CHARACTERIZATION OF RAT AORTIC BODY CHEMORECEPTORS

ANATOMICAL CHARACTERIZATION AND CELLULAR PHYSIOLOGY OF RAT AORTIC BODY CHEMORECEPTORS

By NIKOL A. PISKURIC, B.Sc. (Hons)

A Thesis

Submitted to the School of Graduate Studies

In Partial Fulfilment of the Requirements for the Degree

DOCTOR OF PHILOSOPHY

McMaster University

DOCTOR OF PHILOSOPHY (2012) MCMASTER UNIVERSITY

(Department of Biology) Hamilton, Ontario

TITLE: Anatomical characterization and cellular physiology of rat aortic body chemoreceptors

AUTHOR: Nikol A. Piskuric, B.Sc. (Hons) (McMaster University, Hamilton, Ontario)

SUPERVISOR: Professor Colin A. Nurse

NUMBER OF PAGES: xviii; 194

ABSTRACT

Aortic bodies (ABs) are putative peripheral arterial chemoreceptors located near the aortic arch. They are hypothesized to contribute to O_2 homeostasis by sensing arterial O_2 content and initiating cardiovascular reflexes during hypoxia; however, information on their cellular physiology is lacking. The primary goal of this thesis was to elucidate chemosensory mechanisms among mammalian (rat) AB cells, located specifically at the bifurcation of the left vagus nerve and recurrent laryngeal nerve (RLN), where they are found in association with a group of local neurons (>30). In vagus nerve-RLN whole-mounts, AB chemoreceptor (type I) cells were immunoreactive against the vesicular acetylcholine (ACh) transporter, and were surrounded by nerve terminals immunopositive for purinergic P2X2 and P2X3 receptor subunits, suggesting that ACh and ATP may act as neurotransmitters as in the related carotid body. In a novel dissociated AB culture model, subsets of type I cells exhibited elevated intracellular Ca^{2+} responses to hypoxia, isohydric hypercapnia, isocapnic acidosis, and acidic hypercapnia, demonstrating their direct chemosensitivity for the first time. Interestingly, surviving local neurons also responded to these chemostimuli, suggesting that they are sensory. Patch clamp electrophysiological and Ca^{2+} imaging studies revealed functional heteromeric P2X2/3 and nicotinic ACh receptors on local neurons, consistent with ACh and/or ATP mediating chemotransmission between receptor cells and local neurons. These neurons were also found to be interconnected by electrical synapses. Finally, the short-term survival of red blood cells (RBCs) in AB cultures, along with the finding that blood-borne factors (e.g. ATP released from RBCs) may have access to AB nerve terminals *in situ*, implicates RBCs as O_2-sensors in AB function. Altogether, these results suggest an important role for purinergic P2X2/3 receptors on local neurons/nerve terminals and ATP release from type I cells and RBCs, in the unique ability of ABs to sense and process information about blood O_2 content.

ACKNOWLEDGEMENTS

First and foremost, I would like to thank my supervisor, Dr. Colin Nurse, for sharing with me his enthusiasm and passion for science. Undoubtedly, his tendency to challenge me and offer constructive criticism, along with his unwavering encouragement and confidence in my abilities, were largely responsible for my success as a graduate student. Colin will always have my utmost respect as a scientist and as a person, because of his ability to conduct pioneering research while still remaining a perfect gentleman.

I am absolutely indebted to Cathy Vollmer, without whom this project certainly would not have been possible. Her extraordinary surgical skills only pale in comparison to her *kindness*, loyalty, and steadfast work ethic. She has been a valuable teacher, but more importantly a reliable friend and an endless source of support and inspiration. Thank you to Steve Brown, who "recruited" me to the Nurse lab and then suffered through my incessant questions about everything from MAH cells to mortgages. Steve was truly my mentor and the perfect example of patience, *humility*, and good old-fashioned intelligence. I would like to thank Min Zhang for offering his time and expert patching skills to the cause of my thesis. Despite the days that were "so bad", Min always had a smile on his face, 2 cups of tea on his stool, and a good story about his cat, his grandson, or his home in China. His kindheartedness will not be forgotten. My sincere thanks to Barb Reuter for going the extra mile to ensure that Biology graduate students always felt welcome, cared for, and important. Her encouragement, understanding, and flattery were much appreciated. I would like to thank all past and present members of the Nurse lab with whom I have worked, who, in the past 5 years, have taught me more about myself and about life than I could have imagined. Thank you to Josef Buttigieg, Mike Lowe, Leema Budhu, Katie Clarke, Pablo Reyes, Simon Livermore, Shaima Salman, Sabah and Sana Khan and Sindy Murali. Thanks also to Bart Maslikowski for being an unlikely source of comfort and friendship, and for putting my occasional misery into perspective!

Finally, I would like to thank my family for being endlessly supportive and proud of me. Thank you to Mom and Dad for believing that I could do anything I wanted, and for always saying "*yes*" when I asked for help. Thank you to Baka for being a constant source of wisdom and unconditional love, and for reminding me of my priorities. Last, but certainly not least, thank you to Jacob for consoling me through bad times and celebrating with me in good times; more importantly, thank you for giving my life meaning beyond work, and for making me truly happy. Without a doubt, my husband and family are my greatest source of pride.

TABLE OF CONTENTS

LIST OF FIGURES AND TABLES

CHAPTER 1

CHAPTER 2

CHAPTER 3

CHAPTER 4

CHAPTER 5

LIST OF ABBREVIATOINS

α,β-MeATP	α,β-methyleneATP
5-HT	5-hydroxytryptamine (serotonin)
6-OHDA	6-hydroxydopamine
AB	aortic body
ACh	acetylcholine
Ado	adenosine
AMP	adenosine monophosphate
AMPK	AMP-activated protein kinase
ASIC	acid-sensitive ion channel
ATP	adenosine triphosphate
BBS	bicarbonate-buffered solution
BK	voltage- and Ca^{2+}-sensitive large (i.e. big) conductance K^+ channel
BSA	bovine serum albumin
Ca_v	voltage-sensitive Ca^{2+} channel
CA	carbonic anhydrase
CAII	carbonic anhydrase II
$[Ca^{2+}]_i$	intracellular free Ca^{2+} concentration
CB	carotid body
CBS	cystathionine β-synthase

ChAT	choline acetyltransferase
CNS	central nervous system
CO	carbon monoxide
CO_2	carbon dioxide
CPG	central pattern generator
CSE	cystathionine γ-lyase
CSN	carotid sinus nerve
DβH	dopamine β-hydroxylase
DA	dopamine
DiI	1, 1'-dioctadecyl-3, 3, 3', 3'-tetramethylindocarbocyanine perchlorate
EC_{50}	concentration of agonist causing a half maximal response
fura-2/AM	fura-2 acetoxymethyl ester
GABA	γ-aminobutyric acid
GAP-43	growth-associated protein 43
GFAP	glial fibrillary acidic protein
GPN	glossopharyngeal nerve
H_2S	hydrogen sulfide
Hb	hemoglobin
hBDNF	human brain-derived neurotrophic factor

hGDNF	human glial-derived neurotrophic factor
Hox	hypoxia
HPLC	high-performance liquid chromatography
IR	immunoreactive
K_c	coupling coefficient
K_d	dissociation constant
LC	locus coeruleus
Mec	mecamylamine
mRNA	messenger ribonucleic acid
nAChR	nicotinic acetylcholine receptor
NF, NF70	neurofilament (70 kDa)
Nic	nicotine
NO	nitric oxide
N_2O	nitrous oxide
nNOS	neuronal nitric oxide synthase
NPY	neuropeptide Y
NT-3	neurotrophin 3
NTS	nucleus tractus solitarius
O_2	oxygen
P2X	ionotropic purinergic receptor

P2Y	metabotropic purinergic receptor
PBG	phenylbiguanide
PBS	phosphate-buffered saline
PCO_2	partial pressure of carbon dioxide
pH_e	extracellular pH
pH_i	intracellular pH
PKC	protein kinase C
PN	petrosal neuron
PNMT	phenylethanolamine N-methyltransferase
PNS	peripheral nervous system
PO_2	partial pressure of oxygen
PR	peripherin
RBC	red blood cell
RLN	recurrent laryngeal nerve
S.E.M.	standard error of the mean
SLN	superior laryngeal nerve
sur	suramin
TASK	TWIK-related acid sensitive K^+ channel
TEA	tetraethylammonium
TH	tyrosine hydroxylase

TTX	tetrodotoxin
TWIK	tandem P domain weak inward rectifier K^+ channel
Tx	Triton-X
UTP	uridine triphosphate
VAChT	vesicular acetylcholine receptor
VIP	vasoactive intestinal peptide
VLM	ventrolateral medulla
WGA-HRP	wheat germ agglutinin conjugated to horseradish peroxidase

CHAPTER 1

General Introduction

As the final substrate for oxidative phosphorylation, oxygen (O_2) is vital to cellular energy (i.e. ATP) production and therefore to the survival of all aerobic organisms. The process of respiration involves many coordinated systems that mediate O_2 delivery to the tissues and the concomitant removal of carbon dioxide (CO_2) waste, in a manner that matches the varying energy demands of the organism. In general, the respiratory system and its controlling components ensure that O_2-rich air enters the lungs and that CO_2-rich air is expelled. The cardiovascular system controls the amount and rate of delivery of O_2 to all the cells in the body.

The respiratory and cardiovascular systems are reflexively controlled by a number of specialized organs that sense changes in the chemical composition of the blood; these are the central and peripheral chemoreceptors. The central chemoreceptors are located in the lower brainstem, where they sense interstitial fluid PCO_2/pH and monitor cerebral blood flow and metabolism, increasing sympathetic and respiratory activity in response to acidosis (Neubauer & Sunderram, 2004; Spyer & Gourine, 2009). In contrast, the peripheral arterial chemoreceptors, located strategically along the major arteries of the heart where they sense the chemical composition of arterial blood before it reaches the body tissues, are responsible for eliciting hypoxia-evoked hyperventilation, as well as part of the respiratory response evoked by increased CO_2 tension (hypercapnia) and low pH.

In mammals, the primary peripheral chemoreceptors are the carotid bodies (CBs), situated at the bifurcation of the common carotid arteries. In response to reductions in the partial pressure of O_2 (PO_2), i.e. hypoxia, or increases in CO_2/H^+ (acidic hypercapnia), the CB receptor cells become activated and release a variety of neurotransmitters onto sensory nerve endings, causing an increase in action potential firing in the carotid sinus nerve (CSN). The polymodal properties of CB chemoreceptors are further illustrated by their ability to sense other circulatory factors including hypo-osmolarity, temperature, high K^+, and low glucose (Gonzalez *et al.*, 1994; Lopez-Barneo, 2003; Kumar & Bin-Jaliah, 2007). Afferent petrosal neurons (PNs) transmit chemosensory information to the brainstem, where the respiratory control system or central pattern generator interprets the action potential frequency and initiates an appropriate and proportional ventilatory reflex response (Gonzalez *et al.*, 1994; Teppema & Dahan, 2010).

Another group of peripheral chemoreceptors, the aortic bodies (ABs), are located diffusely in the region of the aortic arch. Although they contribute little, if at all, to the hypoxic ventilatory response, ABs are thought to play a significant role in hypoxia-evoked cardiovascular reflexes, possibly owing to their sensitivity to changes in blood flow and arterial O_2 content. However, this chemosensory role is still controversial, in part because of a lack of information on the cellular physiology of ABs relative to the well-studied CBs. A major goal of this thesis is to fill a critical gap in the AB literature and provide the first physiological characterization of mammalian ABs at the cellular level. It is anticipated that cellular studies of AB cells will provide a novel perspective on their ability to function as chemoreceptors, and possibly help explain the physiological differences between AB and CB chemoreceptors. Because the CB is the model peripheral arterial chemoreceptor organ, a brief overview of the relevant information regarding CB anatomy and chemosensory mechanisms is outlined below.

General anatomy of the carotid body chemoreceptors

The CBs are tiny bilaterally paired organs (<1 mm diameter in the rat, McDonald & Blewett, 1981) located at the bifurcation of the common carotid arteries. Their

constituent receptor type I (glomus) cells are assembled in clusters surrounded by a layer of connective tissue. Type I cells have spherical or ovoid cell bodies ~10 μm in diameter, with large concentric nuclei, and many possess one or more short cytoplasmic processes. Their cytoplasm appears granular because of abundant dense-core and small clear-core vesicles, both of which tend to aggregate at the periphery of the cell near contacts with nerve endings (see below), or other type I cells (see Figure 1). Indeed, dye and electrical coupling experiments, in addition to morphological evidence, suggest the presence of gap junctions between adjacent type I cells within a cluster (McDonald, 1981; Abudara *et al.*, 1999; Jiang & Eyzaguirre, 2003; Eyzaguirre, 2007).

Surrounding receptor cell clusters are the glia-like type II (sustentacular) cells, which are ~4x less abundant than the type I cells. Their elongated cell bodies (~10 μm in length) extend fine cytoplasmic processes that ensheath or penetrate type I cell clusters. Also in contact with type I cells are numerous nerve endings from various sources; on average, each type I cell in the rat CB is contacted by ~1 nerve ending (Gonzalez *et al.*, 1994). Most nerve endings are derived from sensory nerve bundles of the CSN, a branch of the glossopharyngeal nerve (GPN), whose cell bodies lie in the rostral portion of the sensory (petrosal) ganglion. Afferent endings contact type I cells as either small bouton-like endings or wide calyx-shaped endings, and contain ~10x more small clear-core vesicles than dense-core vesicles (McDonald & Mitchell, 1975). A minor source (~5%) of CB innervation is from autonomic efferent neurons, whose cell bodies reside in microganglia embedded within the CSN and GPN. Finally, sympathetic, post-ganglionic fibres enter the CB, though these mostly innervate blood vessels within the organ.

Numerous blood vessels penetrate type I cell clusters, providing a rich blood supply to the CB. These vessels are part of a dense network of thin-walled, fenestrated capillaries (~8-20 μm in diameter), which have a tortuous course throughout the organ. The capillaries arise from non-fenestrated terminal arterioles that are surrounded by 1-2 layers of smooth muscle, rendering them sensitive to vascular regulators. The terminal arterioles emerge from 3 to 4 second order arterioles originating from the main carotid

artery, a branch of the common carotid artery, which delivers the entire blood supply to the CB (McDonald & Larue, 1983).

Chemosensing mechanisms of the carotid body

The CB is a polymodal chemoreceptor capable of sensing multiple blood-borne factors, including arterial PO_2, PCO_2 and acidity. In response to these stimuli, the membrane potential of the receptor type I cells is depolarized, leading to elevations in intracellular free Ca^{2+} concentration ($[Ca^{2+}_i]$) via voltage-gated Ca^{2+} channel entry, and neurosecretion of a variety of neurotransmitters and neuromodulators, ultimately exciting afferent nerve terminals. Although some species and developmental differences do exist, this chemosensing pathway appears to be generally applicable to hypoxic, hypercapnic and acidic stimuli.

The initial effect of hypoxia or acidity (e.g. increased PCO_2 or $[H^+]$, or both) is to cause a depolarizing receptor potential in the type I cell. In the case of hypoxia, this response is mediated by the closure of an O_2-sensitive K^+ channel (Lopez-Barneo *et al.*, 1988), which shifts the membrane potential away from the K^+ equilibrium (or Nernst) potential and towards the equilibrium potential of other active background channels (likely including a Na^+ channel) (Buckler, 2007). The identity of the O_2-sensitive K^+ channels is still controversial, although in the rat there is strong evidence in support of 2 candidates, i.e. a voltage- and Ca^{2+}-sensitive large-conductance (BK) channel (Peers, 1990; Peers & Wyatt, 2007), and a voltage-insensitive, TWIK-related acid-sensitive (TASK)-like tandem-P domain background K^+ channel (Buckler, 1997; Buckler *et al.*, 2000). Recent studies suggest the main O_2-sensitive background K^+ channel in the rat consists of a TASK1/3 heteromultimer (Kim *et al.*, 2009). In the case of acid chemotransduction, inhibition of TASK channels and activation of cation-selective, acid-sensitive ion channels (ASIC 1 & 3) are thought to be the main mechanisms in rat type I cells (Tan *et al.*, 2007). In some species that express voltage-gated Na^+ channels (e.g. rabbit), stimulus-induced depolarization can trigger action potentials (Lopez-Barneo *et al.*, 1988).

Membrane depolarization is normally required for the activation of voltage-gated Ca^{2+} channels and extracellular Ca^{2+} entry. In rat type I cells, this was confirmed using dual electrophysiology and fluorescence $[Ca^{2+}]_i$ recordings, whereby clamping the membrane potential of type I cells near the resting potential (-60 mV) during exposure to hypoxia or hypercapnia prevented the stimulus-evoked rise in $[Ca^{2+}]_i$ (Buckler & Vaughan-Jones, 1994a, b). Furthermore, removal of Ca^{2+} from the extracellular medium significantly inhibited the $[Ca^{2+}]_i$ responses to hypoxia and hypercapnic acidosis, suggesting a role for extracellular Ca^{2+} entry via voltage-gated channels (Buckler & Vaughan-Jones, 1993, 1994a, b).

Type I cells express a variety of Ca^{2+} channels, including L-type (Ca_v1), N-, P/Q- and R-type (Ca_v2), and T-type (Ca_v3) channels (Rocher *et al.*, 2005). Of these, the L-type Ca^{2+} channel appears to conduct the majority of the stimulus-evoked Ca^{2+} current, as indicated by the sensitivity of the hypoxia and hypercapnia responses to selective L-type Ca^{2+} channel antagonists, i.e. the dihydropyridine derivatives nicardipine and nisoldipine (Buckler & Vaughan-Jones, 1994a, b; Rocher *et al.*, 2005). In the rabbit CB, the residual response to hypoxia and hypercapnic acidosis is mediated by P/Q-type Ca^{2+} channels; simultaneous blockade of L- and P/Q-type channels results in complete inhibition of stimulus-induced secretion (Rocher *et al.*, 2005).

Different chemostimuli evoke different intracellular Ca^{2+} responses. Hypoxia, for example, elicits a fast, sustained increase in $[Ca^{2+}]_i$, which is often accompanied by Ca^{2+} fluctuations. The magnitude of the $[Ca^{2+}]_i$ response is graded with the degree of hypoxia (i.e. $\Delta[Ca^{2+}]_i$ increases with decreasing PO_2), similar to CSN discharge (Buckler & Vaughan-Jones, 1994b). Hypercapnic (respiratory) acidosis, on the other hand, elicits a rapid initial rise in $[Ca^{2+}]_i$ followed by a monoexponential decline, which eventually reaches an asymptotic value considerably higher than the baseline $[Ca^{2+}]_i$ (Buckler & Vaughan-Jones, 1993). This biphasic response appears to result from the combined effects of CO_2 and H^+ on the intracellular pH (pH_i) of the type I cell. That is, the initial phase of the $[Ca^{2+}]_i$ response is due to the reversible hydration of CO_2 via the enzyme carbonic anhydrase (CA), which causes a fast intracellular acidification. Indeed,

membrane permeant CA inhibitors (i.e. methazolamide, acetazolamide) slow the rate of intracellular acidification in type I cells (Buckler *et al.*, 1991b); consequently, inhibition of CA also slows the hypercapnia-evoked membrane depolarization in type I cells, as well as the rate and magnitude of the afferent nerve response (Iturriaga *et al.*, 1991; Zhang & Nurse, 2004). The second phase of the $[Ca^{2+}]_i$ signal evoked by high $PCO_2/[H^+]$ results from a sustained decrease in pH_i attributable to prolonged extracellular acidification (low pH_e). In fact, isocapnic (metabolic) acidosis (low pH in normal PCO_2) mainly causes a sustained rise in $[Ca^{2+}]_i$, whereas isohydric hypercapnia mainly causes an initial $[Ca^{2+}]_i$ peak (Buckler & Vaughan-Jones, 1993). These responses parallel the effects of CO_2 and H^+ on pH_i, suggesting that $[Ca^{2+}]_i$ responses to acidic stimuli are mainly determined by their effects on intracellular pH (Buckler *et al.*, 1991a).

Subsequent to increases in cytosolic $[Ca^{2+}]$, chemostimuli cause secretion of a wide variety of neurotransmitters and neuromodulators from type I cells. Indeed, blockers of voltage-gated Ca^{2+} entry inhibit stimulus-evoked secretion (Gonzalez *et al.*, 1994). Among the substances released by CB type I cells are acetylcholine (ACh), ATP, dopamine (DA), serotonin (5-HT), γ-aminobutyric acid (GABA), adenosine (Ado), and histamine (for review, see Nurse, 2005, 2010). In addition to participating in chemotransmission to sensory afferent neurons, CB neurotransmitters and neuromodulators are involved in a variety of autocrine and paracrine interactions (both excitatory and inhibitory), which occur between type I cells within a cluster, between type I cells and type II cells, and between type I cells and nerve endings. Though neuromodulation in the CB appears an important mechanism for fine tuning CB afferent responses, as well as in mediating CB plasticity (Nurse, 2010), it is not the focus of this thesis and therefore only the major neurotransmitters involved in chemoafferent neurotransmission will be discussed below.

It is worth mentioning that the O_2-sensing pathway upstream of membrane depolarization, i.e. the factor(s) that cause(s) K^+ channel inhibition, is(are) still unclear. For many years, the most popular hypothesis concerning the identity of the actual O_2-sensor has been the mitochondrial hypothesis (Kemp, 2006; Buckler, 2007). This

hypothesis is based on an accumulation of evidence which shows that a variety of inhibitors of mitochondrial energy metabolism (such as uncouplers, electron transport chain inhibitors, inhibitors of ATP synthase) *all* rapidly and robustly activate the CB (Buckler, 2007). Recently, Evans and collaborators proposed that the enzyme AMP-activated protein kinase (AMPK), which is sensitive to the intracellular ratio of AMP:ATP, is the primary effector activated by mitochondria and the critical link between mitochondrial inhibition and initiation of membrane signaling (Evans *et al.*, 2005; Wyatt & Evans, 2007). Even more recently, a second hypothesis implicating H_2S gas as a key component in the CB O_2 sensing pathway – *independent* of mitochondrial inhibition – has gained in prominence (Olson, 2011; Prabhakar, 2012). According to the H_2S hypothesis, hypoxia relieves a tonic inhibition of the H_2S biosynthetic enzyme(s), cystathionine γ-lyase (CSE) and/or cystathionine β-synthase (CBS), leading to the endogenous generation of H_2S (Prabhakar, 2012). Subsequently, H_2S excites CB type I cells by either inhibiting BK channels or activating L-type Ca^{2+} channels (Li *et al.*, 2010; Peng *et al.*, 2010). Indeed, studies using CSE knockout mice have provided compelling evidence for the involvement of H_2S in hypoxia-evoked CSN excitation and hyperventilation (Peng *et al.*, 2010). However, the significance of H_2S in CB O_2-sensing has been questioned by Buckler (2012), who showed that the effects of H_2S on CB type I cells are mediated primarily through the inhibition of mitochondrial metabolism (i.e. complex IV or cytochrome oxidase) rather than through a separate signaling pathway; further, Buckler argued that the levels of H_2S required to mimic hypoxia were non-physiological (Buckler, 2012). Further work is required to clarify the relative importance of these pathways in the CB.

Neurotransmitters involved in carotid body chemoafferent excitation

Dopamine (DA) is the best characterized CB neurotransmitter and its biosynthetic enzyme, tyrosine hydroxylase (TH), is now routinely used for type I cell identification. Moreover, secretion of DA in response to chemostimulation has long served as an important physiological assay for type I cell function in the intact CB, CB tissue slices,

and cultured type I cells (Gonzalez *et al.*, 1994; Jackson & Nurse, 1997; Lopez-Barneo, 2003; Iturriaga & Alcayaga, 2004). However, with the exception of the rabbit CB, where it appears to be excitatory, DA functions mainly as an inhibitory neuromodulator in most species, acting via presynaptic and/or postsynaptic D2 receptors (Gonzalez *et al.*, 1994; Iturriaga & Alcayaga, 2004; Nurse, 2010). By contrast, ACh and ATP are considered the major neurotransmitters involved in fast excitatory chemotransmission between CB receptor type I cells and the terminals of chemoafferent PNs (Fitzgerald, 2000; Nurse, 2010). These transmitters are thought to bind to their respective ionotropic receptors (non-selective cation channels) on post-synaptic nerve terminals causing membrane depolarization. Strong evidence for this claim emerged from *in vitro* studies using co-cultures of rat CB type I cells and juxtaposed PNs. Perforated patch clamp recordings of juxtaposed PNs showed that hypoxia, isohydric hypercapnia, and acidic hypercapnia all increased neuronal excitability; furthermore, these responses were partially blocked by antagonists of purinergic P2 receptors (50 μM suramin) or nicotinic ACh receptors (nAChRs) (100 μM hexamethonium, 1 μM mecamylamine) (Zhang *et al.*, 2000; Zhang & Nurse, 2004). However, *combined* purinergic-cholinergic block almost completely abolished the neuronal responses to low PO_2 and high PCO_2/H^+ (Zhang *et al.*, 2000; Zhang & Nurse, 2004). In an *in vitro* preparation of the isolated, superfused CB-CSN, hypoxia-evoked afferent nerve activity was partially blocked by either nAChR (rat) or P2 receptor (rat and mouse) antagonists (Rong *et al.*, 2003; He *et al.*, 2005; He *et al.*, 2006). In similar preparations, *simultaneous* blockade of purinergic and nicotinic receptors completely inhibited the CSN response to hypoxia (rat) and acidosis (cat) (Zhang *et al.*, 2000; Varas *et al.*, 2003). Importantly, hypoxia-evoked increases in CSN activity were significantly reduced in a knock-out mouse model deficient in the P2X2 receptor subunit, and accordingly, hypoxia-evoked hyperventilation in these mice was markedly attenuated, suggesting a pivotal role for ATP acting via the P2X2 receptor in CB hypoxia chemotransmission (Rong *et al.*, 2003). Still, later studies in the cat maintain that the effects of ATP and ACh on afferent PNs are not enough to account entirely for CB

chemotransmission, suggesting that other neurotransmitters are involved (Reyes *et al.*, 2007b, a).

Additional evidence supports the claim that ACh and ATP are neurotransmitters in the CB. In the case of ACh, CB type I cells have the capacity to synthesize (cat and rabbit; Wang *et al.*, 1989; Fitzgerald, 2000), store (rat and rabbit; Nurse & Zhang, 1999; Kim *et al.*, 2004; Zhang & Nurse, 2004), degrade (rat; Nurse & Zhang, 1999), and release ACh in response to chemostimuli, e.g. hypoxia (cat; Fitzgerald *et al.*, 1999; Fitzgerald, 2000). Still, others have failed to localize the mRNA of the ACh synthetic enzyme, choline acetyltransferase (ChAT), and the vesicular ACh transporter (VAChT) in type I cells of the rat CB (Gauda *et al.*, 2004). Physiological studies demonstrate that exogenously applied ACh excites the CSN in many species (for review, see Shirahata *et al.*, 2007), and functional nAChRs have been identified in cultured rat, cat and rabbit PNs using electrophysiological techniques (Zhong & Nurse, 1997; Shirahata *et al.*, 2000; Varas *et al.*, 2000; Alcayaga *et al.*, 2006). Finally, the nAChR α7 subunit was immunolocalized to nerve terminals surrounding cat and rat CB type I cells, as well as to some afferent nerve fibres and PNs (Shirahata *et al.*, 1998; Niane *et al.*, 2009).

Although present in all cells, a neurotransmitter role for ATP in CB function was supported by luciferin-luciferase bioluminscence and HPLC studies, which revealed hypoxia-evoked ATP release from rat CB cultures, fresh tissue slices and whole CB (Buttigieg & Nurse, 2004; Conde & Monteiro, 2006). Given that ATP is co-stored with classical neurotransmitters in synaptic vesicles, it was not surprising that its release from the CB was sensitive to L-type Ca^{2+} channel antagonists and dependent upon extracellular Ca^{2+} (Buttigieg & Nurse, 2004; Conde & Monteiro, 2006). Indeed, the ATP-sensitivity of afferent PNs has been demonstrated in rat, mouse and cat (Alcayaga *et al.*, 2000; Zhang *et al.*, 2000; Rong *et al.*, 2003). Using a combination of electrophysiological, molecular, and immunofluorescence techniques, the ATP receptors expressed by hypoxia-sensitive PNs were found to consist, at least in part, of the heteromeric P2X2-P2X3 type (Zhang *et al.*, 2000; Prasad *et al.*, 2001). Furthermore, nerve endings that make intimate associations with CB type I cells are P2X2- and P2X3-

immunoreactive *in situ*, as are many cell bodies within the petrosal ganglion (Prasad *et al.*, 2001; Rong *et al.*, 2003). Notably, P2X2/3 purinoceptor expression is characteristic of many sensory neurons of the peripheral nervous system (Burnstock, 2009). As mentioned above, the P2X2 receptor subunit seems to be critical to the maintenance of the hypoxia-evoked ventilatory response, and it was shown that knock-out of the P2X3 receptor subunit had little effect on the respiratory response to hypoxia (Rong *et al.*, 2003). However, in addition to the immunolocalization of P2X3 subunits to afferent nerve terminals of both rat and mouse CB *in situ* (Prasad *et al.*, 2001; Rong *et al.*, 2003), there is electrophysiological and pharmacological evidence for contributions of the P2X3 subunit to the hypoxic chemoafferent discharge (Niane *et al.*, 2011), and the basal discharge (Rong *et al.*, 2003), recorded from rat and mouse CSN *in vitro*. Though not the focus of this thesis, it is noteworthy that the neuromodulator Ado, derived in part from the breakdown of released ATP during hypoxia, can also have excitatory paracrine effects in the CB, at both presynaptic and postsynaptic sites. These pathways involve G-protein coupled adenosine A2A and A2B receptors, and appear to contribute to enhanced secretion of CB neurotransmitters and excitation of afferent nerve terminals (Conde *et al.*, 2008). Interestingly, neither P2X2 nor P2X3 deficiency prevented the ventilatory responses to hypercapnia (Rong *et al.*, 2003).

Other paracrine interactions involving carotid body type I cells

In addition to afferent innervation from the petrosal ganglion, the CB receives autonomic efferent input from neurons located within the CSN and GPN. These GPN neurons, which are themselves O_2-sensitive, are responsible for nitric oxide (NO) mediated inhibition of the CB. Hypoxia-evoked ATP release from CB type I cells activates a variety of purinergic P2X receptors (including P2X2, P2X3, P2X4, and P2X7) on GPN neurons (Campanucci *et al.*, 2006). This causes a rise in $[Ca^{2+}]_i$ in efferent nerve terminals, followed by activation of neuronal NO synthase (nNOS), and NO synthesis and release. Ultimately, NO inhibits CB type I cells via membrane hyperpolarization and/or inhibition of L-type Ca^{2+} channels (Campanucci & Nurse, 2007).

ATP released from type I cells also has paracrine effects on the surrounding glia-like type II cells. In intracellular Ca^{2+} recordings from dispersed rat CB cells, ATP evokes large increases in $[Ca^{2+}]_i$ in type II cells but not type I cells, and these effects are mediated by activation of G-protein coupled P2Y2 purinoceptors (Xu *et al.*, 2003). Recent studies in our laboratory led to the proposal that the functional role of type II cell signaling is to amplify ATP at the CB 'tripartite synapse' (Zhang *et al.*, 2012). Using co-cultures of rat CB type I cells, type II cells, and PNs, we showed that activation of P2Y2 purinoceptors on type II cells results in the opening of a gap junction-like, i.e. pannexin-1, channel. Given that pannexin channels form large ATP-permeable pores when open, pannexin activation in CB type II cells by ATP could lead to further ATP release. Indeed, co-cultured PNs were excited following the selective activation of type II cells with the P2Y2 receptor agonist, UTP, demonstrating that ATP release from type II cells can contribute to afferent nerve excitation.

In addition to DA, Ado, ACh and ATP (see above), other small molecule paracrine mediators in the CB include 5-HT and GABA, which act as positive and negative feedback regulators of sensory transmission respectively (reviewed in Nurse, 2010). The excitatory pre-synaptic effect of 5-HT appears to be mediated via G-protein coupled $5\text{-}HT_{2a}$ receptors on type I cells and involves PKC-dependent closure of a resting K^+ conductance (Zhang *et al.*, 2003). On the other hand, GABA acts presynaptically via $GABA_B$ receptor-mediated activation of TASK-like K^+ channels in type I cells and postsynaptically, via activation of $GABA_A$ receptors on petrosal terminals (Fearon *et al.*, 2003; Zhang *et al.*, 2009). Both effects of GABA lead to inhibition of CB sensory discharge.

Anatomy of aortic body chemoreceptors

Comroe (1939) was the first to suggest a location for the AB, though his assertion that it was a discrete entity within the aortic arch (akin to the CB which consistently lies at the carotid bifurcation) has been proven inaccurate. Subsequent studies have shown

that CB-like paraganglia are scattered diffusely throughout the cardiac vasculature and surrounding peripheral nerves, with an especially high frequency at nerve branch points (McDonald & Blewett, 1981; Easton & Howe, 1983; Kummer & Neuhuber, 1989); see Figure 2). The most comprehensive study to describe the number, distribution, size, and morphology of ABs within the cervical and thoracic nerves was performed by McDonald and Blewett (1981). They stained paraganglia using Evans Blue dye which, when injected intravenously, labels tissues with high vascular permeability more rapidly and darkly than surrounding tissues. On average, ~13 putative AB paraganglia (per side) were found along the vagus nerves, superior laryngeal nerves (SLNs), and recurrent laryngeal nerves (RLNs). Despite their abundance, the combined volume of vagal and laryngeal paraganglia was still found to be less than that of one CB (i.e. ~0.7 x 10^6 μm^3 versus 25 x 10^6 μm^3, respectively), because AB paraganglia were significantly smaller than the CBs (~156 μm versus ~600 μm in diameter).

The most commonly studied mammalian ABs include those at the termination of the aortic nerve (a branch of the vagus nerve) near the bifurcation of the common carotid and subclavian arteries (i.e. subclavian bodies; Hansen, 1981; Cheng *et al.*, 1997a), and those within the superior and recurrent laryngeal nerves (Dahlqvist *et al.*, 1984; Kummer & Neuhuber, 1989; Dahlqvist *et al.*, 1994; Dvorakova & Kummer, 2005). Although endoneural in position, vagal paraganglia are separated from bypassing nerves by a capsule of connective tissue emerging from the perineurium (Kummer & Neuhuber, 1989); this capsule ensures staining of discrete blue spots using Evans Blue dye, because it prevents dye diffusion into the bypassing nerve bundle (McDonald & Blewett, 1981).

Except for the obvious size differences, all AB paraganglia are essentially indistinguishable from the large CB paraganglion (McDonald & Blewett, 1981). A typical AB consists of as few as 6 to more than 50 type I (glomus) cells in irregularly shaped clusters, surrounded partially or completely by glia-like type II (sustentacular) cells (Hansen, 1981; McDonald & Blewett, 1981; Kummer & Neuhuber, 1989). Similar to CB receptor cells, AB type I cells are spherical or ovoid, 8-12 μm in diameter, with large round nuclei and occasional cytoplasmic processes that interdigitate adjacent cells

(Hansen, 1981; McDonald & Blewett, 1981). Numerous large, dense-core vesicles and fewer small, clear-core vesicles are found within their cytoplasm; these often aggregate at the periphery of the cell forming asymmetrical, mostly presynaptic, junctions with other chemoreceptor cells or apposed nerve terminals (see below). Interestingly, the density of dense-core vesicles in the AB exceeds that in the CB, though the significance of this is unknown (see Kummer & Neuhuber, 1989). Type II cells are agranular, possess elongated nuclei, and cytoplasmic processes that ensheath type I cells and nerve terminals. Based on estimates obtained from AB paraganglia in the cardiac branches, and aortic, laryngeal and vagus nerves, the ratio of type I to type II cells is ~4:1 (Hansen, 1981; McDonald & Blewett, 1981; Kummer & Neuhuber, 1989).

Clusters of type I cells are penetrated by an anastomosing network of small, densely-packed, thin-walled, fenestrated capillaries (Hansen, 1981; McDonald & Blewett, 1981; Kummer & Neuhuber, 1989). In contrast to the CB, arterioles ringed with smooth muscle are not present within AB paraganglia (Hansen, 1981; Kummer & Neuhuber, 1989); therefore, intraglomerular blood vessels are incapable of local vascular regulation. In one study, serial sectioning of the aortic, cardiac and vagus nerves revealed an AB blood supply derived entirely from one arteriole, which travels a long distance in the epineural sheath (reviewed in Kummer & Neuhuber, 1989). This parent arteriole splits in two and only one branch forms the AB capillary bed. Interestingly, a limiting blood supply has also been inferred from *physiological* studies of cat ABs (Lahiri *et al.*, 1980a; Lahiri *et al.*, 1981b). Indeed, the lack of a multiple, direct blood supply in the AB as compared to the CBs may have important implications concerning their sensitivity to blood-borne stimuli.

Another difference between ABs and CBs is the occasional presence of neuronal cell bodies at the periphery of AB paraganglia (McDonald & Blewett, 1981; Kummer & Neuhuber, 1989; Dahlqvist *et al.*, 1994; Cheng *et al.*, 1997a; Dvorakova & Kummer, 2005). Intravagal ganglion cells are especially numerous (≥30) at the branching of the vagus nerve and RLN, where they are associated with a particularly high density of type I

cells (Dvorakova & Kummer, 2005; see Kummer & Neuhuber, 1989). In contrast, few neuronal cell bodies are found at the periphery of CB.

Innervation of aortic bodies

The perineurium surrounding AB paraganglia is penetrated by nerve fibres that branch into many calyx-shaped or bouton-like endings on AB type I cells. These terminals are strikingly similar to those in the CB, containing numerous mitochondria and small, clear vesicles, and few large, dense-core vesicles (Hansen, 1981; Kummer & Neuhuber, 1989). Based on ultrastructural observations, nerve endings within AB paraganglia form almost exclusively (>95%) afferent endings on type I cells, whereas the remaining terminals form either presynaptic (~1-2%) or reciprocal (<1%) synapses with type I cells (Hansen, 1981).

It is generally accepted that the major source of AB innervation is derived from neurons whose cell bodies lie in the vagal sensory (nodose) ganglia. Several denervation studies have demonstrated that infranodose – but not supranodose – vagotomy causes degeneration of most (~95%) nerve terminals within ABs (aortic nerve, Hansen, 1981; cardiac branches and vagal trunk, Kummer & Neuhuber, 1989; RLN and SLN, Dahlqvist *et al.*, 1994). Furthermore, injection of the anterograde tracer, wheat germ agglutinin conjugated to horseradish peroxidase (WGA-HRP), or the lipophilic dye, DiI, into the nodose ganglion labels arborizing axons and bouton-like terminals on AB type I cells (aortic nerve and cardiac branches, Kummer & Neuhuber, 1989; Cheng *et al.*, 1997a; RLN and SLN, Dahlqvist *et al.*, 1994). Apparently, the sensory afferent axons that innervate the subclavian bodies travel exclusively via the aortic nerve, because cervical vagotomy (i.e. intact aortic nerve but severed distal branches) does not affect the innervation of ABs in this region (Cheng *et al.*, 1997a). Furthermore, Cheng *et al*. (1997a) observed that ~15% of aortic nerve fibres innervated type I cells (chemoreceptor afferents), whereas the rest bypassed the paraganglia and innervated the aortic arch (baroreceptor afferents). Based on the *physiological responses* of ABs following nerve section experiments, Comroe (1939) surmised that chemoreceptor afferents travelled via

the RLN to the aortic nerve before reaching the brain, though this was based on the assumption that AB paraganglia were located within the ascending aorta.

The remaining ~5% of terminals that do not degenerate following vagotomy make exclusively efferent synapses with AB type I cells (Hansen, 1981; Kummer & Neuhuber, 1989). These terminals are thought to originate from autonomic efferent neurons (Hansen, 1981; Kummer & Neuhuber, 1989), though this remains unproven. To investigate the possible contribution of postganglionic sympathetic (i.e. noradrenergic) neurons to AB innervation, Hansen (1981) injected the neurotoxin 6-hydroxydopamine (6-OHDA), which selectively kills catecholaminergic neurons, prior to examining subclavian body ultrastructure. Animals treated with 6-OHDA showed no signs of axonal degeneration within their subclavian bodies, suggesting the absence of a postganglionic sympathetic innervation. The remaining terminals were therefore presumed to originate from either preganglionic sympathetic neurons, or from the local neurons at the periphery of AB paraganglia, which are generally assumed to be postganglionic parasympathetic (Hansen, 1981).

Immunohistochemical studies support the view that local AB neurons innervate the ABs. Intravagal and laryngeal ABs are innervated by nerve terminals immunopositive for vasoactive intestinal peptide (VIP) and neuropeptide Y (NPY), and the pattern of peptidergic innervation is unaffected by infranodose vagotomy (Kummer & Neuhuber, 1989; Dahlqvist *et al.*, 1994). Interestingly, local neurons at the periphery of AB paraganglia are also VIP- and NPY-positive, suggesting that they may be the source of peptidergic innervation. Consistent with the view that local neurons are postganglionic parasympathetic, one population of neurons at the bifurcation of the vagus and RLN is contacted by vesicle-containing axons, most of which degenerate following infranodose vagotomy (see Kummer & Neuhuber, 1989). Finally, local neurons near the vagus-RLN bifurcation are VAChT- immunopositive and are contacted by VAChT-immunopositive nerve terminals, supporting the idea that they are postganglionic parasympathetic (Dvorakova & Kummer, 2005). Indeed, the absence of immunoreactivity against TH

excludes the possibility that they are catecholaminergic (i.e. noradrenergic) postganglionic sympathetic neurons (Dvorakova & Kummer, 2005).

An alternative, sensory role for AB local neurons has also been proposed based on a number of findings. First, some neurons associated with vagal AB paraganglia appear not to be innervated (see Kummer & Neuhuber, 1989); these neurons may send axons directly to the central nervous system. Indeed, Cheng *et al.* (1997a) noted that DiI injection into the nodose ganglion did *not* label nerve terminals around neurons near the subclavian bodies, excluding the possibility of sensory vagal innervation. Second, tracer injection into the nodose ganglion sometimes labeled the *cell bodies* of local neurons, which were thought to represent 'displaced' sensory, nodose neurons (Kummer & Neuhuber, 1989; Cheng *et al.*, 1997b). Finally, of the neurons that are innervated (see above), some retain an intact innervation of unknown source following vagotomy (Hansen, 1981; Kummer & Neuhuber, 1989). Considering that local neurons are themselves VAChT-positive and are surrounded by VAChT-positive terminals (Dvorakova & Kummer, 2005), it is tempting to speculate that local neurons may innervate each other, which explains why some innervation remains after vagotomy.

Aortic body neurotransmitters

The classical marker for localizing thoracic, cervical, and abdominal paraganglia is TH, which labels catecholaminergic type I cells. Of the catecholamines, the ABs are thought to be mostly dopaminergic, and to a lesser extent, noradrenergic, because all type I cells are directly stained by DA antiserum, only some are labeled by dopamine β-hydroxylase (DβH), and none are labeled by phenylethanolamine N-methyltransferase (PNMT) (see Kummer & Neuhuber, 1989). Furthermore, using HPLC, the RLNs and SLNs were found to contain high levels of DA (~ 2 pmol) and noradrenaline (~1 pmol), but lacked adrenaline (reviewed in Kummer & Neuhuber, 1989). More recently, Dvorakova and Kummer (2005) investigated the neurotransmitter profiles of rat and guinea pig type I cells within the vagus nerve and RLN. In both species, all type I cells

were immunoreactive against 5-HT and cholinergic markers (VAChT, rat; ChAT, guinea pig), whereas positive TH-immunoreactivity characterized *all* rat ABs and only *some* guinea pig ABs. In the guinea pig, however, all type I cells were labeled by nNOS. Although these findings suggest species-specific coexistence of transmitters in vagal and RLN AB paraganglia, they are consistent with the neurotransmitter profiles of the CBs of the same species (Dvorakova & Kummer, 2005). A role for the major CB transmitter, ATP, has not been previously investigated in ABs of any species.

In summary, investigations of AB and CB anatomy have revealed mostly similar findings, with two important exceptions, i.e. the presence of local neurons and the limited blood supply in the ABs. Indeed, the presence of two conspicuously similar peripheral arterial chemoreceptors raises a number of questions; in particular, what is the significance of having two groups of peripheral chemoreceptors? How are they different, in terms of the sensory information they process or the systemic/local reflexes they initiate? These questions remain largely unanswered, though a few pioneering studies have made significant progress in advancing our current understanding of AB chemoreceptor function.

Physiology of aortic body chemoreceptors

Reflexes and nerve recording

On examination of the classic 1939 paper by Julius H. Comroe, Jr., entitled *"The location and function of the chemoreceptors of the aorta"* (see Editorial Focus by Neubauer, 2004), it is intriguing that the author's very first statements are as true today as they were almost 75 years ago. Comroe noted that, although the presence of a hypoxia- and hypercapnia-sensitive site within the aortic arch was recognized years before the CBs were even discovered, investigations of the latter proliferated whereas the former received little attention. Consequently, the location, function, and even existence, of AB chemoreceptors were uncertain. The same sentiments are applicable today; the field of peripheral arterial chemoreception is dominated by research on the CBs and the existence of functional AB chemoreceptors is still controversial.

Comroe's detailed studies on dogs and cats provided the first functional distinction between AB and CB chemoreceptors. By comparing the respiratory and cardiovascular responses of intact *versus* CB denervated (i.e. CSN sectioned) animals to systemic anoxia (produced by inhalation of nitrous oxide, N_2O), he found that ABs were relatively more important in eliciting hypertension whereas the CBs were more important in eliciting hyperventilation, even though both chemoreceptors initiated respiratory and cardiovascular reflexes; this effect was more pronounced in dogs than in cats (Comroe, 1939). Indeed, the remaining responses after CB denervation (presumably attributable to the ABs) were abolished by sectioning the vagus (aortic) nerve above, but not below, its bifurcation with the RLN, suggesting that AB chemoafferents ran via the RLN to the vagus (or aortic) nerve.

Following the seminal work of Comroe, few groups pursued investigations of ABs and CBs with the purpose of highlighting distinctions between them. In fact, several nerve recording studies led to an emerging view that ABs were non-functional or low-responding CB counterparts. In the cat, Paintal and Riley (1966) found hypoxia- and nicotine-sensitive AB chemoafferents by recording from single vagus or aortic nerve fibres; however, inhalation of hypercapnic (i.e. ~5% CO_2) air had variable and small effects on nerve activity, whereas the same stimulus was known to strongly activate CB chemoreceptors (Paintal & Riley, 1966). Later, in the same species, Lahiri et al. (1979) showed that single aortic nerve chemoafferents *did* respond to increases in PCO_2 (with the associated changes in $[H^+]$), though the response was largest in the hypocapnic range rather than in the normocapnic to hypercapnic range. In the rat, Sapru and Kriger (1977) compared CB and AB chemoafferent nerve activity by recording from the CSN and vagus nerve, aortic nerve, or RLN, respectively. Though injection of respiratory stimulants (e.g cyanide) into the external carotid artery evoked increases in CSN activity and respiratory rate, injection of the same stimuli into the ascending aorta (presumably activating AB chemoreceptors) caused smaller increases in respiration. In the latter case, however, the reflex hyperventilation was completely abolished after sectioning the CSN, suggesting that it was mediated entirely by the CBs rather than the ABs (Sapru &

Krieger, 1977). Finally, an exhaustive study in cats directly compared the responses of simultaneously recorded single or few-fibre AB and CB chemoafferents to different levels of arterial PO_2 and PCO_2 (Lahiri *et al.*, 1981a). The main finding was that AB chemoafferent responses were qualitatively similar to, but quantitatively less than, those of the CB; i.e. at every stimulus level, CB chemoreceptors were more strongly activated, and this was especially true for hypercapnic stimuli. Therefore, the ABs were classified as "low-responding" chemoreceptors.

In an attempt to explain the differences in chemosensitivity between ABs and CBs, Lahiri speculated that either there were inherent differences in the basic properties of the constituent chemoreceptor (type I) cells, or that different stimulus levels reached the respective chemoreceptors. The latter hypothesis was supported by a number of studies, which ultimately implicated different local microenvironments in the ABs versus the CBs. First, a decrease in hematocrit caused an increase in AB chemoafferent discharge in cats, whereas the CBs showed no consistent change in activity (Hatcher *et al.*, 1978). The rate of aortic nerve firing was proportional to the degree of anemia, despite the fact that arterial PO_2, PCO_2, and pH were maintained at normal physiological levels. Therefore, the ABs appeared to respond to a decrease in O_2 *content*, rather than PO_2. Second, systemic hypotension induced by partially blocking venous return to the heart significantly increased aortic nerve discharge rate but had little effect on CSN activity (Lahiri *et al.*, 1980a). Notably, the AB chemoafferent response was attenuated by hyperoxia, suggesting that AB activation was attributed to a decrease in O_2 availability at the tissue level. Given that the same degree of hypotension did not excite CB chemoafferents, it is likely that CB tissue PO_2 was relatively unaffected by this treatment. Third, in simultaneous chemoafferent nerve recording experiments, injection of excitatory drugs (e.g. cyanide, nicotine) into the venous circulation excited CB chemoafferents first, despite the closer proximity of AB chemoreceptors to the heart; in contrast, AB chemoafferents were first to respond to a decrease in arterial blood pressure (Lahiri *et al.*, 1980b). This study pointed to microcirculatory impediments in the AB that are not present in the CB. Fourth, increasing levels of carbon monoxide (CO) poisoning

strongly increased AB chemoafferent discharge rate in cats, whereas CB chemoafferents were only weakly stimulated at very high (i.e. >70%) CO levels (Lahiri *et al.*, 1981b). CO has the dual effect of decreasing O_2 delivery to the tissues (by displacing O_2 from hemoglobin) and increasing hemoglobin O_2 affinity (thereby left-shifting the O_2-hemoglobin dissociation curve). Given that the PO_2 was unchanged in these experiments, the selective activation of AB chemoreceptors in response to CO suggested that oxygenated hemoglobin must play a role in determining tissue PO_2 in the AB, but not in the CB. In fact, the AB blood flow was estimated to be approximately one sixth of that in the CB, and the mean capillary (i.e. tissue) PO_2 of ABs and CBs was estimated at ~39 mmHg and ~65 mmHg, respectively (Lahiri *et al.*, 1981b). Interestingly, it is at very severe levels of hypoxia (i.e. at or below venous PO_2) that AB chemoreceptors are significantly stimulated (Lahiri *et al.*, 1981a), and it is at these levels of PO_2 where the O_2-hemoglobin dissociation curve is steepest, i.e. where there is a significant decrease in arterial O_2 content.

The pioneering studies by Lahiri's group culminated in a hypothesis that provided a physiological explanation for the differences in AB and CB chemosensitivity and reflex output. The main posit was that a limited blood supply combined with a (presumed) high O_2-consumption rate render the ABs sensitive to O_2 delivery; thus, ABs function primarily as arterial O_2 content sensors. Accordingly, restrictions in the availability of oxygenated hemoglobin activate the ABs and initiate appropriate, cardiovascular reflexes, e.g. hypertension, to increase O_2 delivery to the tissues. In contrast, the CBs, which receive a high blood flow per unit volume (Gonzalez *et al.*, 1994), are relatively unaffected by restrictions in blood flow since the O_2 dissolved in plasma is sufficient to satisfy their energy demands. Therefore, CBs sense arterial O_2 tension, and elicit appropriate respiratory responses when PO_2 is reduced. Ultimately, ABs were designated as circulatory O_2 monitors and CBs as respiratory O_2 monitors, and these functions were mutually exclusive because of the requirement of different microenvironments. (Note, it is assumed that following a decrease in arterial O_2 content, the AB receptor cells are actually activated by a secondary decrease in tissue PO_2.)

Demonstrations of functional AB chemoreceptors are less consistent in the rat, although the existence of AB paraganglia and the presence of chemoreceptor fibres in the aortic nerve have been identified morphologically (see Hansen, 1981; Kummer & Neuhuber, 1989; Dahlqvist *et al.*, 1994; Cheng *et al.*, 1997a). For example, Kobayashi and colleagues (1999) expanded on and confirmed the work of Sapru and Krieger (1977), demonstrating that natural chemostimuli (i.e. inspired hypoxic or hypercapnic air) selectively stimulated the CSN and not the aortic nerve; these data were mostly collected using whole-nerve recording, though no differences were observed in a few paucifibre recordings (Kobayashi *et al.*, 1999). Moreover, the chemoreflexes initiated by inhalation of moderate hypoxia, i.e. hypertension and hyperventilation, were completely abolished after sectioning the CSN but were unaffected after aortic nerve section, suggesting that ABs associated with the aortic nerve did not contribute to systemic chemoreflexes in the rat.

In contrast, studies that focused on single or few-fibre nerve recording attest that functional AB chemoreceptors exist in the rat. *In vivo*, intravenous injection of cyanide evoked an increase in aortic nerve activity, which was completely blocked by hyperoxia (Brophy *et al.*, 1999). Likewise, in an *in vitro* preparation of the isolated, superfused SLN, pressure-ejection of cyanide onto the bifurcation region (where the type I cells are most commonly located) increased nerve activity, an effect that was mimicked by moderate hypoxia (O'Leary *et al.*, 2004). In rats with sectioned CSN, vagus nerve, and SLN (i.e. only aortic nerve chemoafferents intact), intravenous administration of the 5-HT_3 receptor agonist, phenybiguanide (PBG), caused an increase in blood pressure, heart rate, and phrenic nerve frequency and amplitude (i.e. indicating respiratory facilitation), presumably due to activation of AB paraganglia in the aortic nerve (Jones, 2000). Indeed, following aortic nerve section, these responses were significantly reduced or abolished. Simultaneous recordings of aortic nerve and phrenic nerve activity revealed that aortic nerve activation by PBG closely coincided with an increase in phrenic nerve activity (Jones, 2000). Although these data suggest that 5-HT_3 receptor activation may have an excitatory role in AB chemotransmission, a 5-HT_3 receptor antagonist was ineffective at

inhibiting the cyanide-evoked aortic nerve activity. Overall, further studies are required to determine whether the few AB chemoafferents that exist in the rat are capable of performing a physiological function in the whole animal.

Cellular physiology of aortic body receptors

Prior to this thesis, the only group to investigate the cellular physiology of AB chemoreceptor cells was Ito and colleagues (1999), who investigated epitheliod cells from the chicken thoracic aorta that are presumed to be equivalent to the mammalian ABs. Given that these cells were previously shown to contain 5-HT (Yamamoto *et al.*, 1989), and release it in response to hypoxia (Ito *et al.*, 1997), putative AB cells were identified using a vital marker Neutral Red (labels 5-HT granules) in dispersed cells enzymatically dissociated from the lumen of the thoracic aorta. Using the whole-cell voltage clamp technique, Neutral Red-positive cells were found to express fast, TTX-sensitive inward Na^+ currents, slow, sustained inward Ca^{2+} currents, and slow, sustained, TEA-sensitive outward K^+ currents (Ito *et al.*, 1999). Together, the voltage-gated Ca^{2+} channel antagonists nifedipine (L-type) and ω-conotoxin GVIA (N-type) completely blocked the sustained component of the inward current; nifedipine alone blocked almost 80% of the response, suggesting that L-type Ca^{2+} channels conduct most of the Ca^{2+} current. This profile of Na^+, Ca^{2+} and K^+ channels is similar to that observed in type I cells of the CB. Interestingly, in 5 out of 7 chicken epitheliod cells tested, hypoxia caused a small (~10%) inhibition of the outward, TEA-sensitive K^+ current. However, given that TEA failed to induce 5-HT release in secretory experiments, it is likely that inhibition of TEA-sensitive K^+ channels is not responsible for initiating hypoxia-induced 5-HT release (Ito *et al.*, 1997, 1999). The authors suggested that incubation of the cells with the vital dye Neutral Red may have compromised the integrity of the other (unidentified) O_2-sensitive channels involved in initiating hypoxia-induced 5-HT release.

Clearly, many gaps in knowledge exist concerning the functional organization of the AB chemoreflex pathway, and one important goal of this thesis is to address this void. The following unified perspective provides a working model based on data obtained in

the cat, dog, rat and chicken, and is illustrated in Figure 3. In response to stimuli that decrease arterial O_2 content, such as anemia, hypotension, or severe hypoxia, AB type I cells within the vagus nerve/aortic nerve/RLN/SLN/aortic arch are activated. Although the cellular mechanisms of chemotransduction are completely unknown, the downstream release of 5-HT and ACh is likely, given that 5-HT and nicotinic ACh receptor agonists are, besides cyanide, the most potent pharmacological stimuli of AB chemoafferents studied thus far. Presumably, neurotransmitter release causes increased firing of AB afferent nerves, whose axons travel via the aortic nerves to cell bodies in the nodose ganglion. Ultimately, the signal is transmitted to the vasomotor centre in the brain, eliciting primarily cardiovascular reflexes, including hypertension.

Techniques used in this Thesis

Confocal immunofluorescence

In order to describe the anatomy and organization of the AB at the bifurcation of the left vagus nerve and RLN (see Figure 2), whole mounts of these nerves were immunostained and visualized using a laser scanning confocal microscope. Briefly, in confocal microscopy a laser system (i.e. excitation source) emits light that passes through a pinhole aperture to a dichromatic mirror. The laser light is reflected by the mirror and scanned across the specimen in a defined focal plane. Fluorescence emission from the excited fluorophores in the specimen is passed through the same mirror and focused onto another pinhole aperture before reaching the detector (i.e. photomultiplier tube). The essence of this technique is that the two pinhole apertures are **con**jugate to the **focal** point of the objective lens (i.e. **confocal**), so that only light within the desired focal plane reaches the detector. Hence, the advantage of confocal microscopy over traditional widefield epi-fluorescence is that fluorescence that occurs above and below the objective focal plane is not confocal with the pinholes, so that it is not detected and is excluded from the resulting image. This greatly enhances image resolution particularly in the z plane, and allows the reconstruction of several serial confocal sections to create an

overall image of thick (i.e. > 2 μm) samples. For our purposes, the confocal technique made it possible to visualize the *intact* AB paraganglion at the bifurcation of vagus nerve and RLN, which could not be done effectively using other techniques, such as serial tissue sectioning.

Cell culture

For the related CB, the generation of an *in vitro*, dissociated cell culture model has proved invaluable to the study of cellular chemosensing mechanisms. In particular, this model solved the debate of whether the type I cells or apposed nerve terminals were the transducers of chemosensory information. Given that mammalian AB type I cells have never been investigated at the cellular level, we supposed that the demonstration of their direct chemosensitivity would strongly support the notion that ABs are physiological chemoreceptors. Upon dissociation of the left vagus nerve and RLN, we obtained an *in vitro* model that contained not only the putative chemoreceptor type I cells, but also glia-like cells, red blood cells, and viable endogenous neurons, allowing for investigations of intercellular signaling among these cell types.

Ratiometric Ca^{2+} imaging

Given that all chemostimuli investigated to date evoke increases in cytosolic $[Ca^{2+}]$ in chemoreceptor cells of the CB, we reasoned that intracellular Ca^{2+} measurement would be a reliable assay for AB type I cell responsiveness. In addition, given the small yield of AB chemoreceptor cells and neurons in our culture model, a significant advantage of Ca^{2+} imaging is that it allows for the simultaneous recording of $[Ca^{2+}]_i$ in many cells. Indeed, many different upstream signals can cause an increase in cytosolic $[Ca^{2+}]$, including opening of plasmalemmal Ca^{2+} channels (selective or non-selective, voltage- or ligand-gated) or release of Ca^{2+} from intracellular stores. Furthermore, cytoplasmic Ca^{2+} contributes to many cellular processes, including cell excitability, metabolism, activation of kinases, gene transcription, and, particularly important for neuroendocrine cells, neurotransmitter release. Ratiometric Ca^{2+} imaging allows the real-

time measurements of absolute changes in intracellular free Ca^{2+} concentration, $[Ca^{2+}]_i$ in living cells. Cells are loaded with a fluorescent dye called fura-2, whose excitation spectrum changes upon binding Ca^{2+}; i.e. the peak excitation wavelength of free versus bound fura-2 is 380 nm versus 340 nm, respectively. A high-speed filter changer excites the sample with rapidly alternating wavelengths of light, and the ratio of emission observed at 340 nm versus 380 nm excitation provides an estimate of the bound:free fura-2. This ratio is obtained at ~2 s intervals throughout the duration of an experiment, thereby monitoring the changes in $[Ca^{2+}]_i$ in response to applied stimuli. To convert ratio values into absolute vales, ratio data are substituted into the Grynkiewicz equation (Grynkiewicz *et al.*, 1985), which is based on a number of parameters, including the dissociation constant of fura-2 (i.e. 225 nm at 37ºC). Ratiometric dyes are advantageous over single wavelength dyes because they negate errors due to differences in cell thickness, uneven dye loading, and photobleaching.

Electrophysiology

Electrophysiological instruments allow the recording of membrane voltage and currents in live cells. Although fewer cells can be sampled relative to Ca^{2+} imaging, the recording electrode provides very sensitive and reliable information with a high temporal resolution (milliseconds, versus seconds in Ca^{2+} imaging, for example). In patch clamp electrophysiology, the recording electrode is a glass micropipette with a small (~1 μm) open tip, which is filled with saline solution that mimics the intracellular fluid (in the case of whole-cell recording). The tip of the electrode is touched to the surface of the cell of interest, and suction is applied to make a high-resistance (i.e. gigaohm) seal between the micropipette and cell membrane. This high resistance seal allows for low-noise recording of electronically isolated currents through the membrane patch. A chlorided silver wire is placed in contact with the pipette solution and conducts the electric current to an amplifier, which controls the experimental parameters (e.g. clamped voltage) and acquires the data. In nystatin-perforated patch electrophysiology, a perforating antibiotic (nystatin) is added to the micropipette solution. The antibiotic forms ion channels in the

sealed membrane patch, which are permeable to monovalent cations (e.g. Na^+, K^+) but impermeable to divalent cations (e.g. Ca^{2+}) and larger molecules. This allows for electrical continuity between the micropipette and the whole cell but preserves membrane integrity, thereby preventing the dialysis of intracellular signaling molecules out of the cell. Therefore, the electrical activity of the whole cell evoked by intracellular signaling pathways can be measured in response to bath-applied stimuli.

Goals and organization of this Thesis

The main goal of this thesis was to provide an anatomical and physiological characterization of ABs at the bifurcation of the vagus nerve and RLN, with a particular focus on elucidating the mechanism(s) of cellular chemotransduction and chemotransmission to afferent neurons. Ultimately, this thesis provides the first demonstration that mammalian AB type I cells are chemosensitive, and presents a working model to explain how ABs sense O_2 content. Furthermore, the development of a novel AB culture during the course of this thesis provides a useful model for future investigations of AB chemosensing and sensory transmission.

The main body of this thesis is written in a 'sandwich' style and is composed of two published, peer-reviewed manuscripts, and one manuscript that is in preparation for submission.

The first data chapter, Chapter 2, describes the organization of the ABs at the bifurcation of the vagus nerve and RLN using a combination of whole mount immunocytochemistry and confocal microscopy. The possible involvement of ATP as a neurotransmitter in juvenile and adult ABs is investigated using markers of ionotropic ATP receptors. In addition, a novel co-culture model of the mammalian AB, containing type I cells, glia-like cells, and endogenous, viable neurons is presented. In Chapter 3, the direct sensitivity of AB type I cells to several chemostimuli, including hypoxia, isocapnic acidosis, and isohydric and acidic hypercapnia, is investigated using the Ca^{2+} imaging technique. The Ca^{2+} responses of AB type I cells are directly compared to those of type I

cells isolated from CBs of the same animals. Moreover, the effects of chemostimuli on endogenous neurons in AB cultures are investigated. In the final data chapter (Chapter 4), electrophysiological and Ca^{2+} imaging techniques are used to characterize the purinergic receptors underlying the ATP responses in endogenous neurons, as a complement to the immunocytochemical studies of Chapter 2. Moreover, the potential for interactions among red blood cells and ABs is investigated *in vitro* and *in situ*, and a working model of O_2 content sensing by ABs is presented. Finally, Chapter 5 presents a general discussion of the data from Chapters 2-4, and provides an updated model of AB chemotransduction and chemotransmission. Possible future directions and implications of this work are discussed.

Figure 1. Anatomical organization of the carotid body (CB).

A, The CB is composed of clusters of type I (glomus) cells, which are innervated by afferent petrosal neurons (PNs) and efferent glossopharyngeal nerve (GPN) neurons. Glia-like type II (sustentacular) cells are at the periphery of clusters and their processes ensheath the type I cells. **B**, Confocal image of a CB tissue section showing type I cells labeled by tyrosine hydroxylase (TH, green) and nerve terminals labeled by neurofilament (NF, red) and growth-associated protein-43 (GAP, red). Note the presence of a blood vessel penetrating the type I cell clusters.

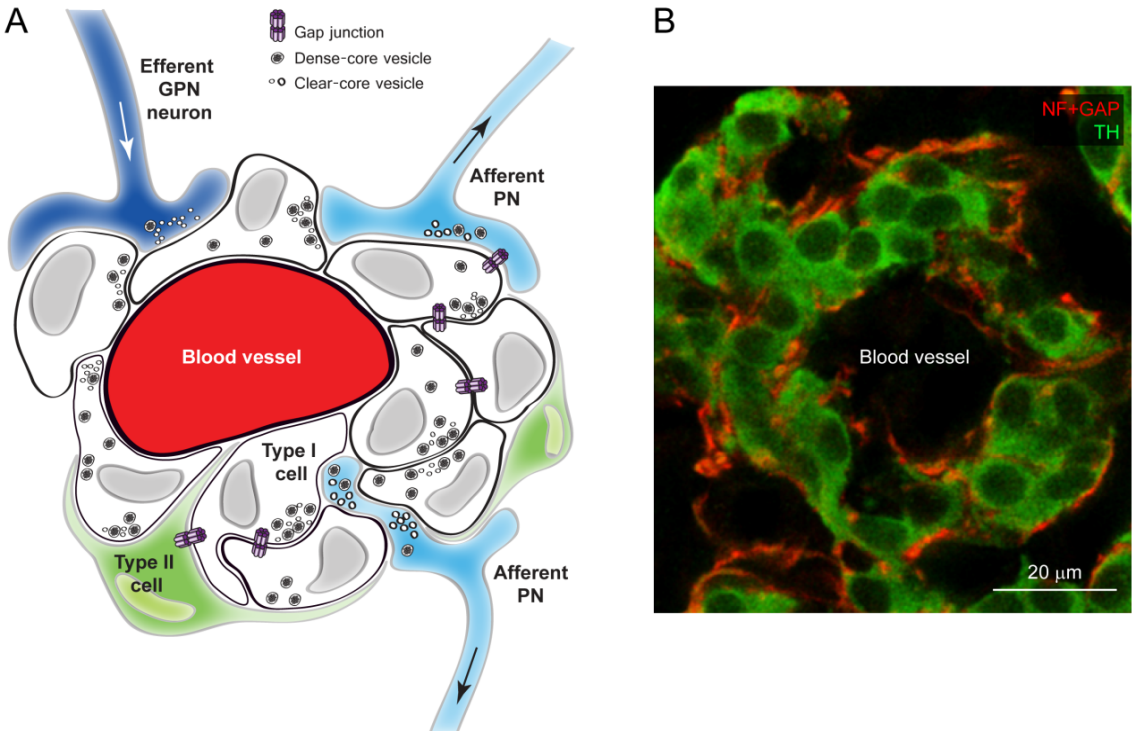
A
Gap junction
Dense-core vesicle
Clear-core vesicle
Efferent GPN neuron
Afferent PN
Blood vessel
Type I cell
Type II cell
Afferent PN
B
NF+GAP
TH
Blood vessel
20 μm

Figure 2. Distribution of peripheral arterial chemoreceptors.

The primary peripheral chemoreceptors in mammals are the carotid bodies (CBs), located bilaterally at the bifurcation of the common carotid arteries; only the left CB is shown here (blue). The aortic bodies (ABs), in contrast, are diffusely distributed throughout the cardiac vasculature and thoracic and cervical nerves (green). The most commonly studied ABs include the subclavian bodies, located at the bifurcation of the common carotid and subclavian arteries, and the laryngeal ABs, located within the superior and recurrent laryngeal nerves, particularly at nerve branch points. The circled AB, located at the bifurcation of the left vagus nerve and recurrent laryngeal nerve, was the one studied exclusively in this thesis.

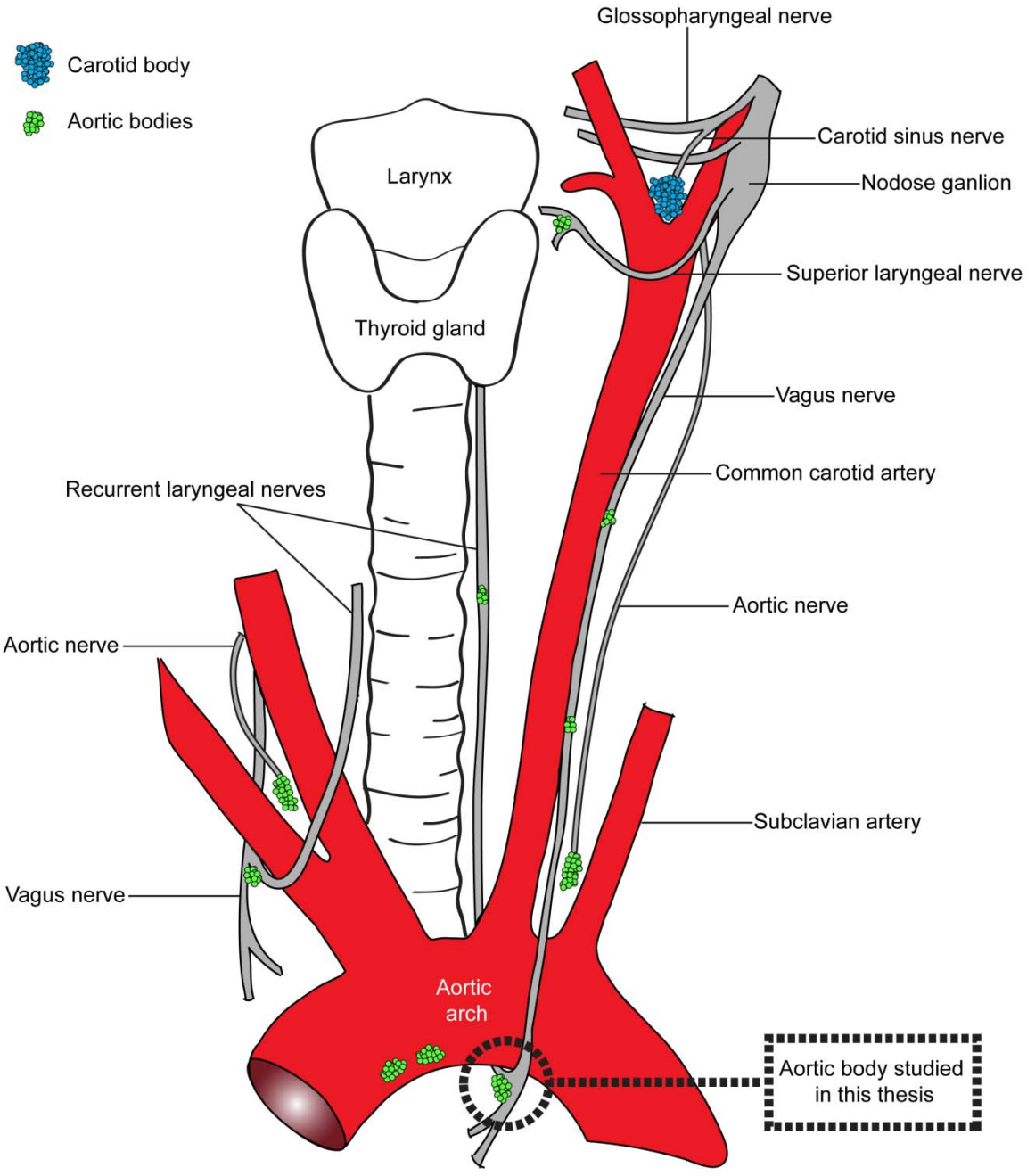
Carotid body
Aortic bodies
Glossopharyngeal nerve
Carotid sinus nerve
Nodose ganlion
Larynx
Superior laryngeal nerve
Thyroid gland
Vagus nerve
Common carotid artery
Recurrent laryngeal nerves
Aortic nerve
Aortic nerve
Subclavian artery
Vagus nerve
Aortic arch
Aortic body studied in this thesis

Figure 3. Proposed functional organization of the aortic body (AB) based on data from the multiple species.

The strongest stimuli for ABs are those which reduce arterial O_2 content, including anemia, hypotension, and carbon monoxide (CO) poisoning (Hatcher *et al.*, 1978; Lahiri *et al.*, 1980a; Lahiri *et al.*, 1981b). ABs are only weakly activated by stimuli that reduce arterial PO_2 or increase PCO_2/H^+ (Lahiri *et al.*, 1981a). It is assumed that the type I cells within AB paraganglia are the actual chemoreceptor cells, which release neurotransmitters onto afferent nerve terminals. Although their mechanism(s) of chemotransduction are completely unknown, the channel(s) responsible for initiating the receptor potential in AB type I cells in response to chemostimuli may include the voltage- and Ca^{2+}-activated BK channels and/or the leak, TASK-1/3 K^+ channels, as in the CB (Gonzalez *et al.*, 1994; Buckler, 2007; Peers & Wyatt, 2007; Kim *et al.*, 2009). Indeed, Ito and colleagues (1999) have shown that epitheliod cells from the chicken thoracic aorta have a similar complement of voltage-gated Na^+, Ca^{2+} and K^+ channels as those of the mammalian CB. The most potent pharmacological stimuli that activate ABs, besides cyanide, include ionotropic 5-HT_3 receptor agonists (i.e. phenylbiguanide, PBG) and nicotinic acetylcholine receptor (nAChR) agonists (i.e. nicotine and α-lobeline) (Comroe, 1939; Comroe & Mortimer, 1964; Brophy *et al.*, 1999; Jones, 2000); however, the site of action of these drugs is unknown. Indeed, dopamine (DA), serotonin (5-HT) and acetylcholine (i.e. VAChT) have been immunolocalized to the AB type I cells, suggesting that they are potential type I cell neurotransmitters (Kummer & Neuhuber, 1989; Dvorakova & Kummer, 2005); of these, only 5-HT release has been observed in response to hypoxia from the chicken thoracic aorta (Ito *et al.*, 1997). Chemoafferent activity has been recorded in the aortic nerve (cat, rat), vagus nerve (cat) and superior laryngeal nerve (rat), and anatomical studies suggest that the cell bodies of afferent neurons reside in the nodose ganglion (Hansen, 1981; Kummer & Neuhuber, 1989; Brophy *et al.*, 1999; Jones, 2000; O'Leary *et al.*, 2004). Ultimately, AB activation evokes primarily cardiovascular chemoreflexes that could lead, for example, to hypertension (Comroe, 1939).

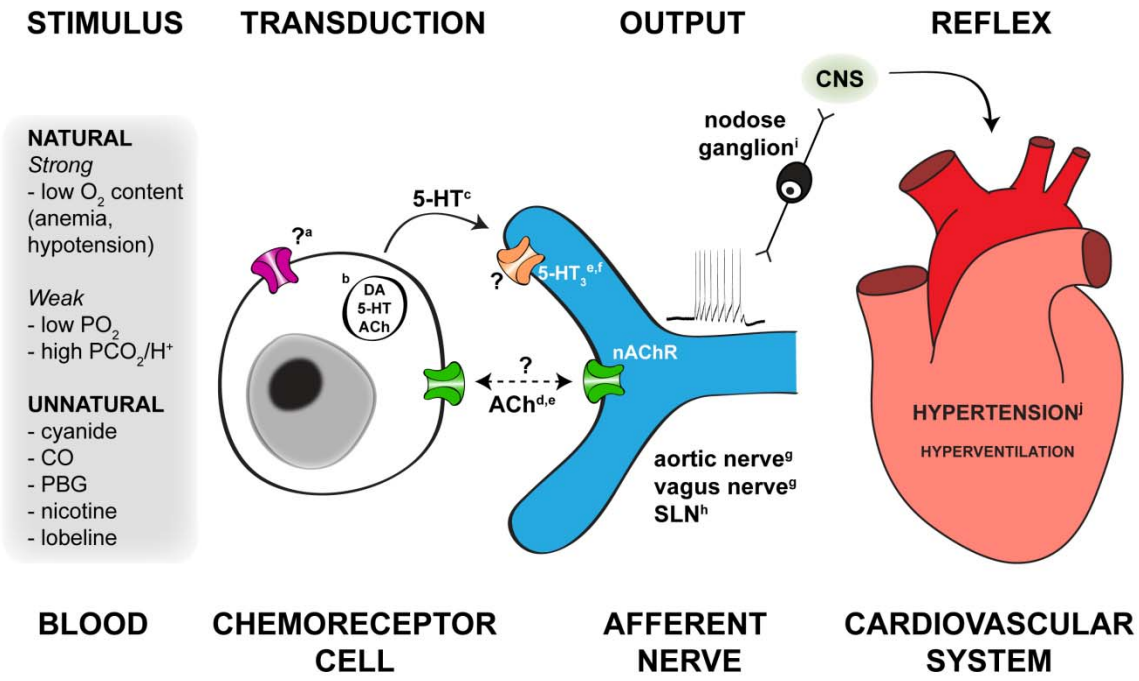

	Description	***Species***	***Reference***
a	Receptor potential possibly caused by inhibition of background K^+ channels, as in the related CB	Chicken, rat	Ito *et al*, 1999; Buckler, 2007; Peers & Wyatt, 2007
b	DA, 5-HT and the vesicular ACh transporter were immunolocalized to AB type I cells	Rat	Kummer & Neuhuber, 1989; Dvorakova & Kummer, 2005
c	Hypoxia-induces 5-HT release from epitheliod cells of chicken thoracic aorta	Chicken	Ito *et al*, 1997
d	Intravenous injection of α-lobeline (a nicotinic ACh receptor agonist) causes hypertension in CB denervated animals	Dog, cat	Comroe, 1939
e	Intra-aortic injection of nicotine, 5-HT and PBG (a $5HT_3$ receptor agonist) activates ABs	Dog	Comroe & Morimer, 1964
f	I.v. injection of PBG increases aortic nerve activity and phrenic nerve activity in CB denervated rats	Rat	Brophy *et al*, 1999; Jones, 2000
g	Single aortic and vagus nerve fibres are activated by low PO_2 (cat) or cyanide (rat)	Cat, rat	Paintal & Riley, 1966; Lahiri *et al*, 1981; Brophy *et al*, 1999
h	Single superior laryngeal nerve (SLN) fibres are activated by cyanide and hypoxia	Rat	O'Leary *et al*, 2004
i	The cell bodies of AB afferent (sensory) neurons are in the nodose ganglion	Rat	Hansen, 1981; Kummer & Neuhuber, 1989
j	Hypoxia causes hypertension, and to a lesser extent, hyperventilation in CB denervated animals	Dog, cat	Comroe, 1939

CHAPTER 2

A confocal immunofluorescence study of rat aortic body chemoreceptors and associated neurons *in situ* and *in vitro*

The work in this chapter has been published as,

Piskuric, N.A., Vollmer, C. and Nurse, C.A. (2011). *The Journal of Comparative Neurology*, **519**: 856-873.

I performed all immunofluorescence and most electrophysiology experiments, data analysis, and preparation of the manuscript. CV performed the dissections and provided the tissue sections.

ABSTRACT

Aortic bodies (ABs) are putative peripheral arterial chemoreceptors, distributed near the aortic arch. Though presumed to be analogous to the well-studied carotid bodies (CBs), their anatomical organization, innervation and function are poorly understood. Using multi-label confocal immunofluorescence, we investigated the cellular organization, innervation and neurochemistry of ABs in whole-mounts of juvenile rat vagus nerve and recurrent laryngeal nerve (RLN), and in dissociated cell culture. Clusters of tyrosine hydroxylase-immunoreactive (TH-IR) type I cells were routinely identified within these nerves. Unlike the CB, many neuronal cell bodies and processes, identified by peripherin (PR) and neurofilament/growth-associated protein (NF70/GAP-43) immunoreactivity, were closely associated with AB type I cell clusters, especially near the bifurcation of the vagus nerve and RLN. Some neuronal cell bodies were immunopositive for P2X2 and P2X3 purinoceptor subunits, which were also found in nerve terminals surrounding type I cells. Immunoreactivity against the vesicular acetylcholine transporter (VAChT) was detected in local neurons, type I cells, and apposed nerve terminals. Few neurons were immunopositive for TH or neuronal nitric oxide synthase (nNOS). A similar pattern of purinoceptor immunoreactivity was observed in adult rat vagus nerve and RLN, except that type I cells were weakly P2X3-IR. Dissociated monolayer cultures of juvenile rat vagus nerve and RLN yielded TH-IR type I cell clusters in intimate association with PR- or NF70/GAP-43- IR neurons and their processes, and glial fibrillary acidic protein (GFAP) -IR type II (sustentacular) cells. Co-cultures survived for several days, wherein neurons expressed voltage-activated ionic currents and were capable of generating action potentials. Thus, this co-culture model is attractive for investigating the role of type I cells and local neurons in AB function.

INTRODUCTION

Peripheral arterial chemoreceptors play a vital role in the maintenance of O_2 and CO_2/H^+ homeostasis by initiating compensatory reflex responses. In mammals, the primary peripheral chemoreceptor organ is the carotid body (CB), which mediates reflex hyperventilation in response to a fall in arterial PO_2 (hypoxia) or an increase in PCO_2 /H^+ (acidic hypercapnia) It is clear, however, that extra-carotid chemoreceptors located in the aortic bodies (ABs) contribute to reflex responses elicited by hypoxia (Comroe, 1939; Cardenas & Zapata, 1983). These ABs appear as paraganglia distributed in the region of the aortic arch near the common carotid and subclavian arteries and within vagal nerve branches, including the laryngeal nerves (McDonald & Blewett, 1981; Kummer & Neuhuber, 1989; Cheng *et al.*, 1997a). Anatomical studies of AB paraganglia in rats have revealed a CB-like organization and morphology, suggesting a putative chemoreceptor function (McDonald & Blewett, 1981; Kummer & Neuhuber, 1989). Similar to CBs, ABs consist of clusters of densely innervated, granule-containing type I (glomus) cells, which are partially or completely ensheathed by glia-like type II (sustentacular) cells (Hansen, 1981; McDonald & Blewett, 1981; Dahlqvist *et al.*, 1984; Dahlqvist *et al.*, 1994). Furthermore, several neurotransmitters implicated in CB chemotransmission, including catecholamines, serotonin (5-HT) and acetylcholine (ACh), have been identified in rat AB type I cells using immunohistochemistry (Kummer & Neuhuber, 1989; Dvorakova & Kummer, 2005).

In contrast to the paired CBs, which are richly vascularized and reputed to have the largest blood flow per unit weight of any body tissue (McDonald, 1981), ABs are diffusely distributed, occur in variable but relatively small sizes, and possess a rather limited blood supply (McDonald & Blewett, 1981; Kummer & Neuhuber, 1989). Also unlike the CB, whose afferent and efferent neurons are predominantly located distally in the petrosal ganglia (Katz & Black, 1986) and glossopharyngeal/carotid sinus nerves, respectively (Campanucci et al., 2003), ABs commonly encompass type I cells in close proximity to many neuronal cell bodies that are presumed to be of parasympathetic

origin, though their function remains unknown (McDonald & Blewett, 1981; Kummer & Neuhuber, 1989; Dahlqvist *et al.*, 1994; Dvorakova & Kummer, 2005). Nonetheless, based on retrograde labelling and axonal degeneration studies, the cell bodies of AB afferent neurons are thought to lie mainly in the nodose ganglia, with their axons travelling via the vagus or aortic nerves toward the ABs (Hansen, 1981; Dahlqvist *et al.*, 1994; Cheng *et al.*, 1997a).

The early classical functional studies of ABs focused primarily on measuring vagal (aortic) chemoafferent activity or systemic output in dogs and cats (Comroe, 1939; Lahiri *et al.*, 1979; Lahiri *et al.*, 1981a). Later, it was suggested that ABs functioned primarily to monitor O_2 delivery (content) and generate compensatory cardiovascular chemoreflexes (Lahiri et al., 1981b). In other species such as the rat, however, a significant role of ABs in cardiovascular physiology has been questioned (Sapru & Krieger, 1977; Kobayashi *et al.*, 1999), even though PO_2-dependent action potential firing has been recorded from the rat aortic (Brophy et al., 1999) and superior laryngeal (O'Leary et al., 2004) nerves. In general, and in contrast to the well-studied CB, the relative inaccessibility and small size of AB paraganglia, together with an incomplete characterization of their neuroanatomical and neurochemical organization, has hampered cellular studies on the physiology of AB chemoreceptors.

As a first step, we address these issues in whole-mounts of juvenile rat vagus nerve and recurrent laryngeal nerve (RLN) by using multi-label confocal immunofluorescence to examine the cellular organization and neurochemical profiles within ABs. To determine whether or not there were any overt developmental changes in neurochemical profiles, we also examined expression patterns in tissue sections from adult nerves as reported in previous studies (Hansen, 1981; McDonald & Blewett, 1981; Dvorakova & Kummer, 2005). However, the use of whole-mount samples from juvenile rats allowed a more accurate reconstruction of the cellular inter-relationships and innervation patterns within the AB. Following our characterization of the interactions between local intra-vagal neurons and AB type I cells, and the expression of a variety of neurochemical markers in whole-mounts, we developed a novel dissociated cell culture

preparation to facilitate future studies at the cellular level. Interestingly, we show that type I cells, local neurons and glia-like type II (sustentacular) cells survive for at least a few days in these co-cultures, where they retain expression of several neurochemical markers present *in situ*.

MATERIALS AND METHODS

Immunocytochemistry

Whole Mounts

Juvenile rat pups, 9–21 days old (Wistar, Charles River, QC, Canada), were rendered unconscious by a blow to the back of the head and then killed immediately by decapitation. All procedures for animal handling and tissue dissections were carried out according to the guidelines of the Canadian Council on Animal Care (CCAC) and institutional guidelines. The left vagus nerve and RLN were routinely excised, and in a few cases, the right subclavian AB located at the bifurcation of the subclavian and common carotid arteries (Figure 1) was also removed. The present study is based on whole mount data obtained from 165 animals. The tissues were fixed as whole-mounts in PBS containing 4% paraformaldehyde overnight at 4°C, and then washed in PBS (3 x 10 min). Whole-mounts were incubated in primary antibody (Table 1) diluted in PBS containing 1% bovine serum albumin (BSA) and 0.5-1% Triton-X (Tx) for 48 hr at 4°C. Subsequently, they were washed in PBS (3 x 10 min) and incubated for 1 hr at room temperature in secondary antibody (diluted in BSA/PBS/Tx; Table 2). After washing with PBS (3 x 3 min), they were mounted on slides using Vectashield Mounting Medium (Vector Laboratories, Burlington, ON, Canada) to prevent photobleaching. In control experiments, omission of primary antiserum resulted in abolition of specific staining in all cases. Preadsorption of the primary antibody overnight at 4°C with excess blocking peptide (where available; ≥ 2 μg peptide/1 μg antibody) resulted in abolition of staining

(see *Antibody Characterization*). Each primary antiserum was tested on at least 5 different preparations.

Cell cultures

The left vagus and recurrent laryngeal nerves were first excised from juvenile rats as described above. The tissues were incubated for 1 hr at 37°C in an enzymatic solution containing 0.1% collagenase–0.1% trypsin (Gibco, Grand Island, NY, USA), prior to mechanical dissociation and trituration. The resulting cell suspension, containing glomus cells and local neurons, was plated onto a thin layer of Matrigel (Collaborative Research, Bedford, MA, USA) that was previously applied to the central wells of modified 35 mm tissue culture dishes (Zhong et al., 1997). Cultures were grown in F-12 nutrient medium supplemented with various additives at 37°C in a humidified atmosphere of 95% air/5% CO_2 (Zhong et al., 1997). Growth factors (Alomone Labs, Ltd., Jerusalem, Israel), i.e. hGDNF (0.01 μg/ml), hBDNF (0.03 μg/ml) and NT-3 (0.05 μg/ml) were added to the nutrient medium in a few experiments. Cell cultures were stained after incubation for 48-72 hr *in vitro*. Cells were washed with warmed PBS and fixed in 5% acetic acid/95% methanol for 1 hr at -20°C. After washing with PBS (3 x 3 min), cells were incubated in primary antibody (diluted in BSA/PBS) for 24 hr at 4°C and washed again (3 x 10 min). Secondary antibody (diluted in BSA/PBS) was applied for 1 hr at room temperature followed by washing (3 x 3 min) and addition of Vectashield.

Tissue Sections

The left vagus and recurrent laryngeal nerves were removed as described above from six adult rats (~35-100 d). The tissue was immersed in 4% paraformaldehyde/1% dimethyl sulfoxide overnight at 4°C. Sections (thickness, 18–20 μm) were cut in a cryostat and collected on glass slides coated with 2% silane (Sigma) and stored at −20°C. For immunostaining, sections were rehydrated with PBS and then incubated overnight with primary antibody diluted in BSA/PBS. This was followed by washing the sections with PBS (3 × 10 min) and incubating in the dark for 1 hr at room temperature with

secondary antibody. After washing 3x with PBS over 15 min, sections were mounted in Vectashield.

Antibody Characterization

1. Rabbit polyclonal anti-TH antibody (Millipore, Temecula, CA, USA) recognizes a major band at ~60 kDa in western blots of rat adrenal gland and rat brain homogenates (our unpublished observations). No binding occurs to the catecholamine biosynthetic enzymes dopamine-β-hydroxylase or DOPA-decarboxylase, and no staining is observed in immunocytochemistry when the antiserum is preadsorbed with rat TH at final dilution (manufacturer's technical information).
2. Mouse monoclonal anti-TH antibody (Millipore, Temecula, CA, USA) recognizes a major band at ~64 kDa in western blots of rat adrenal medulla-derived cells (i.e. PC12 cells), and positively stains rat sympathetic nerve terminals and adrenal gland tissue (manufacturer's technical information).
3. Goat polyclonal anti-VAChT antibody (Millipore, Temecula, CA, USA) recognizes cholinergic neurons and fibres in the rat central (e.g. interpeduncular nucleus of the brain stem and ventral horn of the spinal cord) and peripheral (e.g. autonomic ganglia and adrenal gland) nervous systems (manufacturer's technical information). This antibody recognizes VAChT in VAChT-transfected CV-1 cells but not the vesicular monoamine transporter (VMAT) protein in VMAT2-transfected CV-1 cells; furthermore, it co-localizes with choline acetyltransferase in neurons as indicated by direct double labelling (Arvidsson et al., 1997). In whole-mounts of juvenile rat vagus and recurrent laryngeal nerve, preadsorption of the antibody with the manufacturer's control peptide (Millipore AG260) abolished all specific cellular staining (present study).
4. Guinea pig polyclonal anti-VAChT antibody (Millipore, Temecula, CA, USA) recognizes a single band on western blots of rat brain homogenates corresponding to the size of the predicted rat VAChT protein; no staining occurred in blots incubated

with the antibody that had been preadsorbed with the immunizing peptide (manufacturer's technical information).

5. Mouse monoclonal anti-NF70 antibody (Millipore, Temecula, CA, USA) specifically recognizes the low molecular weight (i.e. 68-70 kDa) subunit of the neurofilament triplet in western blots of purified rat neurofilaments, and shows strong staining of a wide variety of neuronal processes in rat tissues including spinal cord and cerebellum (Debus et al., 1983).
6. Mouse monoclonal anti-GAP-43 antibody (Sigma-Aldrich Canada Ltd., Oakville, ON, Canada) recognizes an epitope present on both kinase C phosphorylated and dephosphorylated forms of GAP-43 (manufacturer's technical information). In western blots of denatured-reduced newborn rat brain tissue, the antibody recognizes a band at 46 kDa, corresponding to the molecular weight of GAP-43 (manufacturer's technical information).
7. Rabbit polyclonal anti-PR antibody (Millipore, Temecula, CA, USA) recognizes a major band at ~57 kDa in western blots of PC12 cell lysate, and does not stain vimentin, GFAP, alpha-internexin or any of the neurofilament subunits (manufacturer's technical information).
8. Rabbit polyclonal anti-P2X2 antibody (Alomone Labs, Jerusalem, Israel) recognizes a single band at ~75 kDa in western blots of differentiated and undifferentiated PC12 cells (manufacturer's technical information). In whole-mounts of the rat vagus and recurrent laryngeal nerves, preadsorption of the antibody with the control peptide abolished all specific staining (present study).
9. Guinea pig polyclonal anti-P2X3 antibody (Millipore, Temecula, CA, USA) stains a single band corresponding to the weight of the P2X3 peptide in western blots of rat trigeminal ganglia, and accordingly, stains the somata of neurons in the rat trigeminal ganglia (Kim et al., 2008). In whole-mounts of the rat vagus and recurrent laryngeal nerves, preadsorption of the antibody with the control peptide (Millipore AG356) abolished all specific staining (present study).

10. Rabbit polyclonal anti-P2X3 antibody (Alomone Labs, Jerusalem, Israel) stains a single band at ~60 kDa in western blots of rat dorsal root ganglion lysates, and this band is abolished by preadsorption of the antibody with the control peptide (manufacturer's technical information). In whole-mounts of the rat vagus and recurrent laryngeal nerves, preadsorption of the antibody with the control peptide abolished all specific staining (present study).
11. Rabbit polyclonal anti-nNOS antibody (ImmunoStar Inc., Hudson, WI, USA) specifically stains a band at ~155 kDa in western blots of rat brain homogenates and demonstrates strongly positive labelling of rat hypothalamus, striatum, cortex and spinal cord, and no cross reactivity with other forms of NOS is observed (manufacturer's technical information). In whole-mounts of rat vagus and recurrent laryngeal nerves, immunolabelling was completely abolished by preadsorption with the manufacturer`s control peptide (Cat. No. 24447; present study).
12. Mouse monoclonal anti-GFAP antibody (Millipore, Temecula, CA, USA) recognizes a band at ~51 kDa on western blots of extracts from a human glioma cell line (manufacturer's technical information). By immunohistochemistry, the antibody recognizes astrocytes and Bergmann glia cells, glioma and glial cell derived tumors and shows no cross-reactivity with vimentin (manufacturer's technical information).

Confocal microscopy

Specimens were first examined using an epifluorescence microscope (Olympus BX60 or Zeiss IM35) in order to identify regions of interest for further confocal examination. Specifically, whole mounts were examined along their entire length, with a particular focus on the bifurcation region between the vagus nerve and RLN. Subsequently, specimens were examined using either the Zeiss LSM 510 or the Leica TCS SP5 II confocal systems, equipped with argon (458/488/514 nm, Zeiss; 458, 476, 488, 515 nm, Leica) and helium-neon (543, 633 nm, Zeiss; 543, 594, 633 nm, Leica) lasers. Images presented here were obtained using objectives with the following magnification/numerical aperture: 20x/0.75 nA air and 60x/1.2 nA water (Zeiss), and

20x/0.7 nA water/glycerine/oil and 63x/1.4 nA oil (Leica). Tissue was scanned in optical sections separated by 1.0-2.5 μm; the average depth of the tissue sampled in this manner was ~20 μm (maximum ~40 μm). Data acquisition was controlled with the aid of LSM Image Browser (version 3.1.0.99, Zeiss) or LAS AF (version 2.1.2, Leica). Digital manipulation of images, including adjustment of brightness and contrast and/or noise elimination, was performed using LSM Image Browser, LAS AF Lite and/or ImageJ (version 1.421, NIH, USA). Images were cropped and/or rotated in Adobe Photoshop CS3 Extended (version 10.0.1) and figures were compiled in Adobe Illustrator CS3 (13.0.1).

Nystatin perforated-patch recording

Cultured neurons (grown with or without growth factors) were used for electrophysiology experiments after 24-48 hr *in vitro*. Nystatin perforated-patch, whole-cell recording was performed according to procedures routinely used in this laboratory (Thompson et al., 1997). Extracellular recording solution contained (in mM): 135 NaCl, 5 KCl, 2 $CaCl_2$, 2 $MgCl_2$, 10 glucose, and 10 HEPES, adjusted to pH 7.4 with NaOH. Pipette solution contained (in mM): 110 K^+ glutamate or gluconate, 25 KCl, 5 NaCl, 0.5 $CaCl_2$, 10 HEPES, and 300 μg ml^{-1} nystatin, at pH 7.2. Other experiments were carried out at 37°C in bicarbonate/5% CO_2-buffered solution (24 mM $NaHCO_3$ substituted for equimolar NaCl) as described previously (Zhang & Nurse, 2000). Records shown in text were obtained at room temperature (20-23°C) with an Axopatch-1D patch-clamp amplifier, digitized with a DigiData 1200 computer interface (Axon Instruments), and stored on a personal computer using pCLAMP software version 9.0 (Axon Instruments).

RESULTS

Localization of type I cells and associated neurons in the vagus nerve and recurrent laryngeal nerve (RLN) of juvenile rats

Aortic body (AB) paraganglia are most commonly found at branch points of the vagus nerve (McDonald & Blewett, 1981; Kummer & Neuhuber, 1989), and in the present study were readily identified within whole-mounts of the left vagus nerve and recurrent laryngeal nerve (RLN) (Figure 1). In all whole-mounts investigated with tyrosine hydroxylase (TH) (n=140), TH-immunoreactive (-IR) type I cells presented as clusters (2 to >150 cells) dispersed along the lengths of the vagus nerve and RLN, as described by Dvorakova and Kummer (2005) in sections of the same tissue from adult rats. These cells were typically small in size (5-10 μm), had a round shape with concentric nuclei, and in some cases appeared to extend TH-IR processes of variable lengths. The largest AB type I cell cluster was consistently found at the bifurcation of the vagus nerve and RLN (i.e. Figure 2A), and consisted of >100 type I cells in close proximity to many (>30) neuronal cell bodies (see below). Together, they were embedded within a compact nerve bundle surrounded by perineurium. A second large type I cell cluster (>50 cells), associated with few or no neuronal cell bodies, was usually located in the cervical vagus that emerged from the distal pole of the nodose ganglion. In a minority of cases (<10%), whole-mounts contained a few (1-4) TH-IR neurons (Figure 2E) located near the AB or in the cervical vagus nerve. These neurons extended long TH-IR processes that joined distinct bundles of TH-IR nerve fibres that travelled within the vagus nerve in the direction of the nodose ganglion.

Antisera against neuron-specific intermediate filaments, such as the low molecular weight (68-70 kDa) neurofilament (NF70; n=17) or peripherin (PR; n=7), revealed the presence of many neuronal cell bodies within the vagus nerve and RLN Neurons of medium (~20 μm) and large (30-40 μm) diameter were easily distinguished from the smaller type I cells, and they tended to have eccentric nuclei. Routinely, a large cluster of up to 30 neuronal cell bodies was found adjacent to the AB receptor cells (Figure 2A) at the bifurcation of the vagus nerve and RLN. Elsewhere, neurons were found in aggregates of 2 or 3 or in small groups (Figure 2F), sometimes associated with small clusters of type I cells. Furthermore, nerve endings identified by positive immunoreactivity against NF70 and the growth-associated protein-43 (GAP-43)

contacted and often encircled type I cells in the vagus nerve and RLN (e.g. Figure 2C), consistent with ultrastructural evidence for a dense innervation of AB type I cells (Hansen, 1981; McDonald & Blewett, 1981; Kummer & Neuhuber, 1989).

In addition to their location in the vagus nerve and RLN, AB paraganglia have also been located at the origin of the subclavian and common carotid arteries (see Figure 1; Hansen, 1981; Cheng *et al.*, 1997a). In this region, TH-IR type I cells were commonly found near the termination of the aortic nerve, affixed to the bifurcation of the subclavian and common carotid arteries (n=3; Figure 2B). Unlike the AB paraganglion at the vagus nerve-RLN bifurcation, however, the subclavian AB was not associated with a cluster of local neurons, except for a minority of cases where only 1 or 2 neuronal cell bodies were present nearby.

Expression of the cholinergic marker VAChT in the aortic body

Previous immunohistochemical studies in the rat CB have led to contradictory results as to whether or not cholinergic markers are expressed in type I cells (Gauda *et al.*, 2004; Zhang & Nurse, 2004). In the adult rat AB, both type I cells and local neuronal cell bodies stained positively for the vesicular acetylcholine transporter (VAChT), though the brightest staining occurred in nerve terminals surrounding local neurons (Dvorakova & Kummer, 2005). Because different antibodies may yield variable staining patterns due to differences in epitope specificity and cell-specific differences in epitope availability following fixation, we tested two different VAChT antibodies on juvenile AB whole-mounts (see Table 1).

Using a goat anti-VAChT antiserum directed against a 20 amino acid C-terminal peptide epitope (AB1578; Millipore), we confirmed that type I cells in the rat vagus nerve and RLN are VAChT-IR (n=11; Figure 3A-C); preadsorption with the blocking peptide abolished VAChT immunoreactivity (Figure 3D), confirming antibody specificity. However, with this antibody, both local neurons (Figure 3A-C, asterisks) and nerve terminals showed negligible staining. In contrast, use of a guinea pig anti-VAChT

antiserum directed against a shorter, 11 amino acid C-terminal peptide epitope (AB1588; Millipore), revealed dense, punctate VAChT-IR nerve terminals surrounding VAChT-IR local neurons in the AB (n=16; Figure 3E, I, J). Furthermore, this antibody produced faint positive staining of type I cells (Figure 3E-H). Despite the variability in staining intensity, these results are consistent with the presence of VAChT in type I cells, neuronal cell bodies, and nerve terminals in the AB at the bifurcation of the vagus nerve and RLN (Dvorakova & Kummer, 2005).

Expression of P2X purinergic receptor subunits in whole mounts of juvenile rat aortic body and surrounding nerves

Because release of ATP from type I cells onto postsynaptic P2X purinergic receptors appears to be a key event during CB chemoexcitation (Nurse, 2005), we tested for the presence of P2X purinoceptor subunits in the juvenile rat AB using immunocytochemistry. Type I cells comprising the large AB paraganglion at the bifurcation of the vagus and recurrent laryngeal nerves, as well as type I cells scattered along these nerves, were contacted by nerve endings that were immunopositive for several P2X purinoceptor subunits. As illustrated in Figure 4 (A-E), antisera against P2X2 subunits labelled nerve terminals contacting TH-IR type I cells in the AB (n=18). Interestingly, a subpopulation (~25%) of local neurons was also positive for P2X2 (Figure 4B), though it was clear that other neurons in the background were negative for both P2X2 and TH (Figure 4C, asterisks). In some cases, it appeared that P2X2-IR fibres emerged from local neurons and that their terminals surrounded and interdigitated type I cell clusters (Figure 4C-E). This raises the possibility of synaptic communication between type I cells and at least some local neurons near the AB at the vagus nerve-RLN bifurcation. P2X2-IR neuronal cell bodies, fibres, and terminals were also found associated with smaller type I cell clusters along the vagus and recurrent laryngeal nerves (not shown).

Similar to the staining pattern for P2X2, P2X3 antisera labelled a subpopulation of large and small neurons (~25%) in the AB region (Figure 4F), as well as many neurons in the vagus nerve caudal to the nodose ganglion (n=10 for both guinea pig and rabbit anti-P2X3 antisera; Figure 4H). Furthermore, dense, bright P2X3-IR nerve fibres and terminals surrounded TH-IR type I cells in the AB (Figure 4F), and elsewhere along the vagus nerve (Figure 4G). To investigate whether or not there was co-localization of P2X2 and P2X3 immunoreactivity, AB whole-mounts were triply immunolabelled for TH, P2X2 and P2X3. As illustrated in Figure 4I-L, P2X2 and P2X3 immunoreactivity were co-localized in nerve terminals surrounding TH-IR type I cells of the AB (n=5). The majority (i.e. >75%) of P2X2-IR local neurons adjacent to the AB were also P2X3-IR (not shown).

P2X purinoceptor expression in tissue sections of adult rat aortic body

To address whether or not P2X purinoceptor subunit expression in the AB is developmentally regulated, we investigated the presence of P2X2 and P2X3 purinoceptor subunits in cryosections of adult (~35-100 d) rat vagus nerve and RLN. As illustrated in Figure 5A, dense innervation of TH-IR type I cells by P2X2-IR nerve terminals was also characteristic of the adult AB (n=4); furthermore, a subset of local neurons were immunopositive for P2X2 (not shown). In contrast, we found no convincing evidence of P2X3-IR nerve terminals in cryosections of adult ABs. Rather, P2X3 immunoreactivity was variable within the cytoplasm of TH-IR type I cells (n=5), as in Figure 5F-H. P2X3-IR neurons were also observed in adult cryosections (e.g. Figure 5E), and were sometimes closely associated with TH-IR type I cells (not shown). Preadsorption with their respective control peptides abolished all specific staining for P2X2 (Figure 5B, C) and P2X3 (not shown) in tissue sections.

Localization of nNOS-immunoreactive neurons in the aortic body microenvironment

Neuronal nitric oxide synthase (nNOS)-IR autonomic neurons have previously been localized in the CB and attached carotid sinus nerve, and are thought to be the basis of NO-mediated efferent inhibition of chemoreceptor function (Wang et al., 1993; Campanucci et al., 2006). We therefore tested for the presence of similar nNOS-IR neurons in juvenile rat vagus and recurrent laryngeal nerves (n=17). As shown in Figure 6A and D, a small subpopulation (~5%) of neuronal cell bodies adjacent to the AB at the bifurcation of the vagus nerve and RLN was nNOS-positive; note in Figure 6A the presence of nNOS-negative neurons denoted by asterisks. Other neurons within the vagus nerve itself were also nNOS-positive (Figure 6B), and these were usually found in the vicinity of nNOS-negative neurons as well (Figure 6B, asterisks). Often, nNOS-IR neurons appeared to extend nNOS-IR processes (Figure 6B, C, D, arrows), that sometimes mingled with neighbouring TH-IR type I cell clusters (e.g. Figure 6D, arrow). Preadsorption of the antibody with the manufacturer's control peptide abolished all specific nNOS staining (not shown).

Monolayer cultures of dissociated aortic body type I cells and local neurons

In contrast to the numerous studies on isolated CB type I cells (Nurse, 2005), comparable studies on AB type I cells are lacking, mainly because techniques for obtaining a viable preparation of dissociated AB type I cells have not yet been developed. To facilitate such studies, we developed a viable monolayer cell culture preparation using enzymatic and mechanical dissociation of the left vagus and recurrent laryngeal nerves. The following observations regarding AB culture composition are based on samples obtained from at least 50 different litters (9-12 pups each), each litter producing 2-4 dissociated cell cultures. Type I cell clusters were readily visible within hours of plating and persisted in culture for several (>3) days. Under phase contrast microscopy, type I cells appeared rounded (5-10 μm in diameter), and had large concentric nuclei with

clearly visible nucleoli (Figure7A, C, D arrowheads). The type I cluster size varied from 5 to >50 cells and though some single type I cells were present, they could not be easily identified under phase contrast microscopy. Staining of the cultures for TH-immunoreactivity (n=19) confirmed the presence of type I cells in clusters (Figures 8A, C, D and 9A-C) and singly isolated (not shown). A conspicuous feature of these AB cultures was the presence of many isolated neuronal cell bodies, not generally seen in dissociated cell cultures of rat CB (Nurse & Fearon, 2002). These local neurons, which were routinely observed during immunostaining of AB whole-mount preparations *in situ* (e.g. Figures 2, 4), were easily identified in culture by their characteristic large size (20-30 μm in diameter), and eccentric nuclei under phase contrast microscopy (Figure 7B, C, D, asterisks). Typically, they occurred singly (Figure 7B, C), or in association with other neurons and/or type I cells (Figure 7D), an arrangement reminiscent of that seen in whole-mounts of the laryngeal AB *in situ*. In culture, these neurons appeared healthy and their viability was confirmed by the fact that they generated large, fast inward currents and sustained outward currents in response to depolarizing voltage steps (Figure 10A, B), as well as repetitive, overshooting action potentials following the injection of depolarizing currents (Figure 10C) (n = 10). Moreover, all neurons were immunopositive for NF70/GAP-43 (n=13; Figure 8C) or PR (n=6; Figure 8B), and their processes appeared to form intimate associations with TH-IR type I cell clusters (Figure 8C, D-F). An occasional TH-IR neuron was found in culture (not shown), though the majority of neurons were TH-negative. Based on routine observations, the addition of growth factors to the culture medium had no obvious effect on the survival of type I cells and/or neurons in short term culture (<3 days).

Besides type I cells and local neurons, juvenile rat AB cultures contained many background cells including glia-like type II (sustentacular) cells, which were identified by positive immunoreactivity against glial fibrillary acidic protein (GFAP) (n=4; Figure 9). This was expected because, similar to the CB, AB paraganglia are known to be ensheathed by glia-like type II cells *in situ* (Hansen, 1981; McDonald & Blewett, 1981; Dahlqvist *et al.*, 1984). As illustrated in Figure 9, these GFAP-IR type II cells had small,

irregular-shaped cell bodies (5-10 μm in diameter) and extended long processes that ramified over the culture surface (Figure 9C-E), similar to that seen in CB cultures (Nurse & Fearon, 2002). Quite frequently, type II cell bodies and their processes were found within type I cell clusters with which they formed an intimate association (Figure 9A-C). Fewer and less intimate associations were observed between local neurons and GFAP-positive type II cells in culture (Figure 9D, E).

DISCUSSION

In the present study we used immunofluorescence and confocal microscopy to characterize aortic bodies (ABs) in whole-mounts of juvenile rat vagus nerve and recurrent laryngeal nerve (RLN). This approach allowed the visualization of clusters of TH-positive type I cells, their innervation pattern, and their relationship to several subpopulations of intra-vagal neurons that were consistently found in close proximity, particularly at the bifurcation of the vagus and recurrent laryngeal nerves. We confirmed the presence of VAChT-IR type I cells and neuronal cell bodies within the AB, as well as VAChT-IR terminals and nNOS-IR fibres. Additionally, we found a few nNOS-IR neuronal cell bodies among these intra-vagal neurons. This study also provided novel information on the distribution of purinergic neurons and nerve fibres expressing P2X2 and P2X3 immunoreactivity. A summary of the main findings is presented in Table 3. We further demonstrate that combined enzymatic and mechanical dissociation of the vagus nerve and RLN could produce a unique co-culture preparation in which both AB type I cell clusters and local neurons survive for at least 3 days. The fact that neuronal processes appeared to form intimate contacts with type I cells in these co-cultures and the neurons were capable of generating overshooting action potentials following injection of depolarizing currents, suggests that this preparation is attractive for future studies on the role of these neurons in AB chemoreception. In this regard, it is noteworthy that though a few VAChT- and nNOS-IR autonomic neurons have been described in the related carotid body (CB) *in situ* (Wang et al., 1993; Hohler et al., 1994), their presence or survival has

not been reported in any of the numerous studies on dissociated rat CB cultures grown under similar conditions (Nurse & Fearon, 2002). Thus, the relationship between type I cells and local, intra-vagal neurons may be unique to the AB and consequently, information processing in the AB may not be identical to that in the CB.

Localization of cholinergic markers in the aortic body

The presence of cholinergic markers in the juvenile rat AB was confirmed using two different VAChT antisera directed at C-terminal epitopes. Though the pattern of immunostaining varied between antisera targeting a short versus long C-terminal epitope of VAChT, antibody specificity has been established in each case by preadsoprtion with the corresponding immunizing peptide (present study and manufacturer's technical information). Thus, the long epitope VAChT antibody showed moderate-to-strong staining of TH-positive type I cells and weak staining of local neurons and nerve endings. In previous studies from this laboratory, this same antibody also produced strong type I cell staining in tissue sections of rat CB (Zhang & Nurse, 2004). On the other hand, the short epitope VAChT antibody showed negligible to weak AB type I cell staining but intense punctate immunostaining of nerve endings surrounding weakly-stained neuronal cell bodies. It therefore appears that, at least after fixation, the microenvironment or configuration of the VAChT C-terminus *in situ* may be different in type I cells versus neurons and nerve endings. Taken together, these data on AB whole-mounts from juvenile rats are consistent with those of Dvorakova and Kummer (2005) on AB tissue sections from adult rats demonstrating the presence of VAChT-immunoreactivity in type I cells and local neurons. The cell bodies of origin of the intense VAChT-IR nerve terminals could not be unambiguously identified in the present study, though it is possible they originate from a subpopulation of local cholinergic neurons. If so, the neurotransmitter acetylcholine (ACh) could participate in a complex local circuit formed by these interconnected neurons with or without involvement of type I cells. Indeed, a common feature of nerve terminals contacting AB type I cells is the presence of small,

clear-cored vesicles (Hansen, 1981; Kummer & Neuhuber, 1989), the presumed storage sites of ACh. Moreover, a role for ACh in AB function was suggested by the earlier observation that nicotine injection into the ascending aorta of dogs elicited cardiovascular responses similar to those elicited by hypoxia, but without involvement of the CB (Comroe & Mortimer, 1964). Though there is still some controversy, the prevailing view in the CB is that ACh acts as an excitatory co-transmitter, released from type I cells onto afferent sensory nerve terminals during chemotransduction (Iturriaga & Alcayaga, 2004; Nurse, 2005; Shirahata *et al.*, 2007). It remains to be determined whether ACh plays a similar role in the AB.

Expression of P2X2 and P2X3 purinoceptor subunits in the aortic body

The present study is the first to report on the immunolocalization of P2X purinergic receptors in juvenile rat AB paraganglia. Using double-label immunofluorescence, the presence of dense P2X2- and P2X3-positive nerve terminals were seen in close contact with type I cells of the AB and elsewhere along the vagus nerve and RLN. Moreover, co-localization of P2X2- and P2X3-immunoreactivity was observed in most nerve terminals and neuronal cell bodies in the AB, similar to that previously reported for sensory afferent terminals in the rat CB (Prasad et al., 2001). These data support the notion that ATP and P2X receptors may play an important excitatory role in the AB, as has been demonstrated for the CB. For example, P2X receptor blockers reversibly inhibited chemosensory transmission in a functional co-culture model of rat CB type I cells and afferent petrosal neurons (Zhang et al., 2000; Prasad et al., 2001) and moreover, the hypoxic ventilatory response was markedly attenuated in transgenic P2X2-deficient mice (Rong *et al*., 2003). Previous ultrastructural studies have shown that AB type I cells are richly innervated by nerve terminals, almost all of which (~95%) are postsynaptic (Hansen, 1981). Based on retrograde labelling and axonal degeneration studies, these afferent nerve terminals are believed to originate mainly from sensory neurons whose cell bodies lie in the nodose ganglion (Hansen, 1981; Cheng *et al.*, 1997a). Thus, it may be that the P2X2/3-expressing nerve terminals

contacting AB type I cells identified in this study originate principally from nodose sensory neurons. Consistent with this view, P2X2 and P2X3 purinoceptor subunit mRNA and protein have been co-localized in rat nodose neurons *in situ* (Lewis et al., 1995; Vulchanova et al., 1997; Xiang et al., 1998). However, because subpopulations of local intra-vagal neurons (~25%) were immunopositive for P2X2 and P2X3 subunits, and were located in close proximity to AB type I cells, it is possible they represent at least a partial source of P2X2/3 purinergic innervation. Indeed, peptidergic innervation by local neurons has been suggested previously by Dahlqvist et al. (1994), following the observation that infranodose vagotomy failed to eliminate neuropeptide Y (NPY) and vasoactive intestinal polypeptide (VIP) -IR innervation of AB paraganglia within the RLN.

Development of the neurotransmitter phenotype in the aortic body

Because developmental changes in neurotransmitter phenotype are common in the autonomic nervous system, including in O_2-sensitive tissues like the adrenal gland and CB (Afework & Burnstock, 2000; Bairam *et al.*, 2007), we investigated purinergic receptor expression in tissue sections of the vagus nerve and RLN from adult rats. Here, we show for the first time the expression of P2X2-immunoreactivity in the adult AB. Moreover, the pattern of P2X2-immunoreactivity in adult rats was similar to that seen in juveniles, where dense P2X2-IR nerve terminals contacted TH-IR type I cells with the occasional presence of a P2X2-IR neuron. Interestingly, P2X3 immunoreactivity was not found in nerve terminals surrounding adult AB type I cells, unlike that in juvenile ABs; rather, adult AB type I cells themselves exhibited variable P2X3 immunoreactivity in the cytoplasm. Functionally, this type of developmental regulation would render adult AB type I cells sensitive to ATP unlike juvenile ABs, which may represent a form of chemoreceptor maturation.

In the CB, it is unclear whether purinergic receptor expression is developmentally regulated. Although there is convincing evidence for P2X2 and P2X3 subunit expression in nerve terminals in the rat CB throughout development (Prasad *et al.,* 2001;

Campanucci *et al*., 2006; He *et al.,* 2006), expression within the chemoreceptor type I cells is debatable. Type I cells in the juvenile rat CB do not express P2X2 and P2X3 purinoceptor subunits (Prasad *et al*., 2001; Campanucci *et al*., 2006). In the adult rat CB, functional studies have provided support for both the absence (Xu *et al*., 2003) and presence (He *et al.,* 2006) of P2X2- and P2X3-containing purinoceptors in type I cells; furthermore, the latter group showed punctate P2X2-immunoreactivity in adult rat type I cells. In adult mice, P2X2 and P2X3 purinoceptor subunits are absent from CB type I cells (Rong *et al.,* 2003), whereas in the cat CB, the expression of P2X2 and P2X3 protein is unchanged over the first 8 months of life (Bairam *et al*., 2007). Thus, it remains to be concluded whether developmental changes in purinergic receptor expression also play a role in CB maturation.

Aortic body type I cells and local neurons in short term co-culture

In order to facilitate future studies on mammalian AB chemoreceptor function at the cellular level we developed an *in vitro* preparation of dissociated left vagus nerve and RLN. Interestingly, these monolayer cultures remained viable for at least 72 hours after the initial plating and it was possible to identify both type I cell clusters and local, intra-vagal neurons under phase contrast microscopy. Whole cell recordings from the neurons indicated they had large, fast inward currents and sustained outward currents, and were capable of generating overshooting action potentials following depolarizing current injections. Moreover, immunocytochemical staining of the cultures revealed that neuronal processes ramified over the culture dish and appeared to form intimate contacts with type I cell clusters. These AB cultures also contained a significant number of GFAP-positive glia-like type II cells that were closely associated with type I cell clusters. While a similar association between type II cells and type I cell clusters has been observed in dissociated cell cultures of the rat CB, the presence of surviving local neurons has not been reported (Nurse & Fearon, 2002). Also, local neurons were not reported in dissociated cell cultures of chicken thoracic aorta, though viable epitheloid O_2-sensitive chemoreceptor cells expressing 5-HT were present (Ito *et al*., 1999). Therefore, our novel

co-culture model of AB type I cells and local neurons should aid future investigations into the cellular organization and function of mammalian ABs and their associated neurons.

ACKNOWLEDGEMENTS

The authors thank M. Zhang for expert technical assistance with electrophysiology experiments. This project was supported by operating grants from the Heart and Stroke Foundation of Ontario (Grant No. NA 6788) and the Canadian Institutes of Health Research (Grant No. MOP-12037). N.A.P. was supported by a Vanier Canada Graduate Scholarship from the Natural Sciences and Engineering Research Council of Canada. The Leica confocal system was purchased with a grant from the Canadian Foundation for Innovation.

Table 1. Details of primary antisera used for immunofluorescence.

Antisera	Antigen	Manufacturer (Cat. No.)	Host	Clone	Dilution
Anti-TH	Purified tyrosine hydroxylase from rat adrenal	Millipore[1] (AB151[2])	rabbit	polyclonal	1:2,000
Anti-TH	Purified tyrosine hydroxylase from a rat pheochromocytoma	Millipore[1] (MAB5280)	mouse	monoclonal	1:2,000
Anti-VAChT	Synthetic peptide corresponding to amino acids 511–530 from the C-terminus of the cloned rat VAChT (CSPPGPFDGCEDDYNYYSRS)	Millipore[1] (AB1578)	goat	polyclonal	1:200
Anti-VAChT	Synthetic peptide corresponding to amino acids 520-530 from the C-terminus of the cloned rat VAChT (CEDDYNYYSRS)	Millipore[1] (AB1588)	guinea pig	polyclonal	1:500
Anti-NF70	Enzymatically dephosphorylated pig neurofilaments	Millipore[1] (MAB1615)	mouse	monoclonal	1:100
Anti-GAP-43	HPLC-purified GAP-43 from neonatal rat forebrain membranes	Sigma-Aldrich[3] (G9264)	mouse	monoclonal	1:10,000
Anti-PR	Electrophoretically pure trp-E-peripherin fusion protein (Gorham *et al*., 1990) containing all but the 4 N-terminal amino acids of rat peripherin	Millipore[1] (AB1530)	rabbit	polyclonal	1:20,000
Anti-P2X2	Synthetic peptide corresponding to amino acids 457-472 from the C-terminus of the rat P2X2 receptor (SQQDSTSTDPKGLAQL)	Alomone Labs[4] (APR-003)	rabbit	polyclonal	1:500
Anti-P2X3	Synthetic peptide corresponding to amino acids 383-397 from the C-terminus of the rat P2X3 receptor (VEKQSTDSGAYSIGH)	Millipore[1] (AB5896)	guinea pig	polyclonal	1:500
Anti-P2X3	Synthetic peptide corresponding to amino acids 383-397 from the C-terminus of the rat P2X3 receptor (VEKQSTDSGAYSIGH)	Alomone Labs[4] (APR-016)	Rabbit	polyclonal	1:200
Anti-nNOS	Synthetic peptide corresponding to amino acids 134-148 of human nNOS coupled to KLH	ImmunoStar[5] (24431)	rabbit	polyclonal	1:200
Anti-GFAP	Purified GFAP from porcine spinal cord	Millipore[1] (MAB360)	mouse	monoclonal	1:2,000

[1] Millipore, Temecula, CA, USA
[2] Antibody replaced with AB152 (Millipore)
[3] Sigma-Aldrich Canada Ltd., Oakville, ON, Canada
[4] Alomone Labs, Jerusalem, Israel
[5] ImmunoStar Inc., Hudson, WI, USA

Table 2. Details of secondary[1] antisera used for immunocytochemistry.

Fluorophore	Antigen	Host	Manufacturer[4]	Dilution
FITC[2]	Rabbit	goat	Jackson ImmunoResearch Laboratories	1:50
FITC[2]	mouse	goat	Jackson ImmunoResearch Laboratories	1:50
FITC[2]	guinea pig	goat	Jackson ImmunoResearch Laboratories	1:50
Texas Red	rabbit	goat	Jackson ImmunoResearch Laboratories	1:50
Texas Red	Mouse	goat	Jackson ImmunoResearch Laboratories	1:50
Texas Red	Goat	donkey	Jackson ImmunoResearch Laboratories	1:50
Cy5[3]	Rabbit	goat	Jackson ImmunoResearch Laboratories	1:500
Cy5[3]	Mouse	goat	Jackson ImmunoResearch Laboratories	1:500

[1] Secondary antisera were conjugated with a fluorescent marker
[2] Fluorescein isothionate
[3] Indodicarbocyanine
[4] Jackson ImmunoResearch Laboratories, Inc., Montreal, QC, Canada

Table 3. Summary of immunoreactivity in whole-mounts and/or cultures of the rat vagus nerve and recurrent laryngeal nerve.

Marker	Structure[1]				
	Type I cells	Neuronal cell bodies	Nerve terminals surrounding type I cells	Nerve terminals surrounding local neurons	Glia-like type II cells
TH	++	+	-	-	-
NF70/GAP-43	-	++	++	++	-
PR	-	++	++	++	-
VAChT	++	++	+	++	-
P2X2	-	+	+	-	-
P2X3	-	+	+	-	-
nNOS	-	+	+	+	-
GFAP	-	-	-	-	++

[1] (-) Indicates negative immunoreaction; (+) and (++) indicate the occurrence of a positive immunoreaction in a minority and majority, respectively, of the indicated cells or nerve terminals; estimates are relative to TH-IR and NF70/GAP-43-IR or PR-IR, which are assumed to label all type I cells and neuronal structures, respectively.

Figure 1. Distribution of aortic body (AB) paraganglia around the aortic arch. Schematic representation of the AB paraganglia and their relation to the major chemosensory organ, the carotid body (CB). The most commonly studied AB paraganglia include the subclavian ABs, located bilaterally at the origin of the common carotid and subclavian arteries, and the vagal paraganglia, which commonly occur at branch points with the superior laryngeal nerves (SLNs) and recurrent laryngeal nerve (RLNs). The present study focused on the AB paraganglion located at the bifurcation of the left vagus nerve and RLN. The right subclavian AB as well as the left vagus nerve and attached RLN (demarcated by solid black bars) were removed for immunofluorescence experiments.

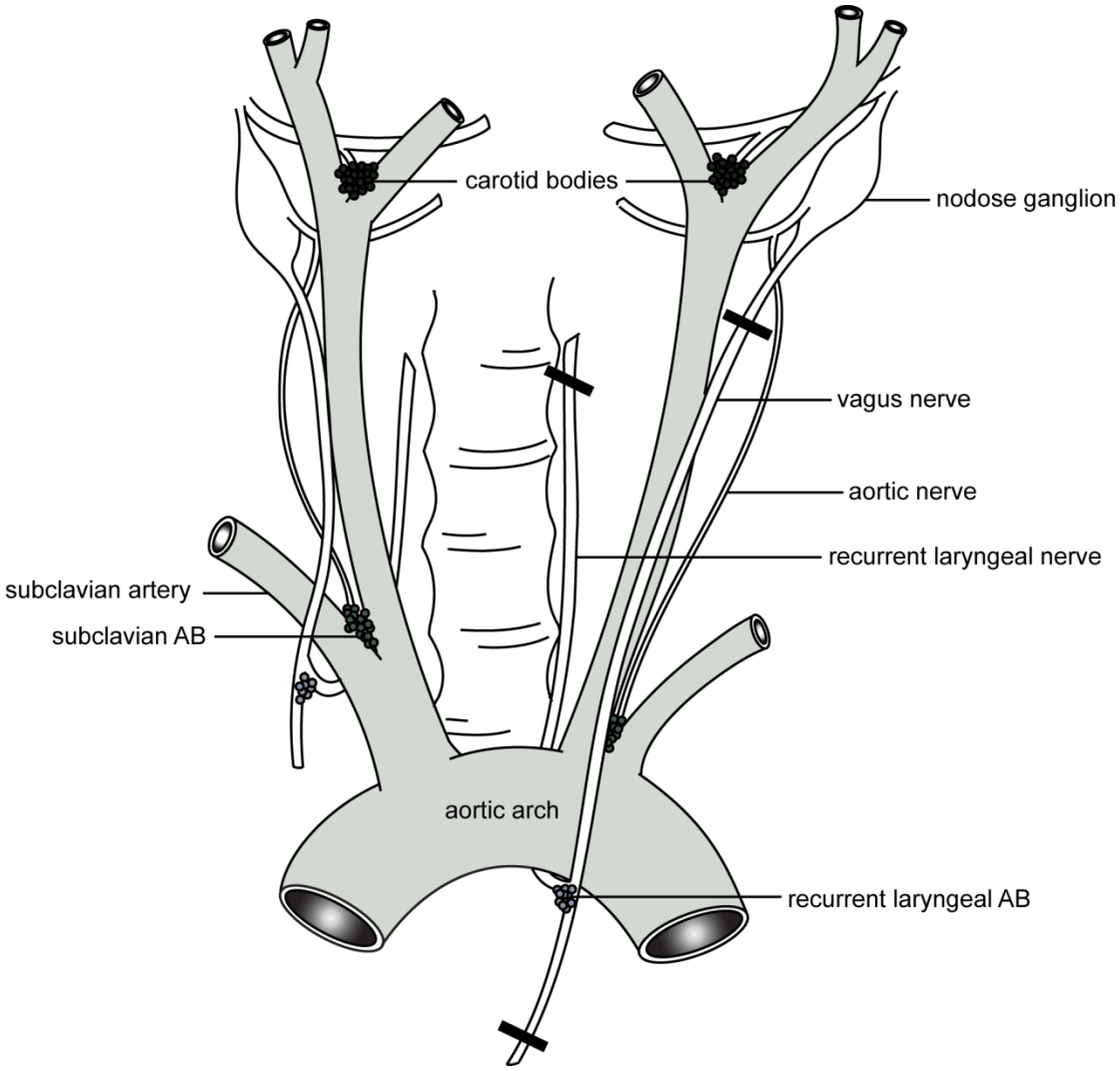
carotid bodies
nodose ganglion
vagus nerve
aortic nerve
recurrent laryngeal nerve
subclavian artery
subclavian AB
aortic arch
recurrent laryngeal AB

Figure 2. Immunolocalization of tyrosine hydroxylase (TH) and neuronal markers in juvenile rat aortic body (AB) paraganglia *in situ*.

A, Near the bifurcation of the vagus and recurrent laryngeal nerves, a large cluster of TH-immunoreactive (-IR) type I cells (green) comprising the AB of interest is adjacent to many peripherin (PR)-IR neuronal cell bodies and nerve fibers (red). This image is a composite of 10 2 μm confocal sections located near the upper (2, green channel) and lower (8, red channel) limits of a 40 μm thick confocal scan. **B**, A cluster of TH-IR type I cells of the subclavian AB (green) is shown embedded within the aortic nerve labelled with neurofilament/growth-associated protein-43 (NF70/GAP-43) (red). One optical section of the green channel (type I cells) is superimposed on a projection of 3 2 μm optical sections of the red channel (nerve fibres); the channels are separated by 4 μm in the z-axis. **C**, Innervation of TH-IR type I cells (green) in the RLN as revealed by NF70/GAP-43-IR (red); note upper isolated NF70/GAP-43-IR neuronal cell body. Images of the same type I cluster from an optical plane 7 μm away are shown in inset; note the intimate association between type I cells (green) and nerve endings (red). **D,** TH-IR type I cell cluster located along the vagus nerve but away from its bifurcation with the RLN. **E,** An example of the rare subpopulation of TH-IR neuronal cell bodies seen in a few whole-mounts (~10%) of the vagus and recurrent laryngeal nerves. In **F**, a cluster of NF70/GAP-43-IR neuronal cell bodies is situated in the RLN near the AB. Scale bars: 50 μm in **A**, **B**; 20 μm in **C-F**.

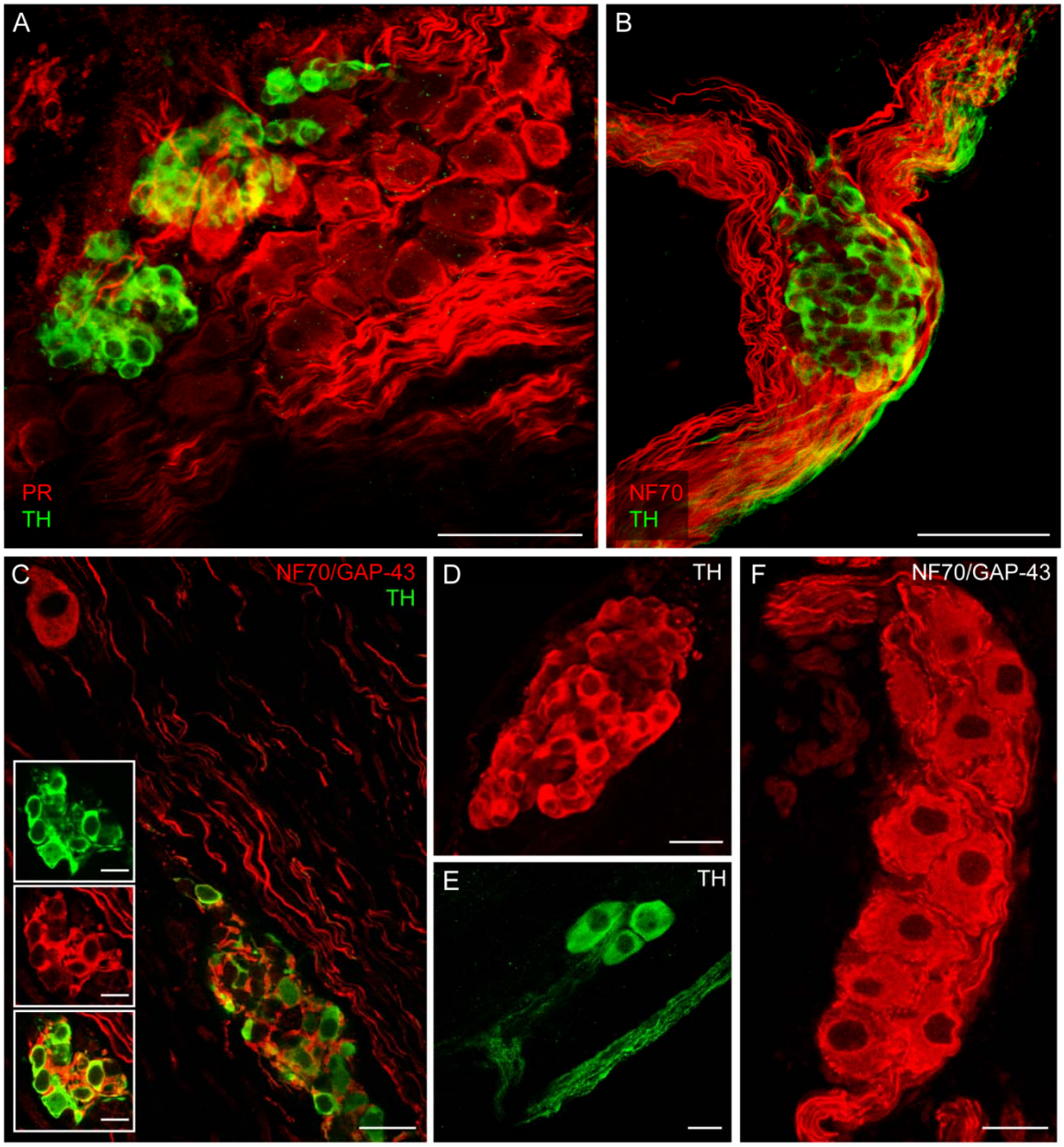
A
PR
TH
B
NF70
TH
C
NF70/GAP-43
TH
D
TH
E
TH
F
NF70/GAP-43

Figure 3. Localization of vesicular acetylcholine transporter (VAChT) immunoreactivity within the vagus and recurrent laryngeal nerves.

A-C, A TH-IR type I cell cluster (**A**; green) is also positively stained by the goat anti-VAChT antibody (**B**; red); overlay of TH- and VAChT-IR images is shown in **C**. The asterisks in **A-C** identify neuronal cell bodies that were negative for both TH and this VAChT antibody. **D**, Region of the vagus nerve near its bifurcation with the RLN incubated with the goat anti-VAChT antibody preadsorbed with the control peptide; note the absence of specific staining. **E-H**, Immunostaining of neuronal cell bodies and nerve terminals (**E**; green) adjacent to a type I cell cluster within the vagus nerve using a different VAChT antibody raised in guinea pig against a shorter C-terminal epitope; TH-IR type I cells (red) are faintly positive for this VAChT antibody (**F-H**). Images in **F-H** are from the same type I cell cluster as in **E** (arrow), but from an adjacent optical plane 1.95 μm away. The guinea pig anti-VAChT antiserum also positively labels neuronal cell bodies and nerve terminals at the bifurcation of the vagus and recurrent laryngeal nerve (**I-J**). Note in **I**, VAChT-IR neurons are contacted by dense, bright VAChT-IR nerve terminals; the area outlined by the hatched box is enlarged in **J**. Scale bars: 20 μm in **A-H**, **J**; 50 μm in **I**.

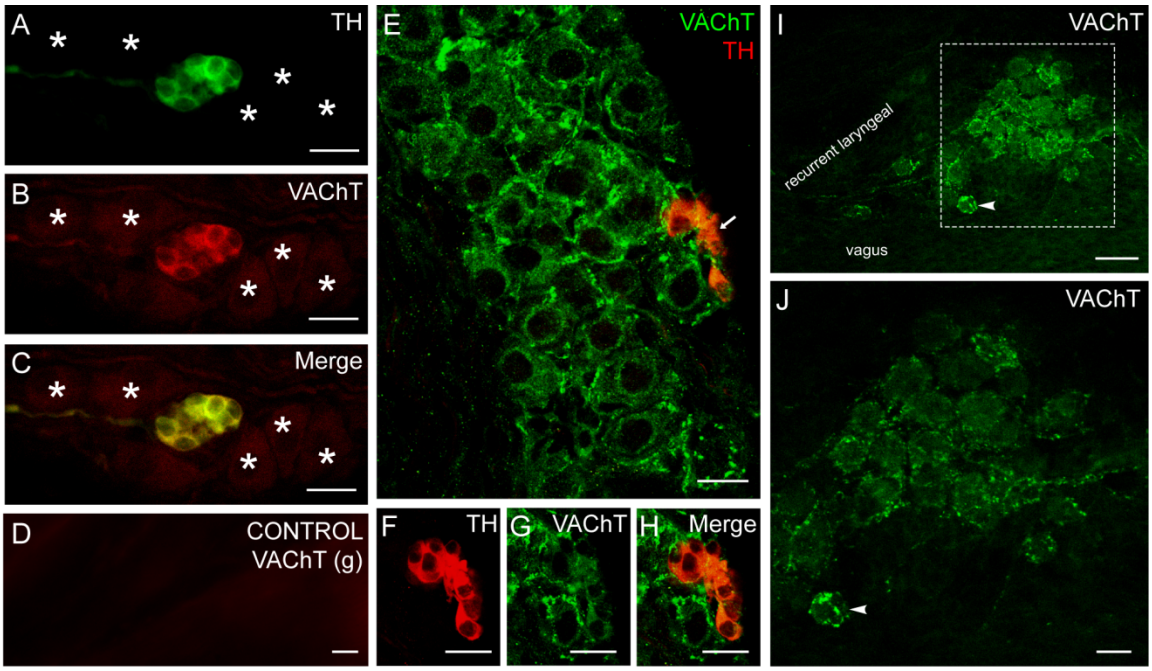
A
TH
B
VAChT
C
Merge
D
CONTROL
VAChT (g)
E
VAChT
TH
F
TH
G
VAChT
H
Merge
I
VAChT
recurrent laryngeal
vagus
J
VAChT

Figure 4. Expression of P2X2 and P2X3 purinoreceptor subunits in local neurons and in nerve endings apposed to aortic body (AB) type I cells.

A cluster of TH-IR AB type I cells (**A**, **C-E**; red) is adjacent to a group of local neurons in the AB; some neurons (and nerve endings) show positive P2X2-immunoreactivity (**B**, **C-E**; blue), whereas others do not (e.g. **C**, asterisks). Images in **A**-**C** are from same optical section, whereas **D** and **E** are from different optical sections within the same AB 2.9 μm and 10.15 μm away, respectively. In **F**, two small type I cell clusters (green) are in close proximity to a few P2X3-IR neuronal cell bodies (asterisks denote neuronal cell bodies that lack or show weak P2X3-IR). In **F**, **G** (arrowheads), TH-IR type I cells are intimately associated with P2X3-IR nerve terminals. Other P2X3-IR (**H**) and P2X2-IR (not shown) neuronal cell bodies are present along the vagus and recurrent laryngeal nerves. **I-L,** One optical section of the AB region, in which TH-IR type I cells (**I**; blue) are surrounded by dense P2X2-IR (**J**; red) and P2X3-IR (**K**; green) nerve terminals; note co-localization of P2X2 and P2X3 in the merged image (**L**). **M-O**, Controls for antibody specificity in the AB region demonstrate that preadsorption of the P2X3 guinea pig (gp, **M**), P2X3 rabbit (r, **N**), and P2X2 rabbit (**O**) antibodies with their respective control peptides abolishes specific cell body and nerve terminal staining. Scale bar: 20 μm in **A-H**, **M-O**; 10 μm in **I-L**.

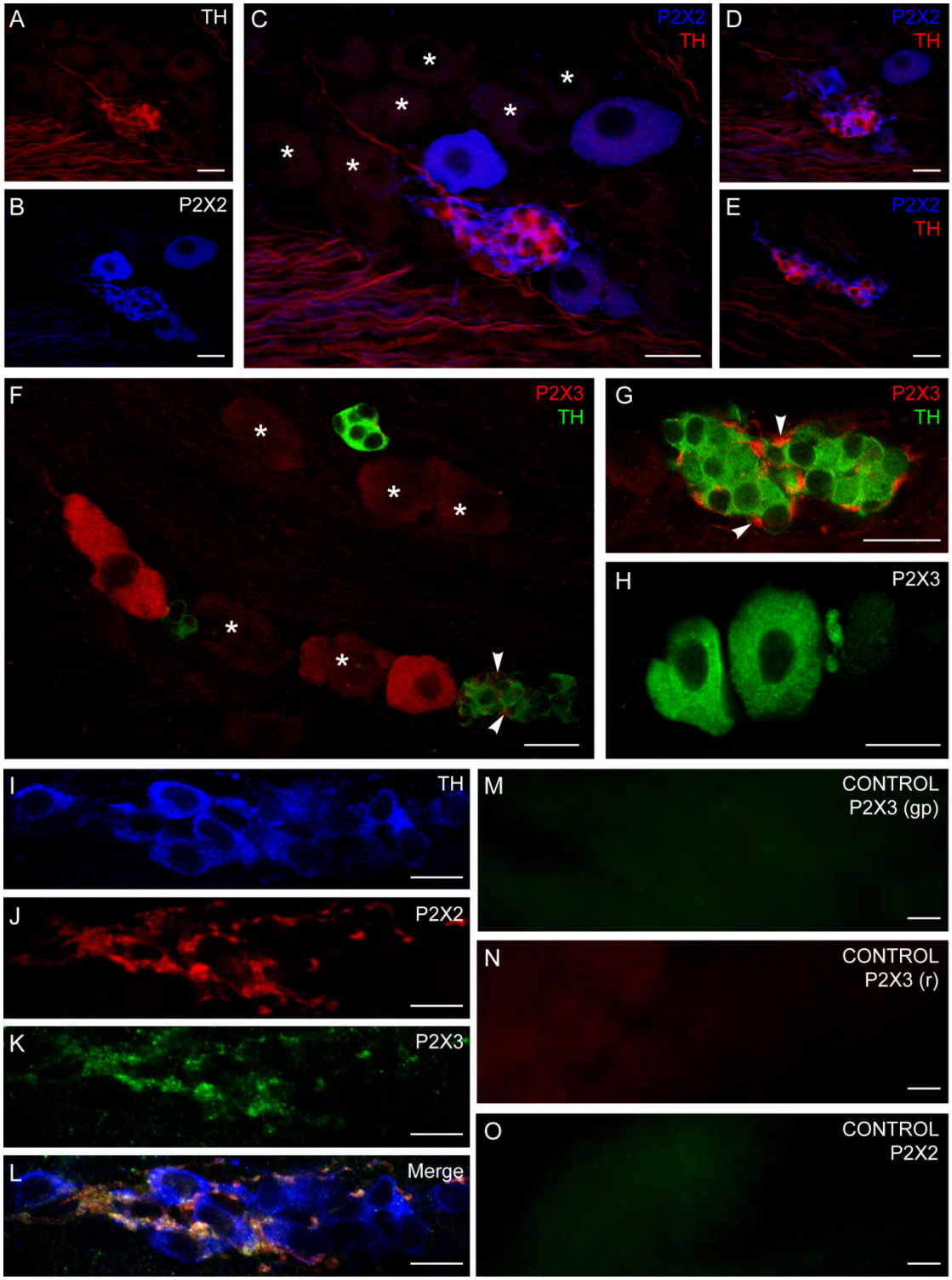
A
TH
B
P2X2
C
P2X2
TH
D
P2X2
TH
E
P2X2
TH
F
P2X3
TH
G
P2X3
TH
H
P2X3
I
TH
J
P2X2
K
P2X3
L
Merge
M
CONTROL
P2X3 (gp)
N
CONTROL
P2X3 (r)
O
CONTROL
P2X2

Figure 5. Purinergic receptors are present in rat aortic body (AB) structures throughout development.

Shown in **A** is one optical section of a cryosection of the left vagus nerve-RLN from a 35-40 day old rat, in which TH-IR type I cells (red) are contacted and interdigitated by brightly P2X2-IR nerve endings (green, e.g. arrowheads). This pattern of staining was also observed in 95-100 day old rats (not shown). In a cryosection where the P2X2 antibody was preadsorbed with the control peptide (**C**), no specific P2X2 immunoreactivity was detected whereas TH immunostaining was unchanged (**B**). In contrast, cryosections double labelled with TH and P2X3 antisera show co-localization of these markers within AB type I cells (e.g. **F**-**H**). P2X3 immunoreactivity (**G**) appears faint within the type I cell cytoplasm (i.e. co-localized with TH) though it is brightest in puncta surrounding type I cells (e.g. arrowheads), suggesting a membranous localization. Furthermore, P2X3-IR neurons are observed in cryosections of the adult AB (**E**). Specific P2X3 immunoreactivity is completely abolished by preadsorption with the control peptide (not shown). P2X3-IR terminals were not obvious in adult cryosections. Note also in image **D** that in some cases, AB local neurons were labelled by TH (arrow). Scale bars: 20 μm.

\\

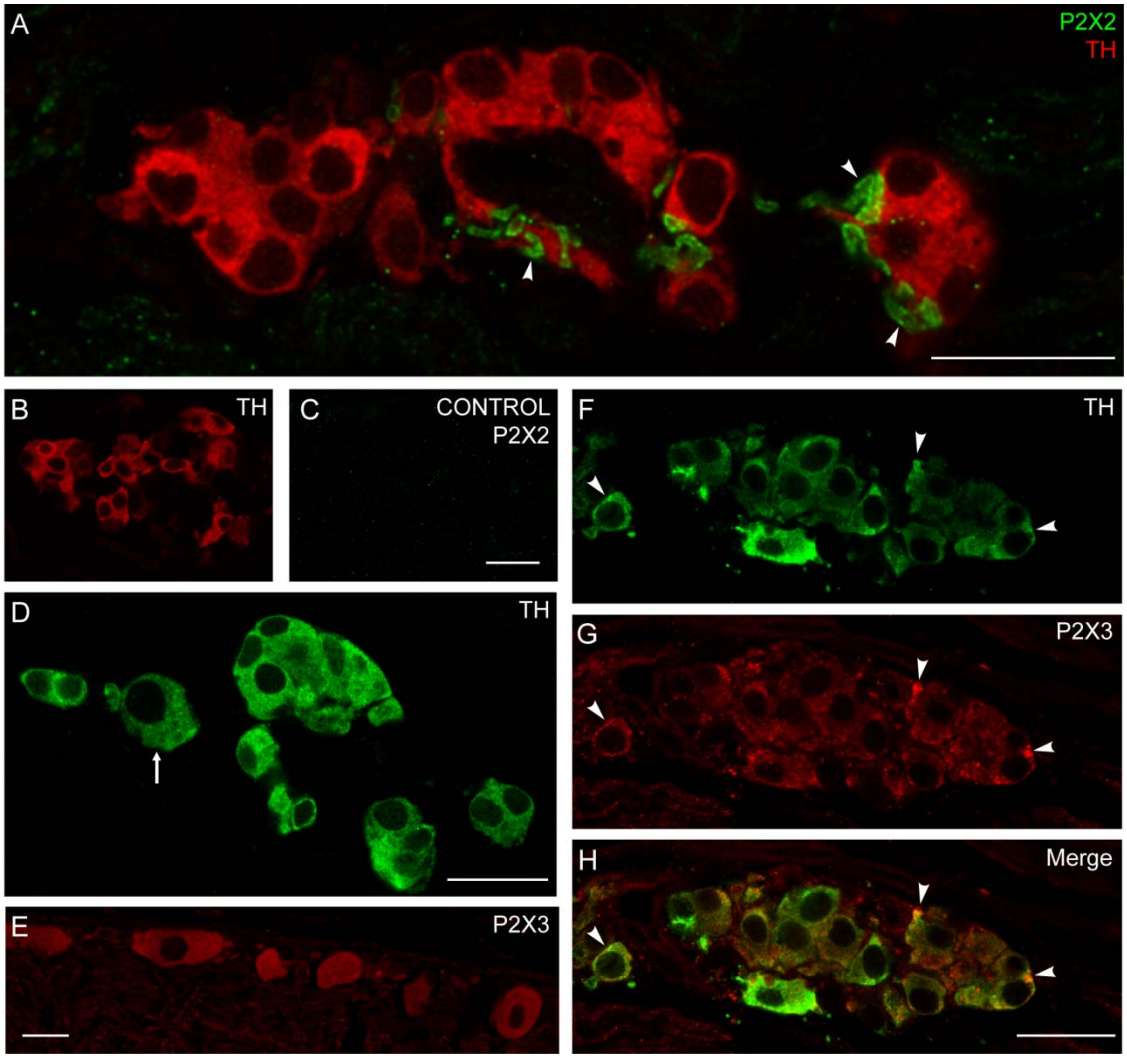
A
P2X2
TH
B
TH
C
CONTROL
P2X2
F
TH
D
TH
G
P2X3
H
Merge
E
P2X3

Figure 6. Expression of neuronal nitric oxide (NO) synthase (nNOS) in local neurons associated with the aortic body (AB).

A, Composite image of an AB paraganglion showing the red channel (nNOS) and green channel (TH) of confocal sections separated by 9.24 μm (i.e. four 2.31 μm sections). Only one neuron is nNOS-IR, representing a minority of the local neuronal population (nNOS-negative neurons are denoted by asterisks). In **C** and **D**, a similar arrangement of TH-IR type I cells in close association with nNOS-IR neurons is seen in one optical section (**C**) or in a projection of sixteen 2.1 μm serial sections of the laryngeal AB (**D**). In both cases, one nNOS-positive neuronal cell body extends an nNOS-positive process (arrows), which in **D**, appears to contact adjacent type I cells. **D, *inset***, Cropped image from a single optical section of the z-projection in **D** showing the nucleus of the neuronal cell body identified by the arrow. In **B**, a projection image of 3 serial 2.5 μm confocal sections shows 5 neuronal cell bodies located within the vagus nerve, only 2 of which are nNOS-IR (nNOS-negative neurons are labelled by asterisks); note that the middle nNOS-IR neuron extends nNOS-positive processes (arrows). Scale bars: 20 μm.

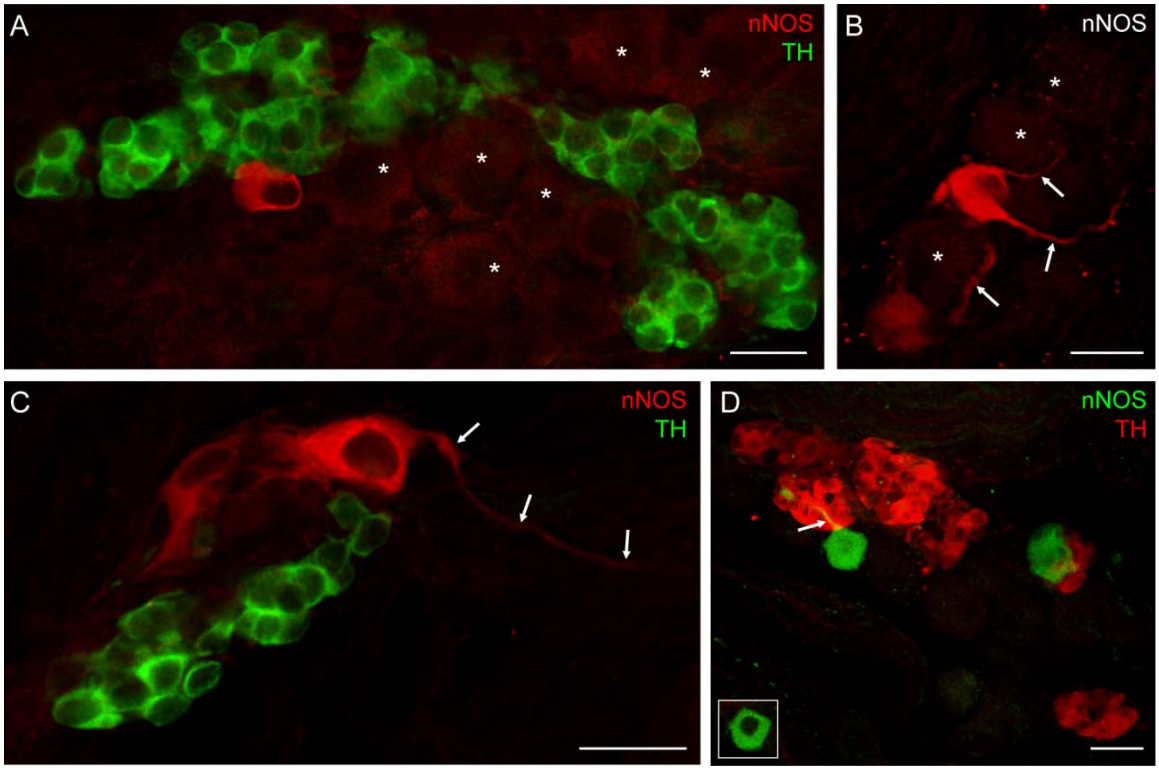
A
nNOS
TH
B
nNOS
C
nNOS
TH
D
nNOS
TH

Figure 7. Type I cells and local neurons survive in short term cultures of dissociated rat aortic bodies (ABs).

Phase contrast micrographs show live type I cell clusters (**A**, **C**, **D**, arrowheads) and local neurons (**B**, **C**, **D**, asterisks) from different AB cultures. Type I cells are typically arranged in clusters (**A**, **C**, **D**), similar to their organization *in situ*, although singles and doubles are also present but are more difficult to identify under phase contrast microscopy. Neuronal cell bodies may occur in isolation (**B**, **C**), but more commonly aggregate, sometimes adjacent to type I cell clusters (**D**). Scale bars: 20 μm in **A**, **B**; 25 μm in **C**, **D**.

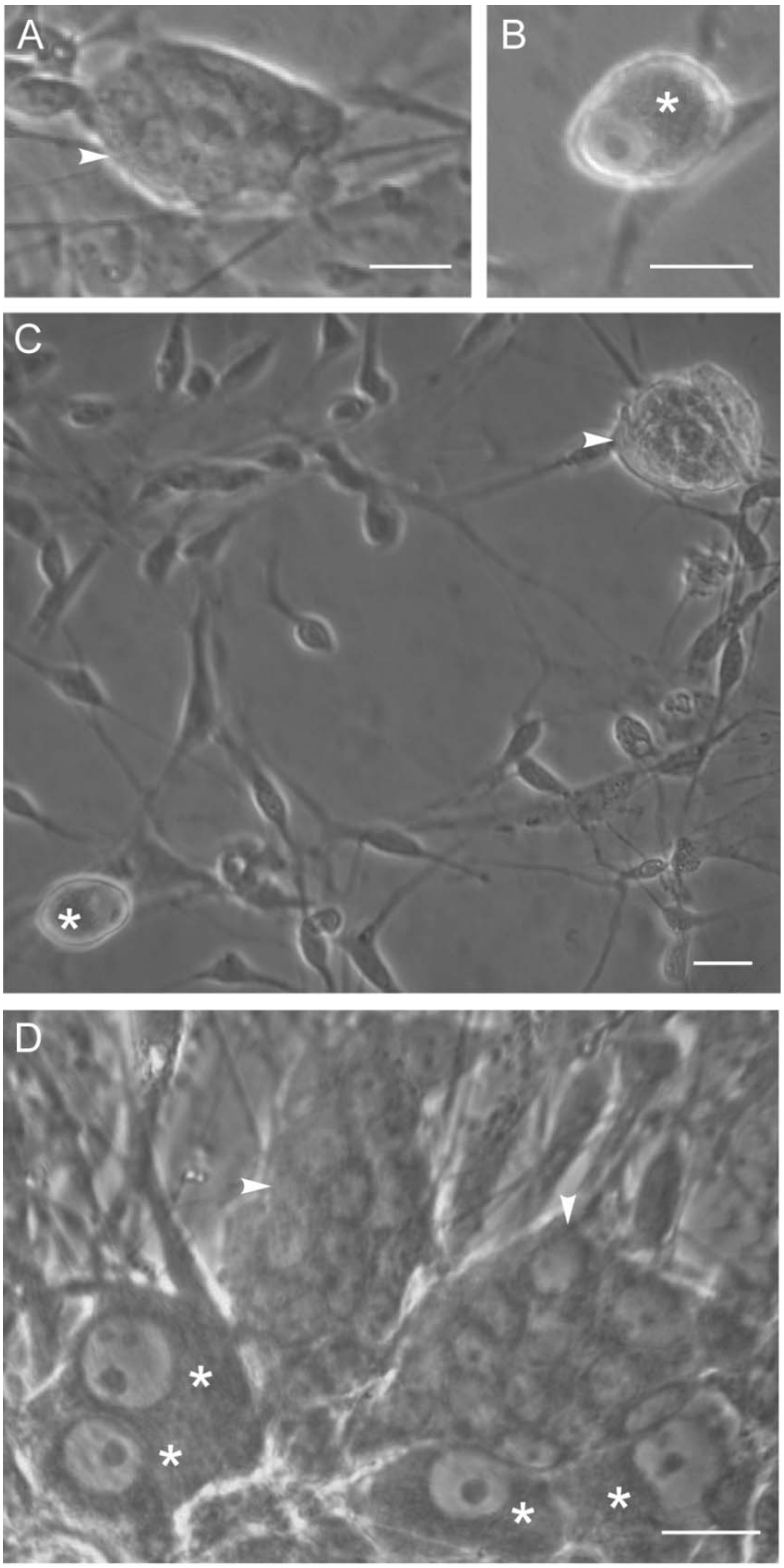
A
B
C
D

Figure 8. Interactions between local neurons and type I cells in dissociated AB cultures as revealed by immunofluorescence staining.

Like their counterparts *in situ*, cultured type I cells stain positively for TH (**A**, **C**, **D**, **F**; green) whereas neuronal cell bodies and their processes stain positively for PR (**B**) or NF70/GAP-43 (**C**, **E, F**; red). **C,** A NF70/GAP-43-IR neuronal cell body (red) extends a process towards a cluster of TH-IR type I cells (green) in culture. Note that the neuronal process appears to emit terminal branches that contact the type I cells. **D-F,** Confocal images from one optical section of a type I cell cluster after 72 hrs in culture; note in the merged image (**F**) that NF70/GAP-43-IR neuronal processes (red) are in intimate contact with TH-IR cells (green). Scale bars: 10 μm **A**, **B**; 20 μm **C-F**.

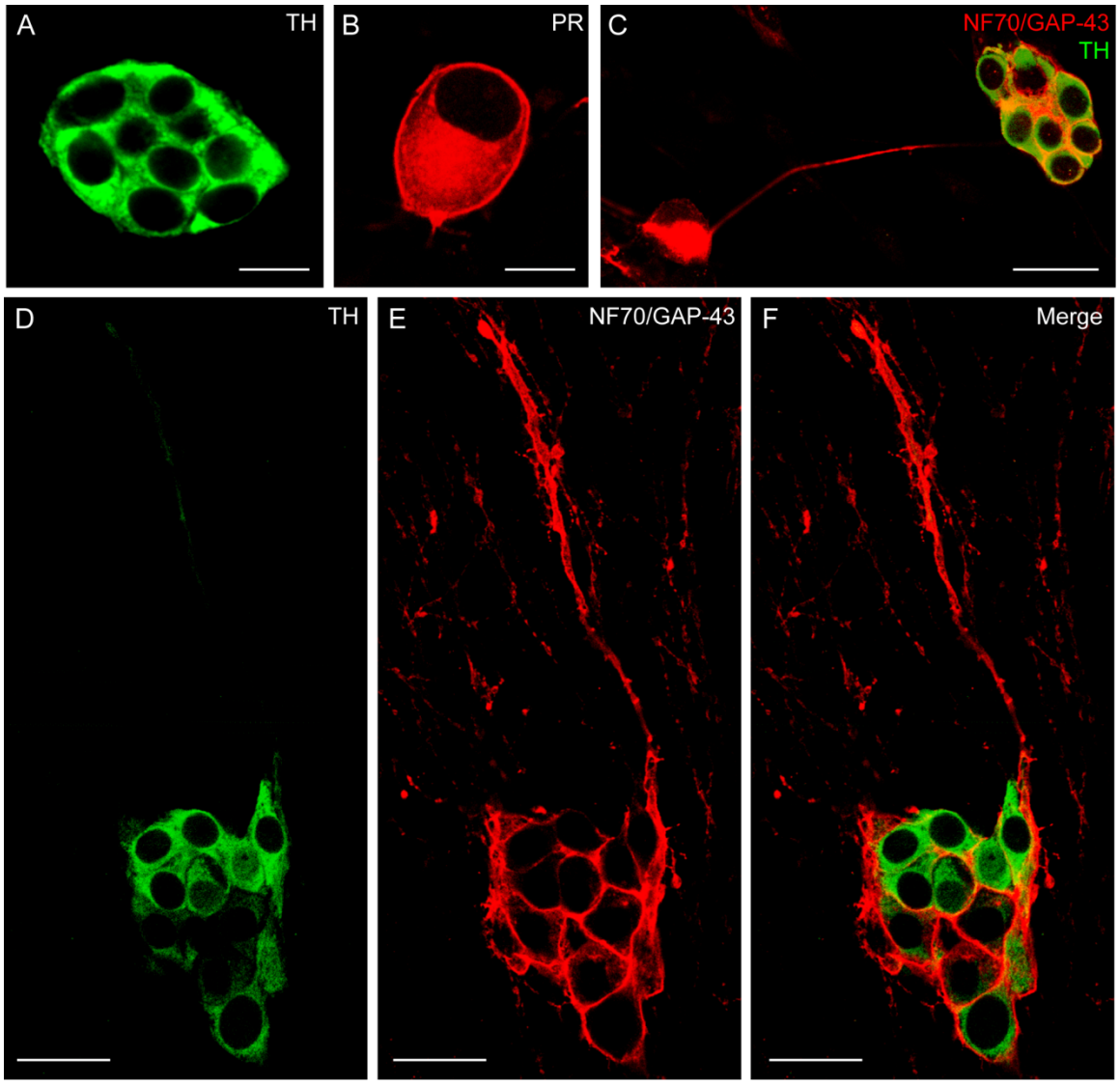
A
TH
B
PR
C
NF70/GAP-43
TH
D
TH
E
NF70/GAP-43
F
Merge

Figure 9. Association of glia-like type II cells with type I cell clusters in dissociated aortic body (AB) cultures.

A-B, Double-label immunofluorescence reveals TH-IR type I cells (red) enveloped by many glia-like type II cells (green), identified by glial fibrillary acidic protein (GFAP)-IR. The GFAP-IR cell bodies are found at the periphery of, and sometimes within, type I cell clusters and extend processes throughout the culture (**A-E**). Images **A** and **B** are from optical sections of the same type I cell cluster separated by seven 2.05 μm sections (i.e. 14.34 μm); note in **A** the presence of a TH-negative, GFAP-negative neuron that is surrounded by GFAP-IR type II cells (arrowhead). **C,** GFAP-IR type II cell bodies are present within a TH-IR type I cell cluster. In the unmerged image (**C**, ***inset***), note the absence of TH-immunoreactivity where the type II cells are present. Images **D** and **E** are from AB cultures showing PR-IR neurons (red) extending elaborate processes that intermingle with GFAP-IR type II cells and their processes. In **D**, note the oval-shaped nuclei of two such type II cells (arrowheads). Scale bars: 20 μm.

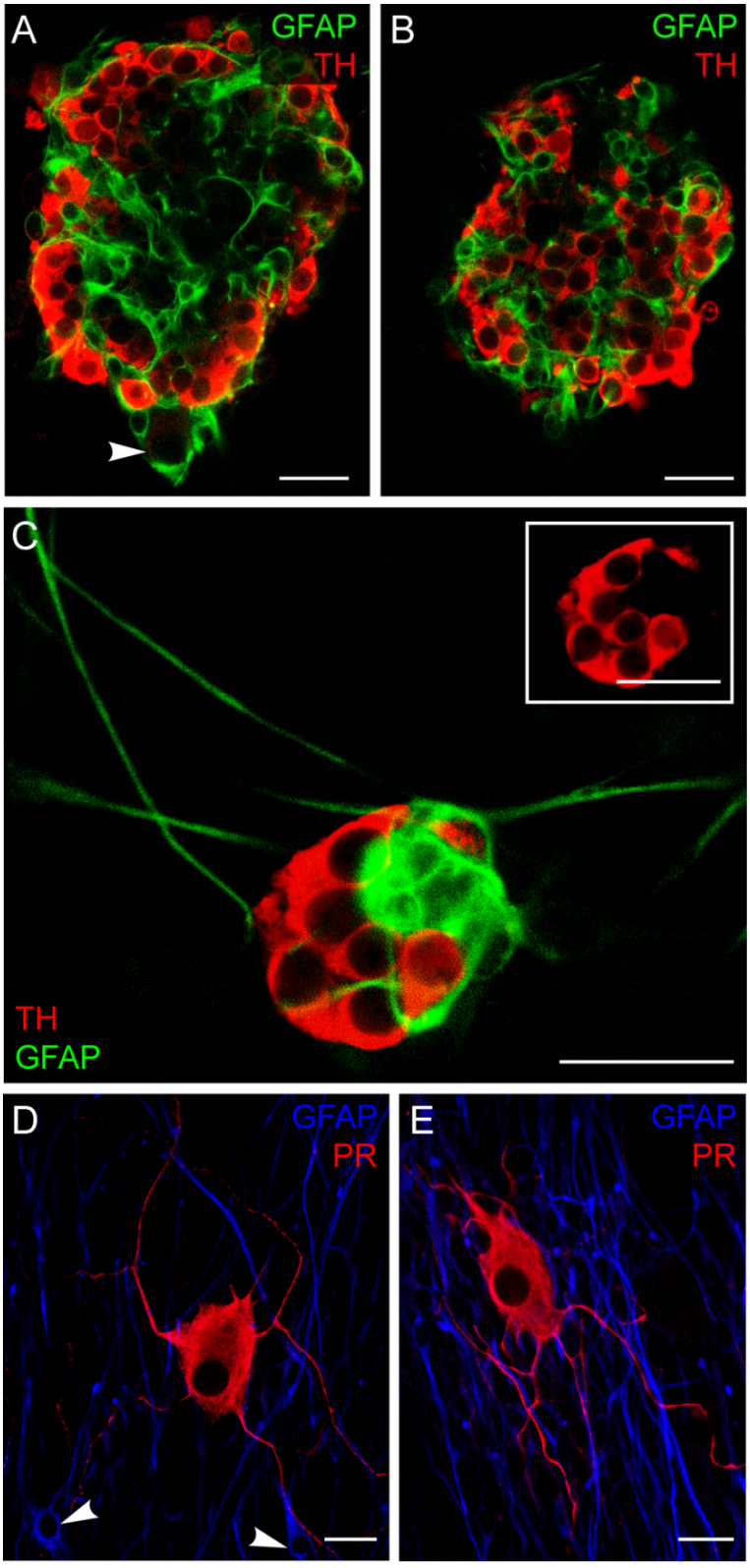
A
GFAP
TH
B
GFAP
TH
C
TH
GFAP
D
GFAP
PR
E
GFAP
PR

Figure 10. Whole-cell currents and membrane excitability of local intra-vagal neurons in short term aortic body (AB) cultures.

A, Exemplar traces reveal that in response to depolarizing voltage steps from a holding potential of -60 mV, neurons elicit large, fast inward currents and sustained outward currents; the I-V relationship for the sustained outward K^+ current is shown in **B**. These neurons generate repetitive overshooting action potentials during injection of sustained depolarizing currents as exemplified in **C**; action potential waveform from the indicated segment of the recording is shown in the expanded trace (top). These data are from AB neurons cultured in the absence of growth factors.

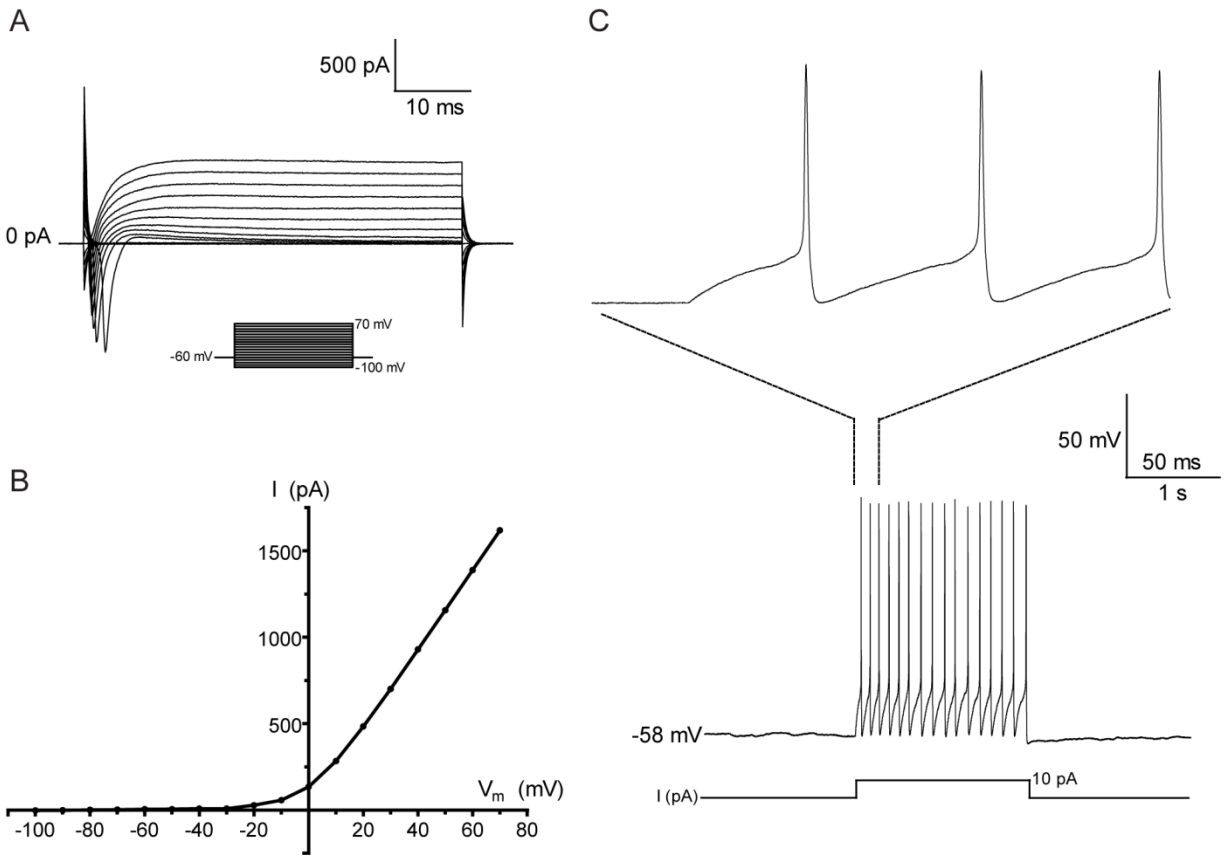
A
500 pA
10 ms
0 pA
70 mV
-60 mV
-100 mV
B
I (pA)
1500
1000
500
V_m (mV)
-100 -80 -60 -40 -20 20 40 60 80
C
50 mV
50 ms
1 s
-58 mV
I (pA)
10 pA

CHAPTER 3

Effects of chemostimuli on $[Ca^{2+}]_i$ responses of rat aortic body type I cells and endogenous local neurons: Comparison with carotid body cells

The work in this chapter has been published as:

Piskuric, N.A. and Nurse, C.A. (2012). *The Journal of Physiology*, 590(9): 2121-2135.

I performed all experiments, data analysis, and preparation of the manuscript.

ABSTRACT

Mammalian aortic bodies (ABs) are putative peripheral arterial chemoreceptors whose function remains controversial, partly because information on their cellular physiology is lacking. In this study, we used ratiometric Ca^{2+} imaging to investigate for the first time chemosensitivity in short-term cultures of dissociated cells of juvenile rat ABs, located near the junction of the left vagus and recurrent laryngeal nerves. Among the surviving cell population were glomus or type I cell clusters, endogenous local neurons, and glia-like cells. A variety of chemostimuli, including hypoxia, isohydric or acidic hypercapnia, and isocapnic acidosis, caused a rise in intracellular $[Ca^{2+}]$ in AB type I cells. The $\Delta[Ca^{2+}]_i$ responses were indistinguishable from those in carotid body (CB) type I cells grown in parallel cultures from the same animals, and responses to acidic hypercapnia were prevented by the non-specific voltage-gated Ca^{2+} channel antagonist, 2 mM Ni^{2+}. Furthermore, we identified a subpopulation (~40%) of glia-like cells in AB cultures that resembled CB type II cells based on their approximately equal sensitivity to ATP and UTP, consistent with the expression of purinergic P2Y2 receptors. Finally, we showed that some local neurons, known to be uniquely associated with these AB paraganglia *in situ*, generated robust $\Delta[Ca^{2+}]_i$ responses to these chemostimuli. Thus, these AB type I cells and associated putative type II cells resemble those from the well-studied CB. Unlike the CB, however, they also associate with a special group of endogenous neurons which we propose may subserve a sensory function in local cardiovascular reflexes.

INTRODUCTION

Peripheral arterial chemoreceptors sense the chemical composition of arterial blood, i.e. PO_2 and PCO_2/H^+, and initiate compensatory reflex responses so as to maintain homeostasis. In mammals, the primary peripheral arterial chemoreceptors are the carotid bodies (CBs), which are located at the bifurcation of the common carotid arteries and mediate their effects via the control of ventilation. Thus, a fall in arterial PO_2 (i.e. hypoxia) is sensed by the CBs, leading to hyperventilation and a restoration of blood PO_2 (Gonzalez *et al.*, 1994). A second group of putative peripheral arterial chemoreceptors, i.e. the aortic bodies (ABs), is distributed diffusely as small paraganglia along the vagus nerve and its branches near the aortic arch (McDonald & Blewett, 1981). These AB chemoreceptors have been the subject of controversy for decades, due to uncertainties about their exact location, adequate stimuli, and indeed, whether or not they are present in all mammalian species (Sapru *et al.*, 1981; Brophy *et al.*, 1999). Nevertheless, there is compelling ultrastructural and immunocytochemical evidence that the vagal AB paraganglia show striking similarities to CB chemoreceptors. For example, the fine structure of parenchymal chemoreceptor glomus or type I cells and their innervation are indistinguishable from those of the CB (McDonald & Blewett, 1981), and in both cases the type I cells express multiple neurotransmitters, including catecholamines, acetylcholine (ACh), serotonin (5-HT) and ATP (Dvorakova & Kummer, 2005; Piskuric *et al.*, 2011).

Despite a consensus about their morphological and biochemical properties, the physiological function of ABs remains controversial. In a classical study, Comroe showed that the respiratory and cardiovascular responses induced by hypoxia and cyanide in cats and dogs were partly due to a second, extra-carotid chemoreceptor located near the aortic arch (Comroe, 1939). Decades later, Lahiri and co-workers carried out an extensive series of physiological studies on ABs in anesthetized, paralyzed and artificially ventilated cats (Lahiri *et al.*, 1979; Lahiri *et al.*, 1981a; Pokorski & Lahiri, 1983). During extracellular recordings from single or few fibers of the aortic nerve, they

found that AB chemoafferents were activated by hypoxia, hypercapnia, metabolic and respiratory acidosis, though their responses (especially to hypercapnia) were significantly lower than those of CB chemoafferents. In the rat, hypoxia and/or cyanide were found to stimulate chemoafferent activity in the aortic and superior laryngeal nerves (Brophy *et al.*, 1999; Jones, 2000; O'Leary *et al.*, 2004); however, the physiological significance of these findings in terms of respiratory or cardiovascular reflexes has been questioned (Kobayashi *et al.*, 1999). One comparative view regarding AB function is that whereas the CB senses oxygen partial pressure (PO_2) and is primarily involved in ventilatory control so as to ensure adequate O_2 supply to the gas exchange surfaces, the AB senses changes in blood O_2 content and its main function is in cardiovascular regulation, ensuring adequate O_2 transport capacity and blood volume (Hatcher *et al.*, 1978; Lahiri *et al.*, 1980a; Lahiri *et al.*, 1981b; Milsom & Burleson, 2007). While this posit is attractive in that it assigns separate and distinct functions to the CB and AB, it fails to provide a satisfactory explanation for how the sensing mechanisms may differ, if at all. In the case of the AB, a major contributing factor is that, to our knowledge, there have been no studies to date that directly address the cellular physiology and putative chemoreceptive properties of mammalian AB type I cells, in marked contrast to the numerous comparable studies on CB type I cells (reviewed in Gonzalez *et al.*, 1994; Nurse, 2010).

In the present study, we address this void for the first time by focusing on a particular group of rat AB chemoreceptors located at the junction of the left vagus nerve and recurrent laryngeal nerve (RLN). The ABs can be routinely identified within this region where they occur in association with a group of local neurons (Dvorakova & Kummer, 2005; Piskuric *et al.*, 2011). Importantly, we previously found that some of these local neurons express purinergic P2X2 and P2X3 receptor subunits, and that dissociation of the tissue yields an *in vitro* preparation where isolated type I clusters, local neurons, and glia-like cells survive for a few days (Piskuric *et al.*, 2011). As a first step towards understanding the cellular mechanisms of AB chemoreception, we used this *in vitro* preparation to investigate the effects of various chemostimulants on isolated AB cells. Because the small size of these ABs resulted in a paucity of type I cell clusters

compared to the well-studied CBs, we used ratiometric fura-2 intracellular Ca^{2+} imaging in order to optimize sampling frequency. As a positive control, as well as to facilitate a direct comparison of chemosensitivity between AB and CB cells at a similar developmental stage, we monitored Ca^{2+} responses in parallel dissociated CB preparations taken from the same animals. We found that AB type I cells were sensitive to hypoxia, isohydric and acidic hypercapnia, and isocapnic acidosis, similar to CB type I cells. Moreover, some local AB neurons were also sensitive to these stimuli, suggesting that they may subserve a sensory function.

MATERIALS AND METHODS

Ethical Approval

All procedures for animal handling and tissue dissections were carried out according to the guidelines of the Canadian Council on Animal Care (CCAC) and institutional guidelines.

Cell cultures

Juvenile rat pups, 9–14 days old (Wistar, Charles River, QC, Canada), were rendered unconscious by a blow to the back of the head and then killed immediately by decapitation. The vagus nerve was cut peripheral to the nodose ganglion and caudal to the bifurcation of the left recurrent laryngeal nerve (RLN); this portion along with the attached RLN was excised. Carotid bodies (CBs) from the same animals were also removed bilaterally and kept separate. The data presented in this study are derived from 20 rat litters, with each litter comprising ~12 pups. All aortic body (AB) tissue harvested was used for the experiments described here; CB tissue was shared between this and other studies being performed concurrently in our laboratory. Tissues were incubated for 1 hr at 37°C in an enzymatic solution containing 0.1% trypsin (Gibco, Grand Island, NY,

USA) and 0.1% collagenase (Gibco, Grand Island, NY, USA or Sigma Aldrich, Oakville, ON, Canada), prior to mechanical dissociation and trituration. The resulting cell suspension, containing either AB or CB cells, was plated onto a thin layer of Matrigel (Collaborative Research, Bedford, MA, USA) that was previously applied to the central wells of modified 35 mm tissue culture dishes (Zhong *et al.*, 1997). Cultures were grown in F-12 nutrient medium supplemented with 5% fetal bovine serum, 1% penicillin/streptomycin, 1% glutamine, 0.3% glucose, and 3 μg/mL insulin, at 37°C in a humidified atmosphere of 95% air/5% CO_2 (Zhong *et al.*, 1997). In a few cases, cells were cultured in the presence of a prophylactic dose of plasmocin (5 μg/mL); data derived from such cells were similar to those obtained from cells cultured without plasmocin. AB and CB cells were used in Ca^{2+} imaging experiments after ~24 hr in culture.

Intracellular Ca^{2+} measurement

Intracellular free Ca^{2+} concentration ($[Ca^{2+}]_i$) was monitored using the fluorescent Ca^{2+} indicator, fura-2/AM (Molecular Probes, Eugene, OR, USA). Cells were loaded with 2.5 μM fura-2/AM diluted in standard bicarbonate buffered solution (BBS) for 30 min at 37ºC, and subsequently washed for ~15 min to remove free dye. Ratiometric Ca^{2+} imaging was performed using a Nikon Eclipse TE2000-U inverted microscope (Nikon, Mississauga, ON, Canada) equipped with a Lambda DG-4 ultra high-speed wavelength changer (Sutter Instrument Co., Novato, CA, USA), a Hamamatsu OCRCA-ET digital CCD camera (Hamamatsu, Sewickley, PA, USA) and a Nikon S-Fluor 40x oil-immersion objective lens with a numerical aperture of 1.3. Dual images at 340 nm and 380 nm excitation (510 nm emission) were acquired every 2 s, with an exposure time of 100-200 ms. Pseudocolour ratiometric data were obtained using Simple PCI software version 5.3. All experiments were performed at 21-23ºC, and cells were continuously perfused with BBS to maintain an extracellular pH of ~7.4.

The imaging system was calibrated using the Fura-2 Calcium Imaging Calibration Kit from Molecular Probes (Cat. No. F-6774). Photometric data at 340 nm and 380 nm

excitation (510 nm emission) were obtained for 11 buffers of known Ca^{2+} concentration (from zero free Ca^{2+} to saturating Ca^{2+}, i.e. 39 μM). After correcting for background fluorescence, these values were used to calculate the following ratios (where 'R' is the 510 nm emission intensity with excitation at 340 nm, to 510 nm emission intensity with excitation at 380 nm); R_{min}, the ratio at zero free Ca^{2+}; R_{max}, the ratio at saturating Ca^{2+}; and β, the fluorescence intensity with excitation at 380 nm for zero free Ca^{2+} ($F380_{max}$), to the fluorescence intensity at saturating free Ca^{2+} ($F380_{min}$). Substituting these ratios into the Grynkiewicz equation,

$$[Ca^{2+}]_i = K_d * \frac{[R - R_{min}]}{[R_{max} - R]} * \beta$$

where R_{min} = 0.18, R_{max}= 7.81, β = 12.29, K_d = 225 nM, and R is the ratio obtained during an experiment, gave the intracellular free $[Ca^{2+}]$ for a given cell (Grynkiewicz *et al.*, 1985).

Solutions and drugs

Cells were perfused with standard BBS containing (in mM): 24 $NaHCO_3$, 115 NaCl, 5 glucose, 5 KCl, 2 $CaCl_2$ and 1 $MgCl_2$, and the pH was maintained at ~7.4 by bubbling with 5% CO_2/95% air mixture. Hypoxic solution was made by aerating BBS with 5% CO_2/95% N_2. PO_2 was measured using a Micro Dissolved Oxygen Electrode (Model DO-166 MT-1; Lazar Research Laboratories, Inc., Los Angeles, CA, USA). The electrode was calibrated in room air and used to measure the PO_2 (~25 mmHg) in the bathing solution. Isohydric hypercapnia was generated by doubling the concentration of $NaHCO_3$ to 48 mM (maintaining osmolarity by reducing NaCl to 91 mM) and aerating with 10% CO_2/90% air (pH ~7.4). Isocapnic acidosis contained 8.6 mM $NaHCO_3$ (130.4 mM NaCl) and was aerated with 5% CO_2/95% air mixture (pH ~6.9). Finally, acidic hypercapnia was generated by bubbling standard BBS with 10% CO_2/90% air (pH ~7.1). High extracellular K^+ solution (30 mM KCl) was made by equimolar substitution of NaCl

for KCl. Nickel(II) chloride hexahydrate was purchased from Sigma Aldrich (Cat. No. N6136; Oakville, ON, Canada).

Statistical analysis

Cells with a basal $[Ca^{2+}]_i$ greater than 200 nM, or cells whose baseline exhibited continuous ramping throughout the experiment, were excluded from analyses. Furthermore, only those cells that responded to 30 mM KCl with a rise in $[Ca^{2+}]_i$ greater than 100 nM (peak minus baseline) were included in statistical analyses (excluding glia-like cells). Data are reported as mean ± standard error of the mean (S.E.M.), where the mean is the average $[Ca^{2+}]_i$ during application of the stimulus (usually 2 min) minus the averaged baseline immediately preceding the stimulus (30 s). Cells were classified as 'responsive' if their mean $\Delta[Ca^{2+}]_i$ was >20 nM. Differences between data sets were analyzed using the repeated measures Friedman Test with Dunn's multiple comparison post hoc tests (for nonparametric data). The significance level was set at 0.05. Statistical analyses were performed in GraphPad Prism 5.

Immunocytochemistry and confocal imaging

Whole-mounts

Procedures for processing whole mounts of the left vagus nerve and RLN for tyrosine hydroxylase (TH)-immunoreactivity were similar to those described in detail elsewhere (Piskuric *et al.*, 2011) .

Cell cultures

AB and CB cultures were stained after 24 hr *in vitro*. Cells were washed with warmed PBS and fixed in 5% acetic acid/95% methanol for 1 hr at -20°C. After washing with PBS (3 x 10 min), cells were incubated in primary antibody diluted in 1% BSA/PBS for 24 hr at 4°C. Primary antibodies were rabbit anti-tyrosine hydroxylase (TH)

polyclonal antibody at 1:2000 (Millipore, Cat. # AB152, Temecula, CA, USA) and mouse anti-glial fibrillary acidic protein (GFAP) monoclonal antibody at 1:500 (Millipore, Cat. # MAB360, Temecula, CA, USA). After washing off primary antibody 3x with PBS (10 min each), secondary antibodies (diluted in BSA/PBS) were applied, including DyLight goat anti-mouse (1:500) and FITC goat anti-rabbit (1:50) (both from Jackson ImmunoResearch Laboratories, Inc., West Grove, PA, USA). After 1 hr at room temperature, specimens were washed 3x (5 min each), and Vectashield (Vector Laboratories, Burlington, ON, Canada) was applied to prevent photobleaching. No control peptides were available for control staining; however, it is noteworthy that each antibody specifically labeled only one cell type within these heterogeneous cultures. Stained specimens were first examined using a standard epifluorescence microscope (Zeiss IM35) in order to identify regions of interest for further confocal examination. For the best specimens, coverslips were removed from the undersides of the dishes and placed upside-down onto a dab of Vectasheild on a microscope slide, and the edges were sealed with nail polish. Images presented here were obtained using the Leica TCS SP5 II confocal system, equipped with argon (458, 476, 488, 515 nm) and helium-neon (543, 594, 633 nm) lasers, and a 63x oil objective with a 1.4 numerical aperture (Leica). Specimens were scanned in optical sections separated by 1.0-2.5 µm. Data acquisition and adjustment of brightness and contrast were controlled with the aid of LAS AF (version 2.1.2, Leica). Images were cropped and/or rotated in Adobe Photoshop CS3 Extended (version 10.0.1) and figures were compiled in Adobe Illustrator CS3 (13.0.1).

RESULTS

In this study, all data on aortic body (AB) cultures were derived from ABs located at the junction of the left vagus nerve and recurrent laryngeal nerve (RLN) from 9-14 d old rats. The location and distribution of type I cells, identified by positive tyrosine hydroxylase (TH) immunostaining in tissue whole mounts of this region, are illustrated in the confocal immunofluorescence images of Figure 1A, B. Details on the relationship

between type I cells and endogenous local neurons in this region have been described in detail in our recent study (Piskuric *et al.*, 2011).

Appearance and composition of aortic body cultures

The appearance of AB cultures under phase contrast microscopy was similar to that reported in our previous study (Piskuric *et al.*, 2011). The small size of the AB (with ~100 glomus or type I cells) at the bifurcation of the vagus nerve and RLN meant that there was generally a poor yield of isolated type I cell clusters even after pooling dissociated cells from nerve bundles from ~12 rat pups (e.g. Figure 1C). Given the bilateral asymmetry of the vagus and recurrent laryngeal nerves, only nerves from the left side were used because of their proximity to the aortic arch, contributing also to a low cell yield. In fact, some cultures appeared to be devoid of recognizable type I cell clusters. A characteristic feature of these AB cultures was the presence of occasional, easily-identified cell bodies of local neurons (Figure 1D, E). This contrasts with the bilateral rat carotid bodies (CBs), which can be individually isolated relatively free from attached nerves and contains ~9,000 type I cells per CB (McDonald & Mitchell, 1975). These CB cultures usually give rise to many dispersed islands of type I clusters, but lack viable neurons under our growth conditions (Nurse, 1990; Nurse & Fearon, 2002).

A comparison of fluorescence micrographs from typical dissociated 24 hr AB and CB cultures after immunostaining for the type I cell marker, TH, and the glial-cell marker, glial fibrillary acidic protein (GFAP), is shown in Figures 1F and G, respectively (n=3). Whereas GFAP-positive cells in rat CB cultures correspond predominantly to glia-like, sustentacular or type II cells (Nurse & Fearon, 2002), the situation is more complex for AB cultures. In particular, because the ABs reside within nerve bundles, AB cultures contain a much higher proportion of GFAP-positive cells (cf Figures 1G, F; see also (Piskuric *et al.*, 2011), the majority of which likely originate from glial (e.g. Schwann) cells associated with the large peripheral vagus nerve and RLN. Because of these morphological considerations, we initially focused on small, putative chemoreceptor type

I clusters (< 5 cells) for monitoring stimulus-evoked intracellular Ca^{2+} responses, so as to minimize contamination from interspersed glial cells.

Ca^{2+}_i responses in aortic body vs carotid body type I cells during chemostimulation

In the majority of experiments, intracellular Ca^{2+} responses were recorded from parallel AB and CB cultures derived from the same litters ~24 hr after plating. Putative single, and small clusters (2-4 cells) of type I cells were identified morphologically under brightfield optics prior to data acquisition, and evidence in support of their identity was obtained at the end of each trace by a positive response to the depolarizing stimulus, high extracellular K^+ (30 mM KCl). It should be noted, however, that at 24 hr it is difficult to distinguish type I from type II cells morphologically, especially when both are present in the same cluster. Pooled data from all cultures revealed that the mean resting intracellular Ca^{2+} concentration, $[Ca^{2+}]_i$, recorded from putative type I cells in AB cultures was 39.7 ± 1.2 nM (range = 10.1 – 138.1 nM; n=265); this value appeared similar for type I cells in parallel CB cultures (mean = 39.3 ± 1.3 nM; n=341). Often, AB type I cells showed random baseline $[Ca^{2+}]_i$ fluctuations that included spikes of variable amplitudes. As exemplified in Figure 2, type I cells from parallel AB and CB cultures showed increases in $[Ca^{2+}]_i$ in response to several chemostimuli including hypoxia (PO_2 ~25 mmHg), isohydric hypercapnia (10% CO_2; pH ~7.4), acidic hypercapnia (10% CO_2; pH ~7.1), and isocapnic acidosis (5% CO_2; pH ~6.9). A subset (7/24, 29%) of AB type I cells in smaller clusters (<5 cells) responded to hypoxia with a significant increase in $[Ca^{2+}]_i$, corresponding to a $\Delta[Ca^{2+}]_i$ of ~60 nM above basal (Figure 3). A comparable response to the same hypoxic stimulus was seen in small clusters (< 5 cells) of CB type I cells from parallel cultures, where a larger proportion of cells (10/22, 45%) responded with a mean $\Delta[Ca^{2+}]_i$ of ~86 nM above basal (Figure 3).

Compared to hypoxia, isohydric hypercapnia and isocapnic acidosis elicited more robust $\Delta[Ca^{2+}]_i$ responses in AB type I cells and a greater proportion of cells responded. As illustrated in Figure 3, 65% (11/17) of AB type I cells responded to isohydric

hypercapnia with a mean $\Delta[Ca^{2+}]_i$ of ~81 nM, whereas 62% (8/13) responded to isocapnic acidosis with a mean $\Delta[Ca^{2+}]_i$ of ~90 nM. Surprisingly, when AB type I cells from small clusters were challenged with acidic hypercapnia (10% CO_2; pH ~7.1), the proportion of responsive cells (14/37, 39%) and mean $\Delta[Ca^{2+}]_i$ (~73 nM) appeared lower than that seen with isohydric hypercapnia. Though not studied in detail, a common occurrence in AB type I cells after exposure to isocapnic acidosis was a prolonged oscillating Ca^{2+} response that continued for several minutes after termination of the stimulus (Figure 2A, C). This observation suggests that these cells may be quite acid sensitive. Data from comparable studies in parallel CB cultures are summarized in Figure 3; 67% (6/9) of CB type I cells responded to isohydric hypercapnia, 56% (i.e. 5/9) responded to isocapnic acidosis, and 42% (14/33) responded to acidic hypercapnia. In general, for hypercapnic stimuli the magnitude of $\Delta[Ca^{2+}]_i$ responses and proportion of responsive were similar in both sets of cultures when comparing single, and small (<5 cells) clusters of, type I cells. Combined data for all chemostimuli based on measurements of Ca^{2+} responses in type I clusters of *all sizes* are summarized in Table 1. It should be noted that contaminating glial cells are more likely to be present within the larger cell clusters.

Effect of Ni^{2+} on the chemosensory responses of AB vs CB type I cells

It is well established that rat CB type I cells respond to hypoxia and acidic hypercapnia via extracellular Ca^{2+} entry through predominantly L-type voltage-gated Ca^{2+} channels (Buckler & Vaughan-Jones, 1994a, b). To investigate the source of $Ca^{2+}{}_i$ in the responses of AB type I cells to chemostimuli, we tested the effects of the non-specific voltage-gated Ca^{2+} channel antagonist, 2 mM Ni^{2+}. First, we confirmed that under our recording conditions 2 mM Ni^{2+} was effective in inhibiting CO_2/H^+-induced $Ca^{2+}{}_i$ responses in CB type I cells (Figure 4A). Of 59 CB type I cells tested, acidic hypercapnia elicited a significant rise in $[Ca^{2+}]_i$ in 45 cells (i.e. 76%); the mean $\Delta[Ca^{2+}]_i$ in responsive cells was 85.9 ± 8.0 nM. As illustrated in Figure 4A, B and D, this $Ca^{2+}{}_i$ response was

completely abolished in the presence of 2 mM Ni^{2+} (Friedman Test with Dunn's Multiple Comparison post hoc test, $p<0.0001$, n=45). In fact, the $\Delta[Ca^{2+}]_i$ during Ni^{2+} application was -4.07 ± 1.07 nM, which is consistent with a *reduction* in baseline spontaneous $Ca^{2+}{}_i$ activity after application of Ni^{2+} (e.g. Figure 4B). The response to acidic hypercapnia was completely recoverable after washout of Ni^{2+} (Fig. 4A, B, D); the $\Delta[Ca^{2+}]_i$ after recovery was 78.92 ± 8.97 nM (Friedman Test with Dunn's Multiple Comparison post hoc test, p=ns, n=45). It was routinely noted, however, that there was a "rebound" in $[Ca^{2+}]_i$ immediately after washout of Ni^{2+}, characterized by a large, fast spike in $[Ca^{2+}]_i$ followed by prolonged spontaneous activity (e.g. Figure 4B), consistent with previous reports (Buckler & Vaughan-Jones, 1994b).

A similar pattern of Ni^{2+} sensitivity was observed in AB type I cells following exposure to acidic hypercapnia (Figure 4C), though the data set was smaller. In a group of 6 cells that responded initially to acidic hypercapnia with a significant rise in $Ca^{2+}{}_i$ (mean $\Delta[Ca^{2+}]_i$ = 68.0 ± 18.2 nM), application of 2 mM Ni^{2+} caused a rapid decrease in the spontaneous $[Ca^{2+}]_i$ activity, and the baseline $[Ca^{2+}]_i$ began to decline (e.g. Figure 4C, hatched lines; Figure 4E). In the continued presence of 2 mM Ni^{2+}, the $\Delta[Ca^{2+}]_i$ response was blocked on re-application of acidic hypercapnia, consistent with a role of Ca^{2+} entry through voltage-gated Ca^{2+} channels (Figure 4C,E; Friedman Test with Dunn's Multiple Comparison post hoc test, p=0.02, n=6). Upon washout of Ni^{2+}, AB type I cells exhibited "rebound" $[Ca^{2+}]_i$ transients, similar to that observed for CB cells; however, the response to a subsequent exposure to acidic hypercapnia was greatly diminished relative to the initial response (mean $\Delta[Ca^{2+}]_i$ = 6.9 ± 14.9 nM; Figure 4C, E).

Effects of P2 purinoceptor agonists on glia-like cells in AB vs CB cultures

Previous anatomical studies indicated that type I cells are more abundant than the surrounding glia-like, type II cells by a factor of 3x in the subclavian AB (Hansen, 1981), and 8x in the recurrent laryngeal AB (Dahlqvist *et al.*, 1984). This ratio compares favorably with similar anatomical studies on the CB indicating that type I cells

outnumber type II cells by a factor of 3x to 5x (McDonald & Mitchell, 1975). Using GFAP-immunostaining as a general marker for glial cells, our routine observations do not support such relative proportions of type I to type II cells in AB cultures, which contain a much higher proportion of GFAP-positive cells (e.g. Figure 1F). This raised the possibility that the majority of GFAP-positive cells in AB cultures were not *bona fide* type II cells, but likely included other glial cells (e.g. Schwann cells) associated with the vagus nerve and RLN. This prompted us to investigate the properties of glia-like cells in AB cultures, especially because type II cells are now thought to participate in paracrine interactions in the CB via purinergic P2Y2 receptors (Xu *et al.*, 2003)

Because P2Y2 receptors display roughly equal sensitivities to ATP and UTP (von Kugelgen, 2006), we first confirmed that ATP and UTP were equally effective in eliciting $[Ca^{2+}]_i$ responses in CB type II cells, as previously reported (Xu *et al.*, 2003). In CB cultures, type II cells occurred within, at the periphery of, or outside type I cell clusters (see Figure 1; Nurse & Fearon, 2002), and were classified as such based on $[Ca^{2+}]_i$ responses to ATP (100 μM) and failure to respond to the depolarizing stimulus, high K^+ (30 mM).

As illustrated in Figure 5Aa and Ab, ATP and UTP elicited similar increases in $[Ca^{2+}]_i$ in CB type II cells as expected, though there was some variability in the magnitude of the responses from cell to cell (Figure 5Aa). UTP (100 μM) elicited responses in 76% of glial cells, all of which were ATP-sensitive. The average ATP- and UTP-induced $\Delta[Ca^{2+}]_i$ in CB glia-like cells were 131.2 ± 17.9 nM and 92.7 ± 21.6 nM, respectively; the average change in $[Ca^{2+}]_i$ following exposure to 30 mM KCl was negligible (-4.4 ± 5.9 nM, n=33).

By contrast, when the same protocol was applied to AB cultures only 37% (59/158) of ATP-sensitive, high K^+ -insensitive cells, responded to UTP (Figure 5Bb). In about one-half of the cases studied, applying UTP first slightly increased the proportion of responsive cells, suggesting that previous exposure to ATP may desensitize P2Y receptors and/or deplete intracellular Ca^{2+} stores. Figure 5Ba shows simultaneous Ca^{2+} recordings from 2 glia-like cells in the same AB culture; both cells responded to ATP,

though only one was UTP-sensitive (i.e. black trace). The UTP-*insensitive* population of glia-like cells is represented in Figure 5Bb by the group of data points indicated by the arrow. Of the UTP-*sensitive* population, the average $\Delta[Ca^{2+}]_i$ in response to 100 μM UTP was 94.6 ± 9.7 nM (n=59), a value very similar to that of CB type II cells; the average $\Delta[Ca^{2+}]_i$ in response to 100 μM ATP was 100.7 ± 6.3 nM (n=158) for the combined UTP-sensitive and UTP-insensitive populations. Again, the average response of the total population to 30 mM KCl was negligible, i.e. -0.5 ± 0.3 nM (n=158).

Are local aortic body neurons sensory?

A unique feature of the vagus nerve-RLN AB *in situ* and in dissociated cell culture is the presence of local neurons, some of which appear to make contact with type I cells (Piskuric *et al.*, 2011). We showed previously that subpopulations of these neurons located at the periphery of AB paraganglia in this region express P2X2 and P2X3 purinoceptors, as do nerve terminals associated with type I cells *in situ*. Because the physiological function of these neurons is unknown, we considered the possibility that they may be sensitive to AB chemostimuli, and perhaps act as sensory relay neurons. Interestingly, we found subpopulations of local neurons that responded to hypoxia, isohydric and acidic hypercapnia, and isocapnic acidosis with a significant rise in $[Ca^{2+}]_i$, as exemplified in Figures 6 A, B, C, E; these neurons also responded to the depolarizing stimulus high (30 mM) K^+ with an increase in $[Ca^{2+}]_i$. We randomly selected a total of 39 AB neurons from 33 different cultures and tested the effects of one or more stimulus(i). The proportion of responsive neurons was variable with 50% (10/20) responding to hypoxia, 67% (4/6) responding to isohydric hypercapnia, 67% (4/6) responding to isocapnic acidosis, and 35% (13/37) responding to acidic hypercapnia. Pooled data of the $\Delta[Ca^{2+}]_i$ in responsive neurons evoked by these various chemostimuli are summarized in the histogram of Figure 6D. In many cases, the $[Ca^{2+}]_i$ responses in these neurons were prolonged and often persisted for several minutes after the stimulus was terminated.

Though the underlying reasons for this effect are presently unclear, the combined data are consistent with the notion that at least some local neurons may have a sensory function.

The above $[Ca^{2+}]_i$ responses observed in AB local neurons could be attributable to a direct chemosensitivity of the neurons themselves or, they may arise secondarily, from interactions with chemoreceptor type I cells and/or other interneurons. Because ATP is a key sensory CB transmitter that is thought to be co-released with ACh from rat type I cells (Nurse, 2010), we wondered whether the neuronal $[Ca^{2+}]_i$ responses in AB cultures could be inhibited by purinergic and/or nicotinic receptor blockers. The results of these experiments were inconclusive (n = 5), in part because of the prolonged, spontaneous $\Delta[Ca^{2+}]_i$ spike activity that commonly occurred after stimulus application (see above), and secondly, the response to multiple stimulus applications tended to run down over time. Nonetheless, in 2 out of 3 cases, one of which is illustrated in Figure 6E, it appeared that the $\Delta[Ca^{2+}]_i$ signal in an AB neuron that responded to acidic hypercapnia was partially inhibited during co-incubation with suramin (100 μM) and mecamylamine (2 μM), i.e. non-specific blockers of P2 and nicotinic ACh receptors, respectively. Clearly, further studies are required to elucidate the mechanisms underlying the intracellular Ca^{2+} responses of local AB neurons to chemostimuli.

DISCUSSION

In this study, we show for the first time that rat aortic body (AB) type I cells located at the junction of the left vagus and recurrent laryngeal nerves are directly sensitive to a variety of chemostimuli. In a previous study using patch-clamp techniques, 5-HT-containing epithelioid cells in the chick AB were found to be hypoxia-sensitive (Ito *et al.*, 1999), and to our knowledge, this represents the only other case where aortic chemoreceptor cells have been directly studied in vertebrates. Using a novel dissociated cell culture model and ratiometric Ca^{2+} imaging, we found that several stimuli that typically activate chemoreceptor type I cells of the mammalian carotid body (CB), including hypoxia and hypercapnia, elicited reversible increases in cytosolic $[Ca^{2+}]$ in the AB type I cells. Interestingly, these stimuli also increased $[Ca^{2+}]_i$ in a population of local

neurons that are endogenous to the ABs in this region. These neurons not only survived our culture conditions but appear to represent a distinct population whose origin and function were previously unknown (Dvorakova & Kummer, 2005; Piskuric *et al.*, 2011). By contrast, innervation of rat ABs by the sensory nodose ganglion has been demonstrated in multiple labeling and immunohistochemical studies (Hansen, 1981; Kummer & Neuhuber, 1989; Dahlqvist *et al.*, 1994), and the presence of chemoafferent fibres, in addition to baroreceptor ones, has been demonstrated in the rat aortic nerve (Cheng *et al.*, 1997a). Moreover, in single- or few fibre recordings from the rat aortic and superior laryngeal nerves, respiratory stimulants (e.g. cyanide) were found to activate AB chemoafferents (Brophy *et al.*, 1999; O'Leary *et al.*, 2004), although other studies appear contradictory (Sapru *et al.*, 1981; Kobayashi *et al.*, 1999).

Sensitivity of aortic body type I cells to chemostimuli

The present study provides strong evidence that rat AB type I cells are directly chemosensitive, responding to a variety of stimuli, i.e. hypoxia, isohydric or acidic hypercapnia, and isocapnic acidosis, with a rise in intracellular $[Ca^{2+}]_i$. In the prototypic CB, these chemostimuli are thought to depolarize type I cells, leading to voltage-gated Ca^{2+} entry, and neurotransmitter release (Gonzalez *et al.*, 1994; Buckler, 2007). Thus, measurements of $\Delta[Ca^{2+}]_i$ in response to chemostimuli have proven to be a useful tool for studying type I cell chemosensitivity in the CB (Buckler & Vaughan-Jones, 1994a, b). Notwithstanding the possibility that the chemosensitivity of AB and CB type I cells may develop along different time courses, it appeared that within the same animals the $[Ca^{2+}]_i$ responses for a given stimulus were similar in cells obtained from the two regions. Also, the $[Ca^{2+}]_i$ responses to acidic hypercapnia in both AB and CB type I cells were inhibited by 2 mM Ni^{2+}, a non-specific blocker of voltage-gated Ca^{2+} channels, consistent with previous studies on CB type I cells (Buckler & Vaughan-Jones, 1994a, b). The present study did not address the ionic mechanisms mediating the presumptive stimulus-induced depolarization of AB type I cells. However, it is noteworthy that at least one background

K^+ channel subunit (i.e. TASK 3), known to contribute to hypoxia- and acid-chemotransduction in CB type I cells (Buckler, 2007), also appears to be expressed in AB type I cells (Yamamoto & Taniguchi, 2003).

Data on single type I cells or small clusters (<5 cells) provided a more reliable estimate of the percentage of responsive AB chemoreceptor cells to the various stimuli. Larger clusters were more likely to be contaminated by non-chemoreceptor, GFAP-positive glial cells, which were much more abundant in AB relative to CB cultures (Nurse & Fearon, 2002; Piskuric *et al.*, 2011). In the present study, glial cells were identified in part by their failure to elicit a $[Ca^{2+}]_i$ response to the depolarizing stimulus high K^+, however, they do respond to ATP which is now thought to be a key excitatory sensory transmitter released from type I cells following stimulus-induced depolarization (see below; Nurse, 2010). Among the smaller clusters, we found a similar percentage of responsive type I cells to elevated CO_2/H^+ in AB and CB cultures, though the percentage of responsive cells to moderate hypoxia appeared lower in AB cultures. Given that previous studies have suggested that the AB is less sensitive to PO_2 than the CB (Lahiri *et al.*, 1981a), it may not be surprising that moderate hypoxia activated a smaller proportion of AB type I cells. This apparent blunting of PO_2 sensitivity in AB type I cells may be related to the idea that the AB resides in a microenvironment where the tissue PO_2 is thought to be lower than that in the CB (Lahiri *et al.*, 1981b). This may have developmental consequences on PO_2 sensitivity, analogous to the situation that occurs when rat pups are raised in a chronic reduced O_2 environment during early fetal and post-natal stages. Such conditions are well known to cause blunting of CB type I cell chemosensitivity, associated with reduced expression of O_2-sensitive K^+ currents (Wyatt *et al.*, 1995). Though acidic hypercapnia appeared to elicit smaller and fewer positive responses than isohydric hypercapnia or isocapnic acidosis in any given cell type, a direct comparison is invalid as corrections for the effect of intracellular acidity on the K_d of the fluorescent probe fura-2 were not taken into account. Indeed, failing to correct for this change means that all $\Delta[Ca^{2+}]_i$ responses to acidic stimuli are likely underestimates. In general, regardless of the stimulus, direct comparisons of the percentage of responsive

cells between this and other studies are not possible because of several unknown factors including: (i) differences in relative sampling of single cells versus cells in clusters of variable sizes and, (ii) differences in the criteria used for classifying cells as "responsive".

A subset of glia-like cells in AB cultures may be analogous to CB type II cells

As mentioned above, a characteristic feature of AB cultures was the high density of GFAP-positive glia-like cells, many of which seemed to overlap clusters of TH-positive type I cells (Figure 1; see also Piskuric *et al.*, 2011). Because earlier studies of AB morphology reported that type I cells are ~3-4x *more* abundant than GFAP-positive, glia-like type II cells *in vivo* (Kummer & Neuhuber, 1989), as is the case for the CB (McDonald & Mitchell, 1975), the origin of glia-like cells in AB cultures was uncertain. A major source of these glial cells is likely to be from the surrounding peripheral vagus and recurrent laryngeal nerves, which are expected to contain GFAP-positive Schwann cells. This is in contrast to the CB cultures, where glial cells are predominantly type II cells (Nurse & Fearon, 2002), which are thought to participate in purinergic paracrine cell-cell signaling via P2Y2 receptors during chemotransduction (Xu *et al.*, 2003). Given that P2Y2 receptors on CB type II cells show roughly equal sensitivities to ATP and UTP (Xu *et al.*, 2003), we compared the effects of these two agonists on $\Delta[Ca^{2+}]_i$ in glia-like cells in AB cultures. Approximately 40% of glia-like cells were sensitive to ATP and UTP, whereas the remainder was ATP-sensitive, but UTP-insensitive. These data suggest that not all glia-like cells in AB cultures are analogous to type II cells of the CB and that the ATP-sensitive, UTP-insensitive populations are probably non-myelinating Schwann cells from the vagus nerve that express P2Y1 purinergic receptors (Mayer *et al.*, 1998).

Possible significance of local neurons to aortic body function

Physiological reflexes initiated by ABs have so far not been well studied in the rat; however, extensive studies on AB chemoafferents in cats may provide some clues. Lahiri and co-workers showed that increases in arterial PCO_2 (with the associated changes in arterial $[H^+]$) increased chemoafferent discharge rates even in hyperoxia, and the combined effects of hypoxia and hypercapnia were additive (Lahiri *et al.*, 1979). Furthermore, they found that although ABs are excited by changes in arterial PO_2 and PCO_2, they are less sensitive than CBs especially to increases in CO_2 (Lahiri *et al.*, 1981a). Also, stressors known to decrease arterial O_2 content while maintaining arterial PO_2 (e.g. anemia, hypotension and carboxyhemoglobinemia) caused significant excitation of AB chemoafferents, but had no effect on the CB (Hatcher *et al.*, 1978; Lahiri *et al.*, 1980a; Lahiri *et al.*, 1981b). These studies led to the hypothesis that the delivery of oxyhemoglobin is important for AB but *not* CB tissue, suggesting a limited blood flow to the AB. This could partially explain why AB chemoafferents had weak responses to increases in arterial PCO_2 *in vivo*, i.e. a lower blood flow resulted in a lower CO_2 delivery to the AB tissue. However, in the present study stimulus levels reaching the cells were similar in both CB and AB cell culture preparations; this resulted in significant and comparable responses to elevations in CO_2/H^+.

A significant and novel finding in this study was that all chemostimuli tested were effective in eliciting $[Ca^{2+}]_i$ responses in at least a subpopulation of local AB neurons. In our recent study, processes from some local AB neurons appeared to contact type I clusters both *in situ* and *in vitro* (Piskuric *et al.*, 2011). It is noteworthy that the pattern of chemosensitivity displayed by AB neurons paralleled that of AB type I cells, i.e. isohydric hypercapnia and isocapnic acidosis excited the largest proportion of neurons and type I cells, and also elicited the largest responses. This would be expected if the neuronal responses were indirect and mediated via chemical synaptic transmission from type I cells. Indeed in the rat CB, release of ATP along with other excitatory co-transmitters (e.g. ACh) from type I cells onto chemoafferent nerve endings is thought to

be the principal mechanism mediating sensory transmission (Zhang *et al.*, 2000; Zhang & Nurse, 2004; Nurse, 2010). In the present study, attempts to block $[Ca^{2+}]_i$ responses in AB neurons using purinergic and nicotinic receptor blockers that are effective in the CB met with only limited success. Thus, although AB type I cells are transducers of the chemostimuli used in this study, we cannot presently exclude the possibility that local neurons may also be directly chemosensitive. In this regard, the proportion of neurons responding to hypoxia may appear higher than that for type I cells. Such inferences, however, should be interpreted with caution. First, all local AB neurons appear to be cholinergic, as indicated by positive immunoreactivity against the vesicular ACh transporter, VAChT (Dvorakova & Kummer, 2005; Piskuric *et al.*, 2011), and could potentially interact with each other via chemical (and possibly electrical) synapses; this could lead to an overestimation of the actual proportion of 'chemosensory' neurons. Second, the effects of weakly-responsive type I cells in a cluster could summate so as to drive a single neuron whose branches made functional contacts with these cells (Piskuric *et al.*, 2011).

What is the purpose of local AB neurons that are present *in situ* as well as in dissociated cell culture (Piskuric *et al.*, 2011)? Previous authors have suggested that local neurons near AB paraganglia are either sensory or autonomic efferent neurons (Kummer & Neuhuber, 1989). Consistent with this view, a small percentage (~5%) of nerve endings on AB paraganglia did not degenerate after vagotomy (Hansen, 1981), and some vagal neurons were retrogradely labeled by tracer injection into the nodose ganglion (Kummer & Neuhuber, 1989). By contrast, the CB is known to contain a small population of nNOS-positive autonomic 'microganglion' neurons thought to be involved in chemoreceptor inhibition (Wang *et al.*, 1993; Campanucci & Nurse, 2007); however, these neurons do not survive our culture conditions. In a previous study (Piskuric *et al.*, 2011), we showed that some local AB neurons expressed purinergic receptor subunits (i.e. P2X2, P2X3) which, incidentally, are characteristic of CB sensory afferent and autonomic efferent neurons (Prasad *et al.*, 2001; Campanucci *et al.*, 2006). Though further studies are required to firmly establish the role of AB local neurons, we suggest

that in addition to relaying chemoreceptor input to the central nervous system, these neurons may participate in the regulation of the local vasculature or cardiac function. Thus, the placement of the AB near the aortic arch at the junction of the vagus and recurrent laryngeal nerves would be strategic, endowing it with a unique physiological function that is separate from the CB, and specific to its niche near the heart.

In summary, we demonstrate for the first time that rat AB type I cells are directly chemosensitive, responding to a variety of chemostimuli with increases in cytosolic [Ca^{2+}]. Moreover, we found that some of the local neurons at the periphery of the AB paraganglion are also chemosensitive, and this is consistent with a putative sensory function. Further studies are required to identify the chemosensory mechanisms and cellular targets of these local neurons.

ACKNOWLEDGEMENTS

The authors thank Cathy Vollmer for her expert technical assistance. This work was supported by an operating grant from the Canadian Institutes of Health Research (MOP 12037) to C.A.N. N.A.P. was supported by a Vanier Canada Graduate Scholarship from the Natural Sciences and Engineering Research Council of Canada (NSERC). The Leica TCS SP5 II confocal system was purchased with a grant from the Canadian Foundation for Innovation-Leaders Opportunity Fund.

Table 1. Summary of $\Delta[Ca^{2+}]_i$ from responsive aortic body and carotid body type I cells.

		Hox; ~25 mmHg	10% CO_2, pH ~7.4	5% CO_2, pH ~6.9	10% CO_2, pH ~7.1	30 mM KCl
AB						
	mean ± SEM (nM)	69.3 ± 8.2	62.8 ± 9.1	89.7 ± 19.4	56.0 ± 5.4	118.6 ± 5
	% responsive	8	63	41	13	100
	n (total)	160	52	37	250	265
CB						
	mean ± SEM (nM)	45.7 ± 3.9	76.7 ± 5.6	53.4 ± 4.8	46.5 ± 2.2	207.5 ± 6
	% responsive	26	84	51	48	100
	n (total)	262	97	76	310	341

Figure 1. Identification of rat aortic body and carotid body cell types *in situ* and/or in dissociated cell culture.

A, Confocal section of a whole-mount containing the vagus and recurrent laryngeal nerve bifurcation reveals aortic body type I cell clusters, immunostained for tyrosine hydroxylase (TH); inset in **A** shown at higher magnification in (**B**). **C-E,** Phase contrast micrographs of dissociated AB cells after 24 hr in culture. An isolated AB type I or glomus cell (GC) cluster is shown in **C**; the soma of local neurons (N) with and without visible processes are shown in **D** and **E**, respectively. Parallel cultures of dissociated AB cells (**F**), and CB cells (**G**) from the same animals, showing type I clusters immunopositive for TH (green), and glia-like cells, immunopositive for glial-fibrillary acidic protein (GFAP, red). Note GFAP-positive cells are more abundant in AB cultures (**F**), relative to CB cultures in which GFAP is known to stain predominantly glia-like, type II cells (**G**).

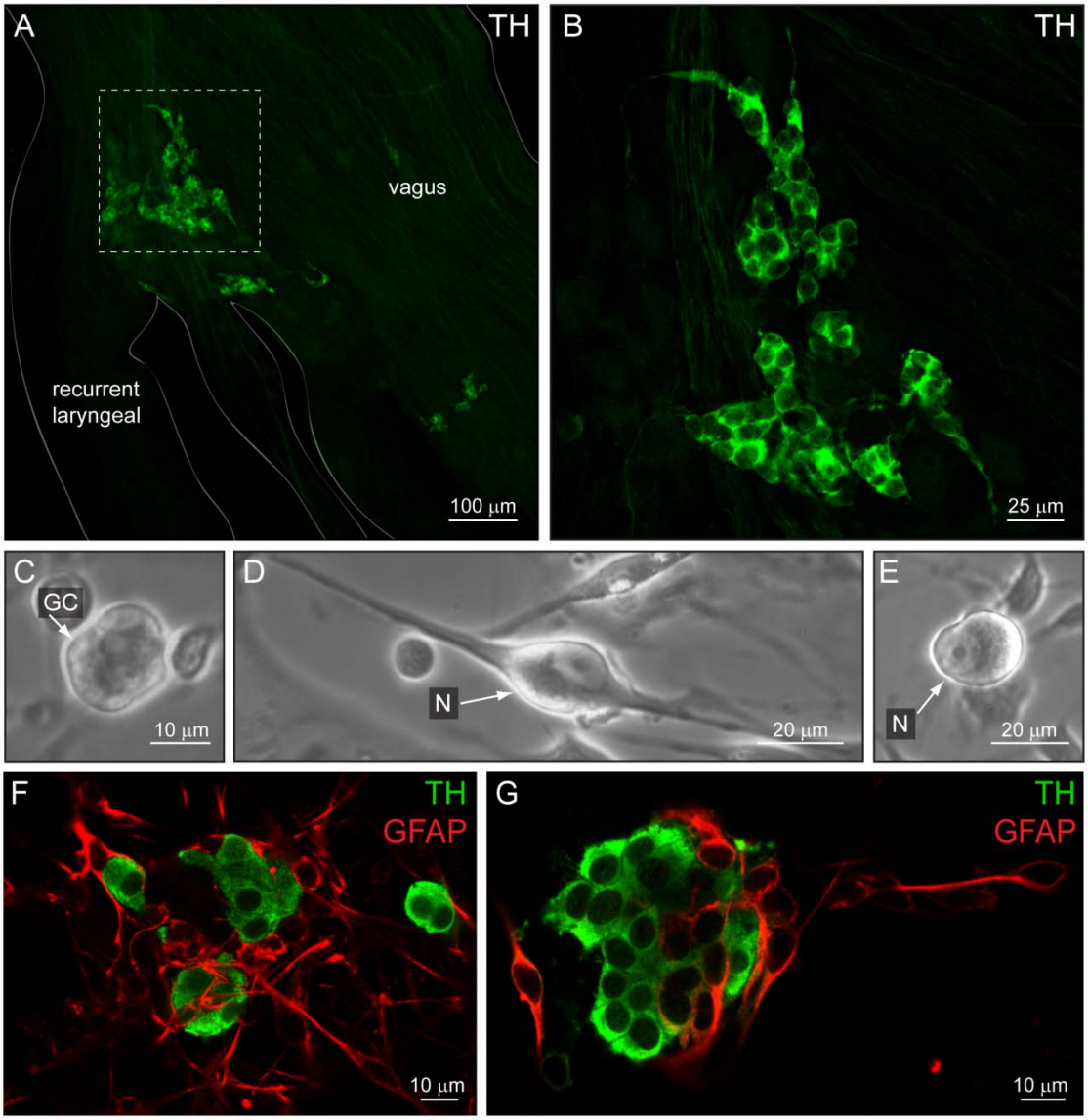
A
TH
vagus
recurrent
laryngeal
100 μm
B
TH
25 μm
C
GC
10 μm
D
N
20 μm
E
N
20 μm
F
TH
GFAP
10 μm
G
TH
GFAP
10 μm

Figure 2. Intracellular calcium (Ca^{2+}_i) responses of aortic body (AB) and carotid body (CB) type I cells to chemostimuli.

Example Ca^{2+} traces from responsive AB type I cells (**A**), and CB type I cells (**B**), to hypoxia (Hox; PO_2 ~25 mmHg), isohydric hypercapnia (10% CO_2, pH =7.4), isocapnic acidosis (5% CO_2, pH~6.9; H^+), and acidic hypercapnia (10% CO_2, pH~7.1). In **C**, a complete Ca^{2+}_i trace from an AB type I cell within a triplet shows responses to all 4 chemostimuli and the depolarizing stimulus, high (30 mM) K^+. Isocapnic acidosis (H^+) elicited the largest responses regardless of stimulus order, but was usually applied last because there was continuous Ca^{2+} activity even after washout.

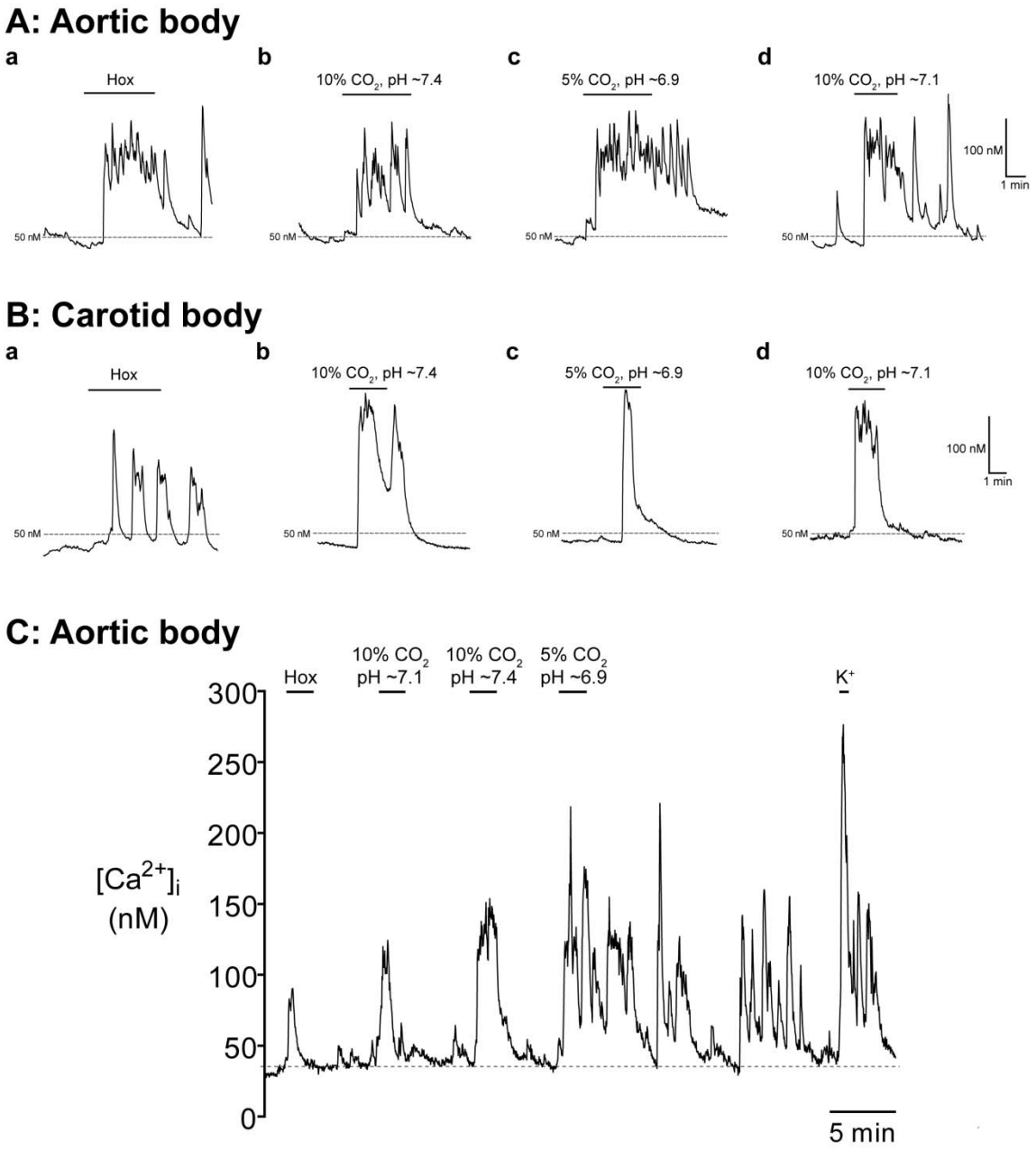
A: Aortic body
a
Hox
b
10% CO2, pH ~7.4
c
5% CO2, pH ~6.9
d
10% CO2, pH ~7.1
100 nM
1 min
50 nM
B: Carotid body
a
Hox
b
10% CO2, pH ~7.4
c
5% CO2, pH ~6.9
d
10% CO2, pH ~7.1
100 nM
1 min
50 nM
C: Aortic body
Hox
10% CO2 pH ~7.1
10% CO2 pH ~7.4
5% CO2 pH ~6.9
K+
[Ca2+]i (nM)
300
250
200
150
100
50
0
5 min

Figure 3. Summary of intracellular Ca^{2+} responses in aortic body (AB) and carotid body (CB) type I cells to various chemostimuli.

Bars represent the mean (+ S.E.M.) increase in $[Ca^{2+}]_i$ induced by the given stimulus in responsive AB (black bars) and CB (white bars) type I cells from small (i.e. <5 cell) clusters, averaged over a 2-4 min interval. The number of responsive cells ('*n*') for each group is given in parenthesis above each bar, as well as the percent of total (*n* responsive/total number of cells sampled).

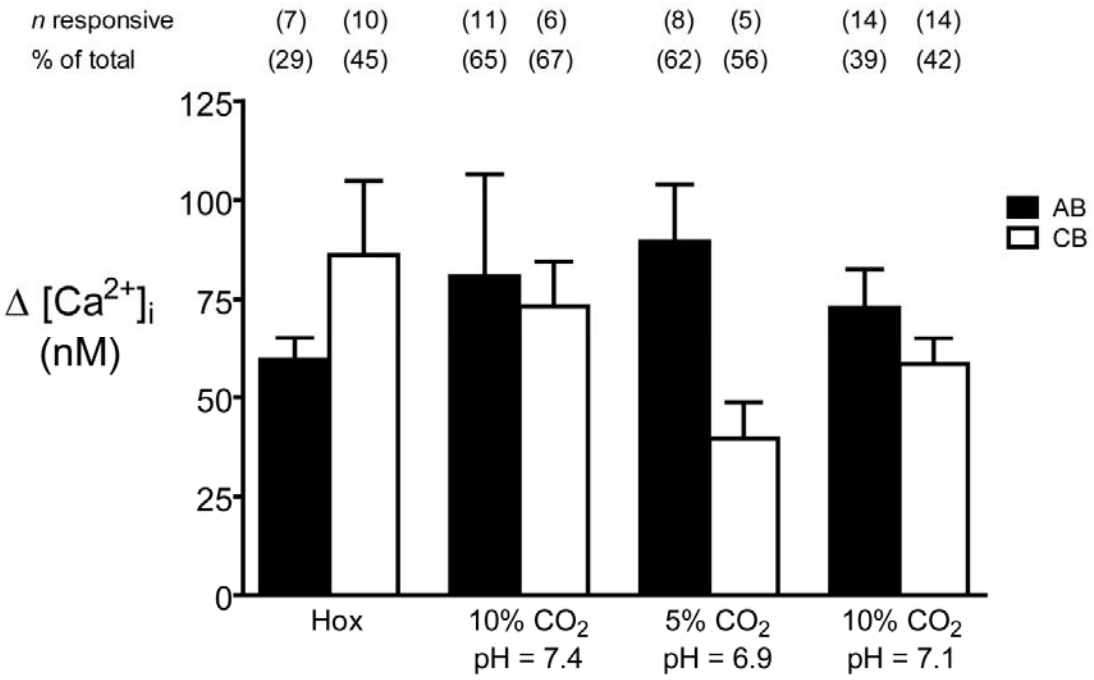
n responsive
(7) (10) (11) (6) (8) (5) (14) (14)
% of total
(29) (45) (65) (67) (62) (56) (39) (42)
125
100
75
50
25
0
Δ [Ca2+]i
(nM)
AB
CB
Hox
10% CO2
pH = 7.4
5% CO2
pH = 6.9
10% CO2
pH = 7.1

Figure 4. Blockade of intracellular Ca^{2+} responses to acidic hypercapnia by 2 mM Ni^{2+}.

A, Acidic hypercapnia (10% CO_2, pH = 7.1) elicited a rise in $[Ca^{2+}]_i$ in a carotid body (CB) type I cell that was reversibly blocked by the non-specific voltage-gated Ca^{2+} channel antagonist, 2 mM Ni^{2+}. The same protocol was applied in **B**, although in this case the CB type I cells exhibited spontaneous $Ca^{2+}{}_i$ activity before and especially after washout of the stimulus; 2 mM Ni^{2+} reversibly blocked the spontaneous activity as well as the response to acidic hypercapnia. In **C**, an aortic body (AB) type I cell with spontaneous $Ca^{2+}{}_i$ activity responded to acidic hypercapnia, and this response was blocked by 2 mM Ni^{2+}; note that application of Ni^{2+} immediately causes a reduction in the baseline $[Ca^{2+}]_i$, as indicated by the hatched lines. Although the effect of acidic hypercapnia was poorly reversible, there was still a detectable response to high K^+. Cumulative data for all 10% CO_2/H^+-responsive CB and AB type I cells exposed to this protocol are illustrated in **D** and **E**.

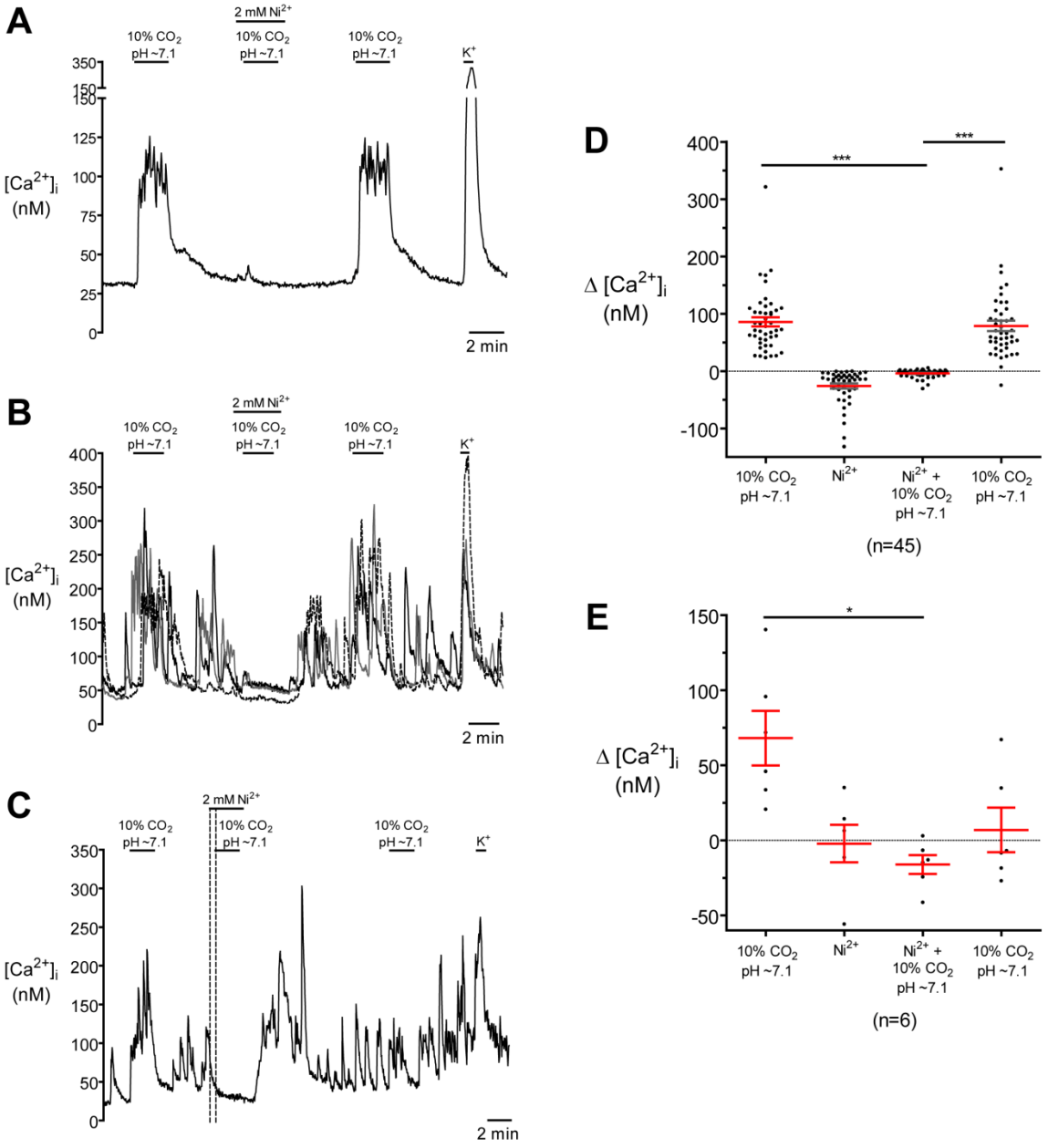
A
2 mM Ni2+
10% CO2 pH ~7.1
10% CO2 pH ~7.1
10% CO2 pH ~7.1
K+
[Ca2+]i (nM)
2 min
B
2 mM Ni2+
10% CO2 pH ~7.1
10% CO2 pH ~7.1
10% CO2 pH ~7.1
K+
[Ca2+]i (nM)
2 min
C
2 mM Ni2+
10% CO2 pH ~7.1
10% CO2 pH ~7.1
10% CO2 pH ~7.1
K+
[Ca2+]i (nM)
2 min
D
Δ [Ca2+]i (nM)
***
***
10% CO2 pH ~7.1
Ni2+
Ni2+ + 10% CO2 pH ~7.1
10% CO2 pH ~7.1
(n=45)
E
Δ [Ca2+]i (nM)
*
10% CO2 pH ~7.1
Ni2+
Ni2+ + 10% CO2 pH ~7.1
10% CO2 pH ~7.1
(n=6)

Figure 5. Comparison of glia-like cells in aortic body (AB) cultures to carotid body (CB) type II cells.

Note that cells were classified as "glia-like" based on positive Ca^{2+}_i responses to ATP (100 μM) but no responses to the depolarizing stimulus, high (30 mM) K^+. Example Ca^{2+} traces from 3 glia-like cells in a CB culture are shown in **Aa**. As expected, all 3 cells respond with almost equal sensitivity to ATP (100 μM) and the P2Y2 receptor agonist, UTP (100 μM), a characteristic profile for the P2Y2 receptors expressed by rat CB type II cells (Xu *et al.*, 2003). The summarized data are shown in **Ab**. **B,** By contrast, only about half of the ATP-sensitive, K^+-insensitive cells in AB cultures responded to UTP. For example, in **Ba**, the red cell responded robustly to ATP but failed to respond to 100 μM UTP. Data are summarized in **Bb**, where the UTP-insensitive cells are represented by the population indicated by the red arrow.

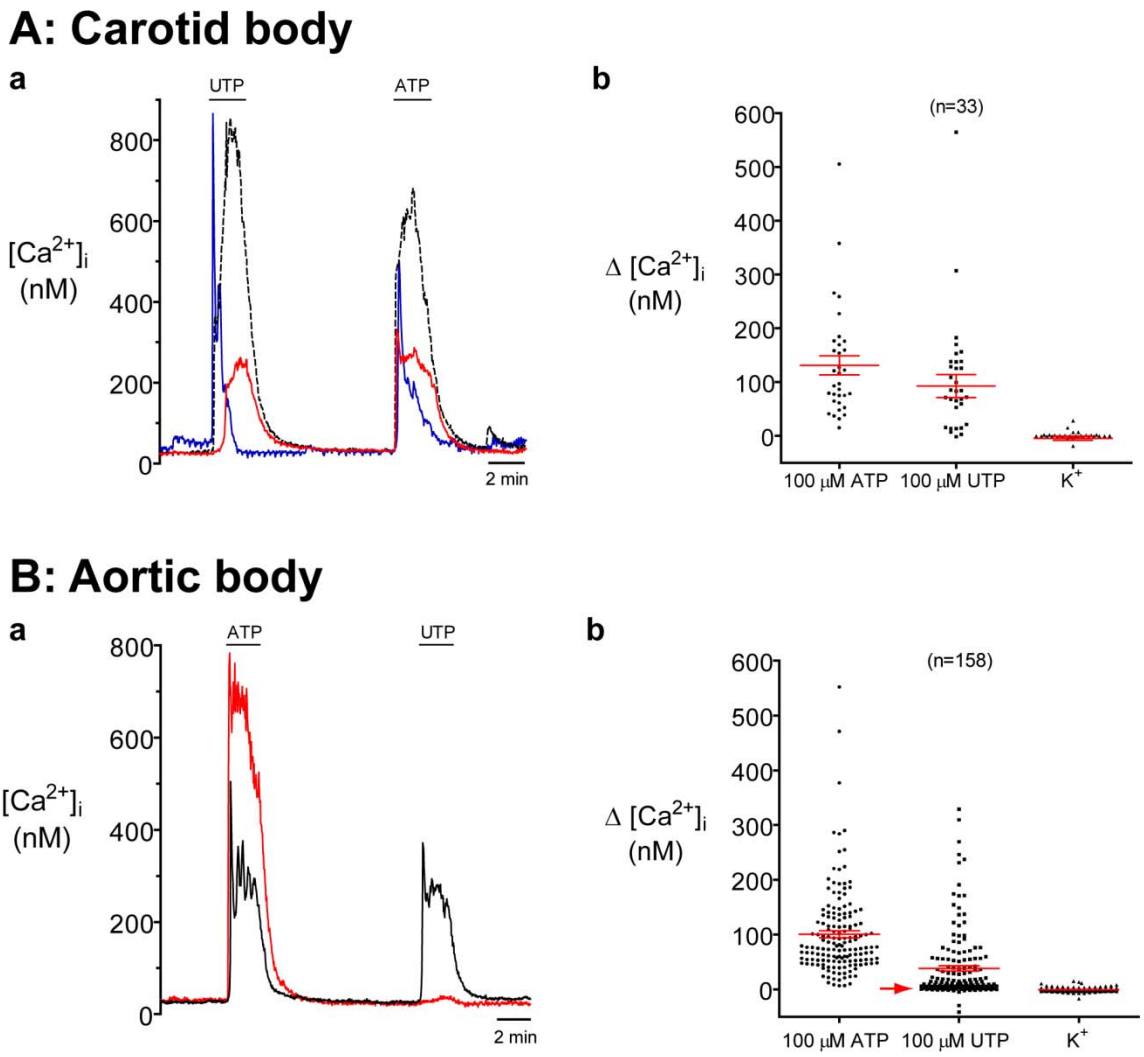
A: Carotid body
a
UTP
ATP
800
600
400
200
0
[Ca2+]i
(nM)
2 min
b
(n=33)
600
500
400
300
200
100
0
Δ [Ca2+]i
(nM)
100 μM ATP
100 μM UTP
K+
B: Aortic body
a
ATP
UTP
800
600
400
200
0
[Ca2+]i
(nM)
2 min
b
(n=158)
600
500
400
300
200
100
0
Δ [Ca2+]i
(nM)
100 μM ATP
100 μM UTP
K+

Figure 6. Intracellular Ca^{2+} responses elicited by chemosensory stimuli in local neurons endogenous to the aortic body (AB).

Upper traces (**A-C**) show $\Delta[Ca^{2+}]_i$ in neurons from different cultures exposed to hypoxia (Hox, PO_2 ~25 mmHg), isohydric hypercapnia (10% CO_2; pH =7.4), isocapnic acidosis (H^+; 5% CO_2, pH =6.9), as well as the depolarizing stimulus high (30 mM) K^+. Pooled data from all chemosensitive neurons, including those exposed to acidic hypercapnia (10% CO_2; pH =7.1), are summarized in the histogram (**D**). **E,** Effect of combined application of purinergic P2 and nicotinic ACh receptor blockers, i.e. suramin (sur; 100 μM) and mecamylamine (mec; 2 μM) respectively, on a neuronal $[Ca^{2+}]_i$ response induced by acidic hypercapnia; note reversible suppression of $Ca^{2+}{}_i$ response by these blockers, as well as the robust response to high K^+ at the end of the experiment (n=3).

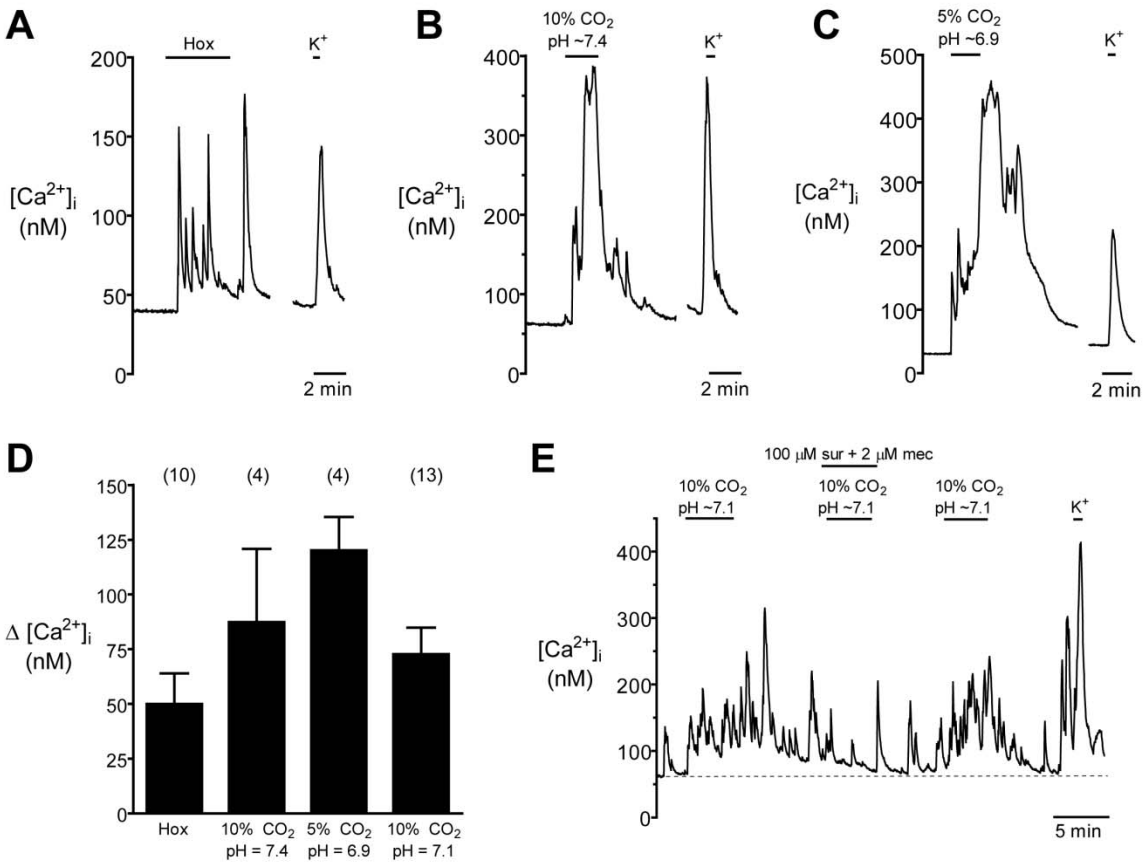
A
Hox
K+
200
150
100
50
0
[Ca2+]i
(nM)
2 min
B
10% CO2
pH ~7.4
K+
400
300
200
100
0
[Ca2+]i
(nM)
2 min
C
5% CO2
pH ~6.9
K+
500
400
300
200
100
0
[Ca2+]i
(nM)
2 min
D
(10)
(4)
(4)
(13)
150
125
100
75
50
25
0
Δ [Ca2+]i
(nM)
Hox
10% CO2
pH = 7.4
5% CO2
pH = 6.9
10% CO2
pH = 7.1
E
100 μM sur + 2 μM mec
10% CO2
pH ~7.1
10% CO2
pH ~7.1
10% CO2
pH ~7.1
K+
400
300
200
100
0
[Ca2+]i
(nM)
5 min

CHAPTER 4

ATP- and ACh-sensitivity, electrical coupling, and Evans Blue dye uptake among rat aortic body local neurons: Potential monitors of blood O_2 content

Piskuric, N.A., Zhang, M., Vollmer, C. and Nurse, C.A.

The work in this chapter is in preparation for submission.

I performed all Ca^{2+} imaging and immunofluorescence experiments, data analysis, and wrote the manuscript. M. Zhang provided technical assistance with electrophysiology experiments. C. Vollmer provided technical assistance with animal dissections and Evans Blue dye perfusion.

ABSTRACT

Aortic bodies (ABs) are arterial chemoreceptors presumed to monitor blood O_2 content by unknown mechanisms, in contrast to their well-studied carotid body (CB) counterparts which monitor PO_2 and PCO_2/pH. However, in our recent studies, rat AB chemoreceptors (type I cells) located at the left vagus- recurrent laryngeal nerve bifurcation responded to PO_2 and PCO_2/pH in a manner indistinguishable from CB type I cells. Because these ABs are uniquely associated with a group of local neurons, which are also sensitive to these stimuli, we hypothesized that they may contribute to monitoring blood O_2 content. During perforated patch recordings, ATP, known to be released from CB type I cells and red blood cells (RBCs) during hypoxia, induced inward currents and excited ~45% of local neurons (EC_{50} 1 μM) mainly via heteromeric P2X2/3 purinoceptors. While ATP also induced a rise in intracellular [Ca^{2+}] in a subpopulation of these neurons, almost all of them responded to nicotinic cholinergic agonists. During paired recordings, several juxtaposed neurons showed strong bi-directional electrical coupling, suggesting coordination of electrical activity within the local AB 'circuit'. Perfusion with Evans Blue dye resulted in labelling of AB paraganglia; when combined with confocal immunofluorescence, the dye-labeled regions coincided with areas containing tyrosine hydroxylase- positive type I cell clusters and P2X2-positive processes. Thus, ABs have ready access to circulatory factors, e.g. ATP released from RBCs during hypoxia. We propose a working model whereby local neurons, RBCs, ATP signaling, and low blood flow contribute to the AB's unique ability to monitor blood O_2 content.

INTRODUCTION

Peripheral arterial chemoreceptors monitor the chemical composition of arterial blood and initiate reflexes to maintain respiratory and circulatory O_2, CO_2, and $[H^+]$ homeostasis. In mammals, the primary and best-studied peripheral chemoreceptors are the carotid bodies (CBs), which sense changes in PO_2 and PCO_2/H^+ and stimulate hyperventilation in response to hypoxia and acidic hypercapnia (Gonzalez *et al.*, 1994). A separate group of poorly-studied arterial chemoreceptors are the aortic bodies (ABs), located diffusely in the nerves surrounding the aortic arch. While the function of the ABs remains controversial, Lahiri and co-workers, based on experiments performed in cats ~30 years ago, proposed that AB chemoreceptors monitor circulatory O_2 *content*, and to a lesser extent arterial PO_2, eliciting adaptive *cardiovascular* reflexes in response to reductions in O_2 delivery to the tissues (Hatcher *et al.*, 1978; Lahiri *et al.*, 1980a; Lahiri *et al.*, 1980b; Lahiri *et al.*, 1981b). In support of this hypothesis, stimuli that reduced arterial O_2 content while maintaining normal arterial PO_2 and pH, such as anemia, hypotension, and carboxyhemoglobinemia, excited AB chemoafferents (in the aortic nerve), but had little or no effect on CB chemoafferents (Hatcher *et al.*, 1978; Lahiri *et al.*, 1980a; Lahiri *et al.*, 1981b). Because stimuli that reduced O_2 flow to the tissues activated AB but not CB chemoreceptors, Lahiri et al. (1981b) postulated that oxygenated hemoglobin (Hb) must contribute to the tissue PO_2 in the AB and not in the CB. In fact, the CB is known to have a very high blood flow per unit volume (Daly *et al.*, 1954), and this might provide a large margin of safety against stimuli that reduce O_2 delivery. In contrast, the blood flow in the AB is estimated to be approximately one sixth of that in the CB (Lahiri *et al.*, 1981b), rendering it very sensitive to reductions in O_2 content.

The question therefore arises, how do ABs and CBs sense arterial O_2 content and PO_2, respectively, if the actual stimulus at both receptor sites is supposedly tissue PO_2? Lahiri et al. (1981a) speculated that these differences were attributable either to fundamental differences in the properties of their constituent chemoreceptor (glomus or type I) cells, or to differences in their local microenvironments which led to different

stimulus levels at the receptor site. In any case, ABs and CBs were classified as "low-" and "high-" responding chemoreceptors, respectively, since stimuli that robustly activated the CBs, i.e. low PO_2 and high PCO_2, only weakly activated ABs (Lahiri *et al.*, 1981a).

In order to test whether or not fundamental differences existed between AB and CB chemoreceptor cells, we recently used the ratiometric Ca^{2+} imaging technique to contrast the chemoreceptive properties of isolated AB type I cells with those of the CB at comparable ages (Piskuric & Nurse, 2012). Using this novel *in vitro* model of the AB, we found that AB type I cells responded to a variety of chemostimuli, including low PO_2, high PCO_2, and low pH, via increases in cytosolic [Ca^{2+}] (Piskuric & Nurse, 2012). Interestingly, in parallel experiments on CB type I cells derived from the same animals, we found that responses to the same chemostimuli were not overtly different from those of the AB, although the proportion of O_2-sensitive type I cells in CB cultures was slightly higher. These results do not support the hypothesis that inherent differences in the cellular physiology of AB and CB chemoreceptors are responsible for their differences in function.

These findings prompted us to explore alternative hypotheses to account for how the AB might function as a sensor of blood O_2 content. An attractive candidate for this role within the AB local circulation is the red blood cell (RBC) which, by virtue of its Hb content, is a determinant of blood O_2 carrying capacity. In fact, RBCs have recently been hypothesized to function as O_2-sensors, responding directly to hypoxia via ATP release and regulating local blood flow to adjust O_2 delivery to tissues (Ellsworth *et al.*, 2009; Jensen, 2009). Moreover, the trigger for ATP release is thought to be a change in Hb conformation in response to O_2 desaturation (Ellsworth *et al.*, 2009). Thus, if oxygenated Hb plays a role in maintaining tissue PO_2 in the AB, ATP release from RBCs may be an important link that signals a decrease in O_2 content. Our interest in RBCs as a key component in the AB signaling pathway was further heightened by the observation that, in contrast to the CB, many 'surviving' RBCs were readily identified in 1 d old AB cultures, suggesting the presence of a special microenvironment.

The posit that RBCs may play a role in AB chemosensing during hypoxia via release of ATP requires that blood-borne factors have ready access to AB cells, which in turn should express receptors for chemicals such as ATP. Interestingly, in a previous study, we showed that some local neurons associated with AB paraganglia in the vagus and recurrent laryngeal nerves expressed P2X2 and P2X3 purinergic receptor subunits using immunocytochemistry (Piskuric *et al.*, 2011). Subsequently, we showed that some of these neurons were chemosensory when tested in short-term culture, though it was unclear whether their responses were direct or indirect (Piskuric & Nurse, 2012). To test the hypothesis that ATP plays a central role in the ability of ABs to monitor O_2 content, we first characterized the ATP sensitivity of local AB neurons using electrophysiology and ratiometric Ca^{2+} imaging. Second, we addressed whether AB local neurons could form functional interconnections with each other that might help coordinate electrical activity within the network, e.g. during sensory processing. Third, using Evans Blue dye perfusion to label paraganglia with fenestrated capillaries, we addressed whether chemical stimuli in the microvasculature (e.g. ATP) have ready access to AB neurons and their purinergic nerve terminals *in situ.*

MATERIALS AND METHODS

Animal handling

All procedures for animal handling and tissue dissections were carried out according to the guidelines of the Canadian Council on Animal Care (CCAC) and institutional guidelines.

Cell cultures

Aortic body (AB) cultures were prepared as previously described (Piskuric & Nurse, 2012). Briefly, juvenile (9-14 d) rat pups (Wistar, Charles River, QC, Canada),

were rendered unconscious by a blow to the back of the head and then killed immediately by decapitation. The vagus nerve was cut inferior to the nodose ganglion and caudal to the bifurcation of the left recurrent laryngeal nerve (RLN); this portion along with the attached RLN was excised. Tissues were incubated for 1 hr at 37°C in an enzymatic solution containing 0.1% trypsin (Gibco, Grand Island, NY, USA) and 0.1% collagenase (Gibco, Grand Island, NY, USA or Sigma Aldrich, Oakville, ON, Canada), prior to mechanical dissociation and trituration. The resulting cell suspension was plated onto a thin layer of Matrigel (Collaborative Research, Bedford, MA, USA) that was previously applied to the central wells of modified 35 mm tissue culture dishes. Cultures were grown in F-12 nutrient medium supplemented with various additives, at 37°C in a humidified atmosphere of 95% air/5% CO_2. Cells were used after ~24 hr in culture.

Electrophysiology

Nystatin perforated patch, whole-cell recording was performed according to procedures described in detail previously (Zhang *et al.*, 2000). Patch pipettes were made from borosilicate glass (World Precision Instruments, Sarasota, FL, USA) using a vertical puller (PP 83; Narishige, Tokyo, Japan). Micropipettes had a resistance of 8-12 MΩ when filled with intracellular recording solution and formed gigaseals >1 GΩ. A junction potential of +14.0 mV was not corrected for unless otherwise noted. Cells were perfused with a standard bicarbonate buffered solution (BBS), which was warmed to ~35°C before entering the recording chamber. Membrane potential and ionic currents were recorded with the aid of a dual headstage MultiClamp 700B patch clamp amplifier and a Digidata 1322A analog-to-digital converter (Axon Instruments Inc., Union City, CA, USA), and stored on a personal computer. Data were acquired using pCLAMP software (version 9.0; Axon Instruments Inc.), and analysis was performed using Origin 8.0 and GraphPad Prism (Version 5.01).

Intracellular Ca^{2+} measurement

Intracellular free Ca^{2+} concentration ($[Ca^{2+}]_i$) was monitored using the fluorescent Ca^{2+} indicator, fura-2/AM (Molecular Probes, Eugene, OR, USA). Cells were loaded with 2.5 μM fura-2/AM for ~ 30 min, in either modified BBS at 37ºC or HEPES buffered saline at room temperature, and subsequently washed for 10-15 min to remove free dye. Ratiometric Ca^{2+} imaging was performed using a Nikon Eclipse TE2000-U inverted microscope (Nikon, Mississauga, ON, Canada) equipped with a Lambda DG-4 ultra high-speed wavelength changer (Sutter Instrument Co., Novato, CA, USA), a Hamamatsu OCRCA-ET digital CCD camera (Hamamatsu, Sewickley, PA, USA) and a Nikon S-Fluor 40x oil-immersion objective lens with a numerical aperture of 1.3. Dual images at 340 nm and 380 nm excitation (510 nm emission) were acquired every 2 s, with an exposure time of 100-200 ms. Pseudocolour ratiometric data were obtained using Simple PCI software version 5.3. All experiments were performed at ~37ºC, and cells were continuously perfused in modified BBS to maintain an extracellular pH of ~7.4. Data analysis, including estimation of intracellular free $[Ca^{2+}]$ according to the Grynkiewicz equation (Grynkiewicz *et al.*, 1985), was similar to that described in detail elsewhere (Piskuric & Nurse, 2012).

Solutions and Drugs

Bicarbonate buffered saline (BBS) used in patch clamp experiments contained (in mM): 24 $NaHCO_3$, 120 NaCl, 10 glucose, 12 sucrose, 5 KCl, 2 $CaCl_2$ and 1 $MgCl_2$, and the pH was maintained at ~7.4 by bubbling with 5% CO_2/95% air mixture. Pipette solution contained (in mM): 115 K^+-glutamate, 25 KCl, 5 NaCl, 10 HEPES, 1 $CaCl_2$, and 300 μg/mL nystatin. BBS used in Ca^{2+} imaging experiments contained (mM): 24 $NaHCO_3$, 115 NaCl, 5 glucose, 5 KCl, 2 $CaCl_2$ and 1 $MgCl_2$. For Ca^{2+} free experiments, $CaCl_2$ was replaced by 1 mM EDTA disodium salt. Nystatin (Cat. No. N3504), ATP disodium salt hydrate (Cat. No. A1852), α,β-MethyleneATP lithium salt (Cat. No. M6517), acetylcholine choloride (Cat. No. A-2661), mecamylamine hydrochloride (Cat.

No. M9020), and Evans Blue (Cat. No. E2129) were all obtained from Sigma-Aldrich (Oakville, ON, Canada).

Statistical Analysis

In Ca^{2+} imaging experiments, neurons with a basal $[Ca^{2+}]_i$ less than 200 nM and a positive response (i.e. $\Delta[Ca^{2+}]_i$ >50 nM) to the depolarizing stimulus 30 mM KCl were included in statistical analyses. For all other stimuli, cells were classified as 'responsive' if their mean $\Delta[Ca^{2+}]_i$ was >20 nM. Data are reported as mean ± standard error of the mean (S.E.M.). Differences between data sets were analyzed using the repeated measures Friedman Test with Dunn's multiple comparison post hoc tests (for nonparametric data). The significance level was set at 0.05. Statistical analyses were performed in GraphPad Prism 5.

Paraganglia staining

Rat pups (10-14 d) were anesthetized by intraperitoneal administration of sodium pentobarbital (30 mg/kg), before perfusion via the left ventricle with ~10 mL PBS (pH 7.2), followed by ~10 mL Evans Blue, and finally ~10 mL 4% paraformaldehyde. Prior to perfusion, Evans Blue was diluted in PBS (to 5 mM) and filtered through a 0.2 µm Millipore filter. The left vagus nerve and the attached RLN were excised, and the tissue was mounted in fresh PBS. Samples were examined using an Olympus BX60 upright microscope under both light and epifluorescence microscopy (Texas Red filter, 594 nm excitation). Images were captured with a QICAM FAST 12-bit digital camera (QImaging, Burnaby, BC, Canada) with the aid of Northern Eclipse software (Empix Imaging, Mississauga, ON, Canada). In a few cases, whole mounts stained with Evans Blue were further processed for immunostaining as indicated below.

Immunocytochemistry and confocal microscopy

Dissociated AB cultures were stained after 24 hr *in vitro*. Cells were washed with warmed PBS and fixed in 5% acetic acid/95% methanol for 1 hr at -20°C. After washing with PBS (3 x 10 min), cells were incubated in primary antibody diluted in 1% BSA/PBS for 24 hr at 4°C. Evans Blue stained whole mounts (which were previously fixed by paraformaldehyde perfusion) were washed in PBS and then incubated in primary antibody diluted in 1% BSA/PBS/1% Triton-X for 48 hrs. Primary antibodies were: mouse monoclonal anti-tyrosine hydroxylase (TH) at 1:2,000 (Cat. No. MAB5280, Millipore, Temecula, CA, USA), sheep polyclonal anti-human carbonic anhydrase II (CAII) at 1:1,000 (Cat. No. AHP206, AbD Serotec, Raleigh, NC, USA), and rabbit polyclonal anti-P2X2 at 1:500 (Cat. No. APR-003, Alomone Labs, Jerusalem, Israel). After washing off primary antibody 3x with PBS (10 min each), secondary antibodies diluted in BSA/PBS (or BSA/PBS/Triton-X, for whole mounts) were applied. Secondary antibodies included DyLight goat anti-mouse (1:500), FITC donkey anti-sheep (1:50), and FITC goat anti-rabbit (1:50) (all from Jackson ImmunoResearch Laboratories, Inc., West Grove, PA, USA). After 1 hr at room temperature, specimens were washed 3x (5 min each), and Vectashield (Vector Laboratories, Burlington, ON, Canada) was applied to prevent photobleaching. Stained specimens were first examined using a standard epifluorescence microscope (Zeiss IM35) in order to identify regions of interest for further confocal examination. For the best culture specimens, coverslips were removed from the undersides of the dishes and placed upside-down onto a dab of Vectasheild on a microscope slide, and the edges were sealed with nail polish. Images presented here were obtained using the Leica TCS SP5 II confocal system, equipped with argon (458, 476, 488, 515 nm) and helium-neon (543, 594, 633 nm) lasers, and a 63x oil objective with a 1.4 numerical aperture (Leica). Specimens were scanned in optical sections separated by ~2 µm. Data acquisition and adjustment of brightness and contrast were controlled with the aid of LAS AF (version 2.1.2, Leica). Images were cropped and/or rotated in Adobe

Photoshop CS3 Extended (version 10.0.1) and figures were compiled in Adobe Illustrator CS3 (13.0.1).

RESULTS

The electrophysiological properties of aortic body (AB) neurons were examined using perforated-patch whole cell recording in both voltage and current clamp mode. All data reported below were obtained from neurons examined after 24 hr in culture. AB neurons had a mean input capacitance (C_{in}) of 34.9 ± 2.8 pF (range: 22.0 – 43.4 pF), a mean input resistance (R_{in}) of 0.65 ± 0.15 GΩ (range: 0.19 – 0.70 GΩ), and a mean resting potential of -50.2 ± 1.3 mV (n=46).

ATP-sensitivity of aortic body neurons

We showed previously that subpopulations of local AB neurons express P2X2 and P2X3 purinoceptor subunits (Piskuric *et al.*, 2011), a characteristic of many sensory neurons including those innervating the carotid body (CB) (Prasad *et al.*, 2001; Burnstock, 2009). In AB cultures, a dose of ATP expected to activate most P2X receptors (i.e. 10 μM) induced membrane depolarization in 45% (17/38) of neurons. Typically, ATP caused rapid action potential firing followed by a large, sustained membrane depolarization; the mean sustained depolarization over a 2 s interval was 28.3 ± 3.7 mV (n=16; e.g. Figure 1A-i). In a few cases the initial burst of action potentials was followed by a slow decay towards the resting potential (n=2; e.g. Figure 1A-ii). The remaining neurons showed no change in membrane potential (e.g. Figure 1A-iii), except for 2 cases where ATP induced a small subthreshold depolarization. Under voltage clamp at -60 mV, ATP evoked dose-dependent inward currents with an EC_{50} of 1.0 μM (n=7) in AB neurons. After correcting for the junction potential, the reversal potential of the (10 μM) ATP-evoked current occurred near +10 mV (n=6; Figure 1F), suggesting that it was carried by non-selective cation channels. The ATP-evoked current showed strong inward

rectification, as described previously for currents carried by some P2X purinergic receptors (for review see North, 2002).

The kinetic profile of ATP-evoked inward currents in AB neurons consisted of a fast activation phase followed by slow desensitization (e.g. Figures 1B, 2B). Such biphasic kinetics are characteristic of cells expressing both P2X2 and P2X3 homomeric, or P2X2/3 heteromeric receptors (North, 2002). To probe for the presence of heteromeric receptors, we tested the effect of the selective P2X3 agonist α,β-MeATP, on the kinetics of the ATP-evoked current. In ATP-sensitive neurons (n=4), α,β-MeATP (5 μM) evoked slowly desensitizing inward currents with an EC_{50} of ~3.9 μM (n=2, Figure 2C; holding potential= -60 mV), consistent with the presence of heteromeric P2X2/3 receptors (Radford *et al.*, 1997). When applied to the same cells, under current clamp, both ATP and α,β-MeATP (5 μM) showed similar depolarizing responses consisting of a brief burst of action potentials followed by a prolonged membrane depolarization (n=4; Figure 2A). These data suggest that AB neurons express P2X2/3 heteromeric receptors, although the expression of P2X2 and P2X3 homomeric forms cannot be excluded.

ATP-induced Ca^{2+}_i responses in aortic body neurons

Activation of P2X2/3 purinoceptors increases cytosolic Ca^{2+} concentration via Ca^{2+} entry through the P2X channels themselves, as well as through voltage-gated Ca^{2+} channels following membrane depolarization. Thus, we tested the effects of ATP on the intracellular free Ca^{2+} concentration, $[Ca^{2+}]_i$, in AB neurons. In response to 10 μM ATP, 47% of neurons (i.e. 36/77) responded with an increase in $[Ca^{2+}]_i$ greater than 20 nM, with an average $\Delta[Ca^{2+}]_i$ of 154.9 ± 16.0 nM (n=36). Based on these 36 responsive neurons, the estimated EC_{50} for ATP was ~1.9 μM (Figure 3B). Figure 3A illustrates the Ca^{2+}_i responses of 2 neurons recorded from simultaneously, where one neuron was ATP-sensitive (red trace) and the other was not. The effect of extracellular Ca^{2+} removal on the response evoked by 10 μM ATP was investigated in 6 neurons. The ATP-induced Ca^{2+}_i rise was significantly reduced (~78% inhibition) in the absence of extracellular Ca^{2+}

(250.7 ± 12.4 nM in control vs. 55.0 ± 12.1 nM in Ca^{2+}-free solution; Friedman Test with Dunn's Multiple Comparison post-hoc test, p=0.0001, n=6; Figure 3C-D). Because Ca^{2+}-free solution did not completely block the response it is likely that P2Y purinoceptors were also present. This potential contribution from P2Y receptors may explain the right shift in the ATP dose-response curve generated from Ca^{2+} imaging experiments. Interestingly, in 2 out of 6 neurons tested, both ATP (10 μM) and the P2Y2/4 agonist UTP (100 μM), caused a significant rise in intracellular Ca^{2+}, suggesting the 2 neurons expressed a combination of P2X and P2Y purinoceptors.

Functional nicotinic ACh receptor expression in aortic body neurons

Although we showed previously that only a subset of AB local neurons express P2X2 and P2X3 purinergic receptors, all of them were immunopositive for the vesicular acetylcholine (ACh) transporter (VAChT) (Dvorakova & Kummer, 2005; Piskuric *et al.*, 2011). Furthermore, dense VAChT-positive terminals surrounded these neurons, consistent with ACh acting as a local neurotransmitter. Therefore, we tested whether or not AB neurons were sensitive to ACh. Indeed, almost all neurons tested (24/26) responded to 10 μM ACh, which caused a mean rise in $[Ca^{2+}]_i$ of 226.7 ± 22.8 nM (n=26). The nicotinic ACh receptor (nAChR) agonist, nicotine (10 μM), was also effective in activating almost all (37/38) neurons, eliciting Ca^{2+} transients of similar size and shape to ACh (e.g. Figure 4A). The mean $\Delta[Ca^{2+}]_i$ induced by 10 μM nicotine was 217.7 ± 18.3 nM (n=38). Of 46 neurons tested with either ACh or nicotine, 27 (i.e. 59%) responded to 10 μM ATP, indicating that even ATP-*insensitive* neurons were ACh-sensitive (e.g. Figure 4C).

The ACh-evoked $Ca^{2+}{}_i$ transients were completely and reversibly inhibited by the non-selective nAChR blocker, mecamylamine, at a concentration (10 μM) that blocks all or most nAChRs *in vitro*. In the presence of mecamylamine, the $\Delta[Ca^{2+}]_i$ induced by ACh was significantly reduced to 1.4 ± 3.3 nM, from an initial value of 161.9 ± 25.7 nM (Friedman Test with Dunn's Multiple Comparison post-hoc test, p=0.0001, n=6; Figure

4B); after washout of the blocker, the ACh response recovered to 124.7 ± 27.8 nM. Therefore, the ACh-evoked Ca^{2+} responses in AB neurons are due predominantly to nAChR activation, with little or no contribution from muscarinic ACh receptors.

Electrical coupling among aortic body neurons

It was noticeable that within 1 d old AB cultures, neurons were occasionally juxtaposed, overlapping, or grouped within heterogeneous cell clusters; these groupings appeared to represent cases of incompletely dissociated neurons. Given the morphological and biochemical evidence that these neurons might form chemical synapses (see above; Dvorakova & Kummer, 2005; Piskuric *et al.*, 2011), it was of interest to test whether adjoining pairs of these incompletely dissociated neurons were synaptically connected. Interestingly, instead of the expected chemical transmission, we obtained evidence for robust electrical coupling among these closely associated neurons. During whole-cell recordings from pairs of adjoining neurons in current clamp mode, graded depolarizing and hyperpolarizing current pulses were injected into one neuron of the pair while changes in membrane potential were simultaneously recorded in both neurons. As exemplified in Figure 5A-B, current injected into Neuron 1 (N1) induced a membrane potential change in the cell (ΔV1), as well as a potential change in Neuron 2 (ΔV2) of similar size and shape. Given that the synaptic delay between voltage responses was negligible, and that both subthreshold depolarizations and hyperpolarizations were transferred to the adjoining cells, these results indicated the presence of electrical coupling. Coupling was bidirectional, because stimulation of N2 also evoked similar responses in N1.The degree of electrical coupling was quantified using the coupling coefficient (K_c), where $K_c = \Delta V2/\Delta V1$ (Bennett, 1966), for a hyperpolarizing current pulse of 100 pA (over 500 ms) to eliminate the contribution of voltage-activated ion channels. For 5 electrically coupled pairs of neurons, the average K_c (± S.E.M.) was 0.83 ± 0.03 (n=5 pairs of neurons).

To test whether the electrically-coupled pairs of neurons might include ones that expressed functional purinergic P2X receptors, we applied 10 μM ATP. Among 5 pairs of electrically coupled neurons, 3 pairs were insensitive to ATP (e.g. Figure 5D), whereas in the other 2 pairs, ATP evoked almost identical depolarizing potentials in both members of each pair (e.g. Figure 5E). In total, we found 7 examples of non-rectifying, resistive electrical coupling between AB neurons. Confirmation that these neurons can form electrical synapses was obtained in one case where injection of Lucifer Yellow (0.5%) into a single neuron resulted in dye spread to neighboring neurons. This is illustrated in Figure 5C, where injection of Lucifer Yellow into neuron N1 led to dye transfer into 2 nearby neurons, i.e. from N1 into the overlapping neuron N3, as well as from N1 to N2, even though their cell bodies were not in contact. In this example, it appears that electrical coupling occurred among all 3 neurons.

Presence of red blood cells in aortic body cultures

Previously, we described dissociated AB cultures as a heterogeneous mixture of type I cells, local neurons, and glia-like cells (some of which resemble CB type II cells) (Piskuric *et al.*, 2011; Piskuric & Nurse, 2012). Here, we provide evidence for an additional cell type, i.e. red blood cells (RBCs), in 1-day-old AB cultures. As illustrated in Figures 6A-C, these RBCs were easily identified under phase contrast microscopy as characteristically round, biconcave, and anuclear. A histogram of the diameters of 300 RBCs after 24 hr in culture reveals a normal distribution with a mean diameter of 5.9 ± 0.04 μm (Figure 6D), close to the average diameter of typical rat RBCs, i.e. 6.5 μm. The density of RBCs (hundreds/dish) greatly exceeded that of chemoreceptor type I cells and neurons, both of which were relatively difficult to locate. RBCs were randomly distributed throughout AB cultures and surprisingly, many appeared viable at this stage, and in a few cases appeared to adhere to the outer surface of local neurons. As expected, many RBCs were not well adhered to the culture dish and these likely included dead or dying cells.

To verify that these cells were indeed RBCs, we stained AB cultures with an antibody against carbonic anhydrase II (CAII), an enzyme involved in CO_2 transport by RBCs. Brightly stained, CAII-immunopositive cells were numerous and resembled the putative RBCs seen under phase contrast microscopy (e.g. Figures 6E-G). Double-label immunofluorescence using CAII and tyrosine hydroxylase (TH), a classical marker for type I cells, showed that CAII and TH labeled different cell populations, where the TH-positive type I cells were usually about double the size of the CAII-positive RBCs. It was evident, however, that the repetitive washing involved in immunostaining washed away a significant proportion of the RBCs that were present in living AB cultures.

Evans Blue paraganglia staining

To determine whether blood-borne factors (e.g. ATP) have access to AB paraganglia and local neurons within the left vagus and recurrent laryngeal nerves, we perfused 14 rats with PBS, followed by Evans Blue and paraformaldehyde, via intra-cardiac injection. Evans Blue is an acidic diazo dye which, when introduced into the circulation, labels paraganglia more rapidly and distinctly than the adjacent neural tissues because of their relatively high vascular permeability (McDonald & Blewett, 1981). Furthermore, when Evans Blue leaves blood vessels and enters the extravascular space, it is fluorescent under green illumination (i.e. 594 nm excitation, Texas Red; McDonald & Blewett, 1981).

Of the 14 rats subjected to this procedure, successful perfusion was evident in 8 animals based on blue discolouration of the whiskers, nose, and paws. In the excised left vagus nerve and RLN, the darkest staining was typically localized to the region between these nerves; however, discrete blue "spots" were not visible in this area using regular light microscopy. Rather, the nerves emerging from the main vagal trunk, particularly the RLN and presumably the aortic nerve, were diffusely stained blue, and blue-stained pockets were most common in or at the periphery of these nerve branches. Discrete blue staining was less common within the vagal trunk itself.

Under epifluorescence illumination, it was evident that the blue-stained pockets (presumptive paraganglia) were not themselves fluorescent, but rather they were surrounded by red fluorescence. This suggested the presence of extravascular Evans Blue dye in the interstitium surrounding type I cell clusters, as illustrated in Figure 7A-C. An interesting feature was the frequent presence of fluorescent neuronal cell bodies within or adjacent to the fine nerve branches emerging from the main vagal trunk. In a few cases, red fluorescent neurons were associated with what appeared to be small blood vessels (e.g. Figure 7I).

Three whole mounts that had conspicuous blue labeling of presumptive paraganglia were immunostained using antibodies against TH and the P2X2 purinoceptor subunit. In all 3 samples, the area identified by blue staining was found to correspond with TH-immunoreactive type I cells (e.g. Figure 7F, L), and in 2 cases, the TH-positive type I cells were surrounded by dense P2X2-immunoreactive nerve terminals (e.g. Figure 7L).

DISCUSSION

In this study, we first used a cell culture model of dissociated rat aortic bodies (ABs) derived from the left vagus nerve and attached recurrent laryngeal nerve (RLN) to characterize the ATP- and ACh-sensitivities of local AB neurons. This was of interest because at least some of these putative sensory neurons appear to contact chemoreceptor type I cells *in situ* and *in vitro* (Piskuric *et al.*, 2011), and co-release of ATP and ACh from type I cells was a plausible mechanism mediating sensory transmission at such synapses (Nurse, 2010; Piskuric *et al.*, 2011; Piskuric & Nurse, 2012). Moreover, we previously showed that subpopulations of these neurons expressed purinergic P2X2 and P2X3 receptors *in situ*, whereas all were immunopositive for the vesicular ACh transporter (VAChT) (Piskuric *et al.*, 2011). The electrophysiological and Ca^{2+} imaging data presented here provide functional corroboration of our immunolocalization results, demonstrating that ~45% of local neurons express heteromeric P2X2/3 purinoceptors

whereas *all* local neurons express nicotinic ACh receptors. Furthermore, juxtaposed neurons in short-term (24 hr) culture demonstrated bidirectional, resistive, electrical coupling, which would allow for synchronous activation of most or all local AB neurons. Using Evans Blue staining, we also showed that AB type I cells, local neurons, and P2X2-expressing nerve terminals, have access to factors in the microcirculation, such as ATP released from red blood cells (RBCs). Interestingly, apparently 'viable' RBCs were abundant in AB cultures at 1 d *in vitro*, a feature that is uncharacteristic of comparable cultures of the related carotid body (CB), despite its rich vascularization (our routine observations).

Expression of purinergic P2X receptors in aortic body neurons

In the present study, ~45% of AB neurons were found to be homogeneous in terms of their ATP-sensitivity. In general, ATP evoked brief action potential firing and a large, sustained depolarization, in most of the responsive neurons. Under voltage clamp, ATP evoked slowly desensitizing inward currents with an EC_{50} of ~1.0 μM, suggesting they were mediated by homomeric P2X2 (EC_{50} = 0.5 μM), homomeric P2X3 (EC_{50} = 1.2 μM), and/or heteromeric P2X2/3 receptors (EC_{50} = 0.7 μM) (Jarvis & Khakh, 2009). The presence of heteromeric P2X2/3 receptors was confirmed in a few cases where α,β-MeATP evoked slowly desensitizing inward currents. Taken together, these data are consistent with our previous immunofluoescence studies demonstrating that subsets of local neurons express P2X2 and P2X3 purinergic receptors (Piskuric *et al.*, 2011). Notably, the percentage of ATP-sensitive neurons (~45%) was greater than the percentage of neurons that were immunopositive for P2X2 (25%) and P2X3 (25%) subunits. This could be explained by the fact that the P2X2- and P2X3-expressing subpopulations are incompletely overlapping, or, may simply be the result of strong synaptic interactions (e.g. chemical and/or electrical coupling) between ATP-sensitive and ATP-insensitive neurons (see below). Ratiometric Ca^{2+} imaging experiments also demonstrated that ~45% of neurons responded to ATP with a robust rise in $[Ca^{2+}]_i$.

However, although ~80% of the ATP-evoked Ca^{2+} response was blocked in the absence of extracellular Ca^{2+}, consistent with a major role for P2X receptors, there was often a residual Ca^{2+} signal, suggesting Ca^{2+} release from intracellular stores via P2Y receptors. Though the identity of the P2Y receptor(s) is unknown, the fact that a few ATP-sensitive neurons also responded to UTP suggests the presence of P2Y2/4 receptors.

Evidence for synaptic interactions among AB neurons

During simultaneous paired recordings we obtained evidence for strong electrical coupling between near or juxtaposed AB neurons in culture. In 7 cases electrical coupling was bidirectional and resistive and the coupling coefficient was >0.8. Based on our routine observations that dissociation of AB neurons was often incomplete after initial plating, we speculate that electrical coupling between neurons was already present *in situ* and simply carried into culture, rather that the result of *de novo* synapse formation *in vitro*. It is noteworthy that local AB neurons *in situ*, particularly those at the bifurcation of the vagus nerve and RLN, are always found in compact groupings (Piskuric *et al.*, 2011). While the presence of strong electrical coupling may have masked our ability to detect chemical transmission among local neurons, it is plausible that the latter may also occur. First, previous immunofluorescence studies suggest the possibility of a cholinergic circuit involving local neurons, given the localization of VAChT in their cell bodies as well as in surrounding nerve terminals (Dvorakova & Kummer, 2005; Piskuric *et al.*, 2011). Second, in the present study, brief application of ACh (30 s, 10 μM) elicited large and rapid increases in cytosolic [Ca^{2+}] in almost all AB neurons, and these responses were mimicked by nicotine and blocked by the general nicotinic ACh receptor blocker, mecamylamine. Thus, it is plausible that nicotinic cholinergic synapses may form between local neurons; however, this point requires validation in further studies.

Potential role of red blood cells and local neurons in sensing of O_2 content by the AB

Despite the proposed functional differences between AB and CB chemoreceptors, i.e. that the AB senses O_2 content whereas the CB senses O_2 tension, an underlying mechanism to explain these differences remains elusive. Indeed in our recent study, there were no obvious differences between the cellular responses of AB and CB type I cells to chemostimuli such as hypoxia and acidic hypercapnia (Piskuric *et al.*, 2011), suggesting involvement of other factors. Given that red blood cells (RBCs) determine the O_2 content of the blood (via hemoglobin, Hb), we focused on the RBC as a potential contributor to AB chemosensing. It is noteworthy that much current research is directed at understanding the role of RBCs as O_2 sensors, which release ATP in response to hypoxia as a potential mechanism for matching microvascular O_2 supply with local tissue demand (Ellsworth *et al.*, 2009). Given these considerations, the RBC appears perfectly suited to link O_2 content and AB activation, an idea that was strengthened by our observation that unlike CB cultures at 24 hr *in vitro*, AB cultures contained abundant RBCs that appeared viable. While the reasons for this difference between CB and AB cultures are presently unknown, we hypothesized that ATP released from RBCs during hypoxia might contribute to the sensing of O_2 content by acting directly on purinergic P2X-expressing local neurons (see above). This hypothesis necessitates that ATP in the microcirculation has access to the nerve cell bodies and/or terminals of local neurons. Indeed, we found that intra-cardiac perfusion of juvenile rats with Evans Blue led to diffuse blue staining near the bifurcation of the vagus nerve and RLN, and discrete blue spots (presumptive paraganglia) were commonly seen within the RLN (see also, McDonald & Blewett, 1981). Furthermore, under epifluorescence microscopy, it appeared that the blue colour of paraganglia was due to extravascular dye, which surrounded type I cells in the interstitium. Interestingly, the somata of local neurons within the vagus nerve and RLN were also fluorescently labeled, and in addition, there was bright red fluorescence in the surrounding interstitial space (for comparison, see McDonald & Blewett, 1981). We speculate that this is due to retrograde dye uptake by local neurons, a phenomenon that

has been previously reported in other neurons following intravenous or intracardiac injection of Evans Blue (Weiss & Cobbett, 1992; del Valle *et al.*, 2008). This suggests that the nerve terminals of local neurons had access to large dye molecules that left the blood vessels, consistent with the idea that ATP released from RBCs can directly activate local neurons and/or their endings. Moreover, immunolabeling of blue-stained whole mounts confirmed that the blue stained areas did in fact contain TH-immunopositive type I cells, which were contacted by P2X2-immunoreactive nerve terminals.

A physiological model for activation of AB neurons

We propose the following "working model" of O_2 content-sensing by the AB. Under normal physiological conditions, blood flow to the AB is limiting rendering the tissue slightly hypoxic, especially when combined with the high O_2 consumption of chemoreceptor type I cells (see Gonzalez *et al.*, 1994). Thus, the AB depends on oxygenated Hb delivered by RBCs to satisfy its energy demands. In response to physiological stimuli that reduce hemoglobin saturation, such as severe hypoxia (decreased PO_2) or a decrease in O_2 delivery to the tissue, RBCs release ATP into the microcirculation. Because of the high permeability of blood vessels within AB paraganglia, ATP released from RBCs floods the interstitium surrounding AB type I cells and local neurons. As a result, local neurons that express P2X2/3 receptors are activated, and in turn spread the excitatory signal to other neurons (including ATP-insensitive ones) via electrical coupling and, possibly, cholinergic synapses. Simultaneously, type I cells release ATP and ACh in response to hypoxia, aiding neuronal activation. Finally, local neurons transmit this chemosensory information to their targets, which may include the central nervous system where they could initiate cardiovascular reflexes, or the local vasculature. In fact, a recent study found that P2X2- and P2X3-immunoreactive nerve fibre terminals are distributed widely in the aortic arch, atrium, vena cava, and ventricles (Song *et al.*, 2012). It is plausible that AB neurons could modulate the parasympathetic cardiac ganglia in response to sensory stimuli, ultimately playing a role in regulation of

the heart. It should be noted that local AB neurons are central to this model; indeed, they are a constant feature of the AB paraganglion found at the bifurcation of the left vagus nerve and RLN.

Conclusion

In this study, we show that isolated aortic body (AB) neurons, derived from the left vagus and recurrent laryngeal nerves, are excited by ATP and ACh acting via P2X2/3 and nicotinic receptors, respectively. These neurons also exhibit strong bi-directional electrical coupling, and the potential for cholinergic synaptic interactions, allowing for the coordination of signaling within the local neuronal circuit. Furthermore, local neurons and purinergic nerve terminals *in vivo* have access to diffusible factors in the circulation. Based on these findings, we suggest that ATP released from red blood cells in response to hypoxia is the main link between reductions in O_2 content and activation of the entire circuit of local AB neurons. This proposal suggests a sensory function among local neurons, whose central and/or peripheral projections may help control cardiovascular reflexes in conditions such as anemia and hypotension.

ACKNOWLEDGEMENTS

N.A.P. was supported by a Vanier Canada Graduate Scholarship from the Natural Sciences and Engineering Research Council of Canada (NSERC).

Figure 1. ATP-evoked responses of aortic body (AB) neurons after 24 hr in culture. **A**, Current-clamp recordings illustrating the variable effects of ATP on the membrane potential of AB neurons. Most ATP-sensitive neurons responded with an initial burst of action potentials followed by a sustained depolarization (i), whereas a minority of responsive cells showed a slow recovery towards the resting potential after the initial burst of action potentials (ii). The remaining neurons (55%) did not respond to 10 μM ATP (iii). **B**, ATP-evoked inward currents at -60 mV in response to increasing doses of ATP. A dose-response curve, fitted with a nonlinear regression (Hill slope of 1.0; EC_{50} = 1.0 μM) is shown for a group of 7 neurons in (**C**). **D**, Inward currents evoked by 10 μM ATP at different membrane potentials. **F**, I-V plot for currents evoked by 10 μM ATP after correcting for the junction potential (+14 mV), yields a reversal potential, E_R, near +10 mV (n=6); note the presence of strong inward rectification above 0 mV.

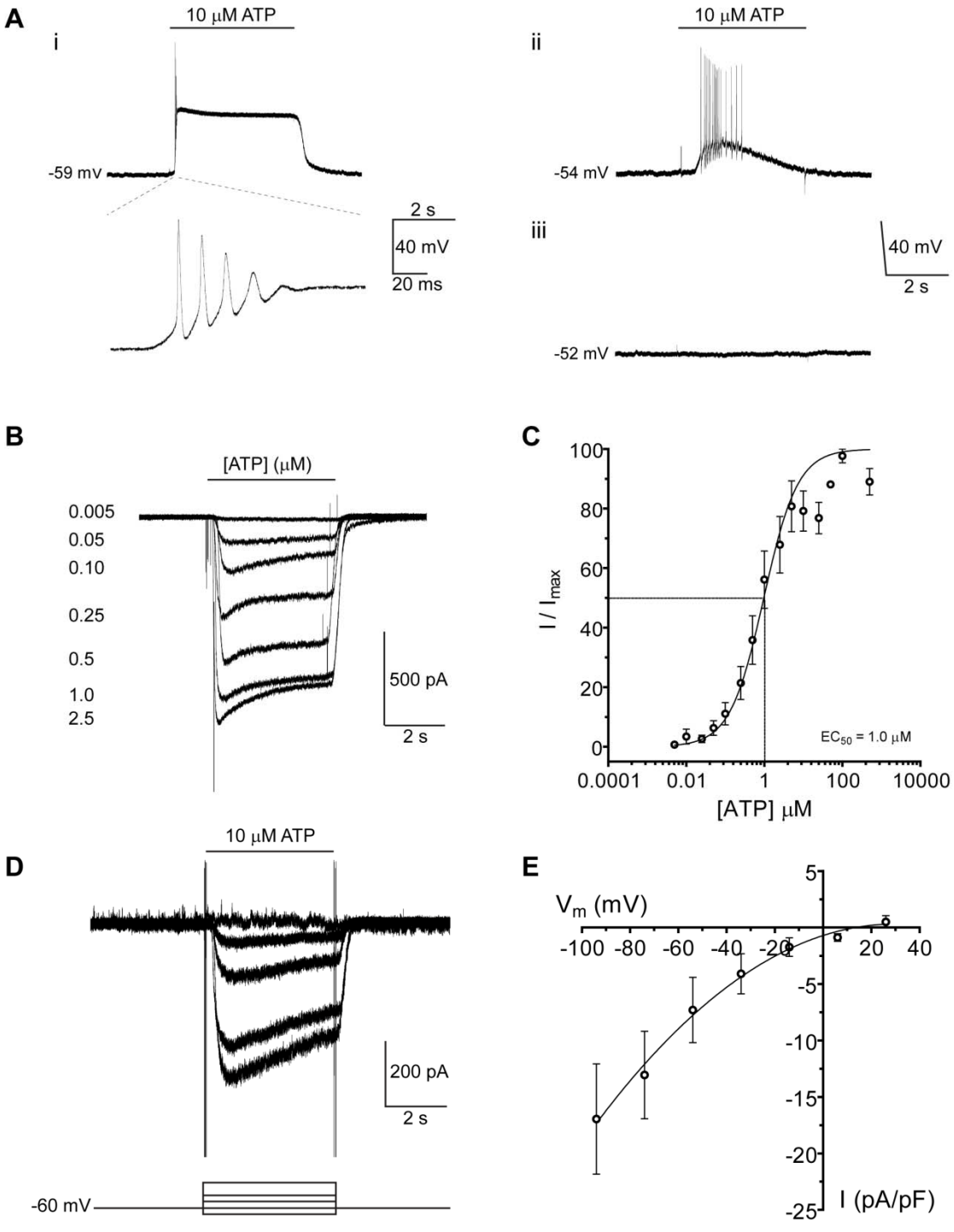
A
i
10 μM ATP
-59 mv
2 s
40 mV
20 ms
ii
10 μM ATP
-54 mV
iii
40 mV
2 s
-52 mV
B
[ATP] (μM)
0.005
0.05
0.10
0.25
0.5
1.0
2.5
500 pA
2 s
C
I / I max
100
80
60
40
20
0
0.0001
0.01
1
100
10000
[ATP] μM
EC50 = 1.0 μM
D
10 μM ATP
200 pA
2 s
-60 mV
E
Vm (mV)
-100 -80 -60 -40 -20 20 40
5
-5
-10
-15
-20
-25
I (pA/pF)

Figure 2. Heteromeric P2X2/3 purinoceptors contribute to the ATP responses in local neurons.

A, In 4 neurons that respond to ATP (*left*), α,β-MeATP causes transient action potential firing and sustained membrane depolarization (*right*). **B**, At a holding potential of -60 mV, both ATP and α,β-MeATP induce fast inward currents that are slowly desensitizing, suggestive of heteromeric P2X2/3 purinoceptors. **C**, The dose-response curve for α,β-MeATP was fitted with a nonlinear regression, with a Hill slope of 1.0 and an EC_{50} of ~3.9 μM (n=2).

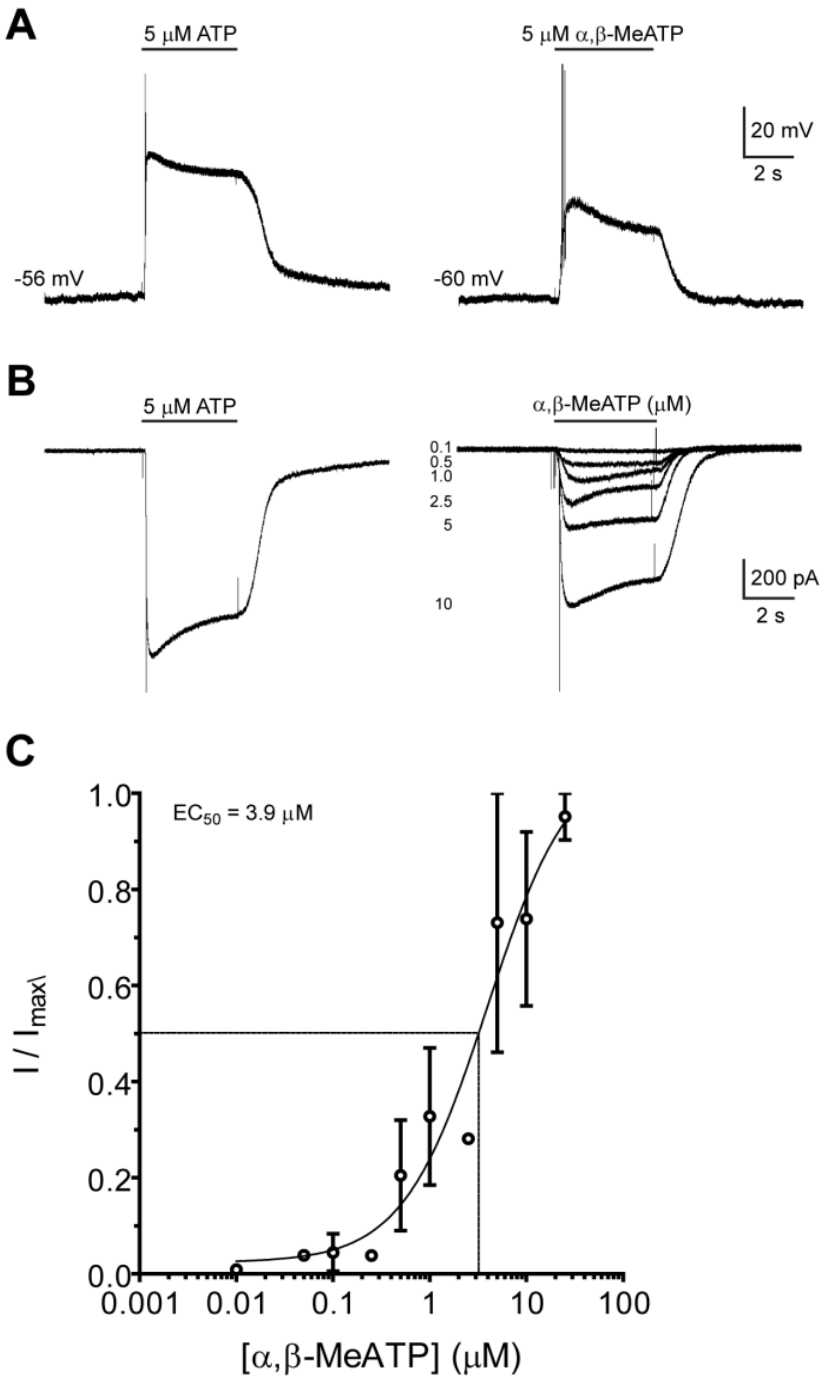
A
5 μM ATP
5 μM α,β-MeATP
20 mV
2 s
-56 mV
-60 mV
B
5 μM ATP
α,β-MeATP (μM)
0.1
0.5
1.0
2.5
5
10
200 pA
2 s
C
EC50 = 3.9 μM
I / Imax\
1.0
0.8
0.6
0.4
0.2
0.0
0.001
0.01
0.1
1
10
100
[α,β-MeATP] (μM)

Figure 3. Intracellular Ca^{2+} responses of aortic body (AB) neurons to ATP.
A, Simultaneous intracellular Ca^{2+} recordings from 2 AB neurons illustrating variable responses to ATP. Note that only one neuron gives a robust response to increasing doses of ATP (red trace), whereas the other neuron is relatively unresponsive. **B**, Dose-dependent increases in cytosolic [Ca^{2+}] evoked by ATP in responsive neurons; combined data from 36 neurons gives an EC_{50} of ~1.9 μM. **C**, Exemplar trace showing the effect of extracellular Ca^{2+} removal on the ATP-induced Ca^{2+} response; summarized data for 6 neurons are shown in (**D**). Note that ~22% of the ATP-evoked responnse remains in Ca^{2+}-free media, suggesting the presence of P2Y receptors.

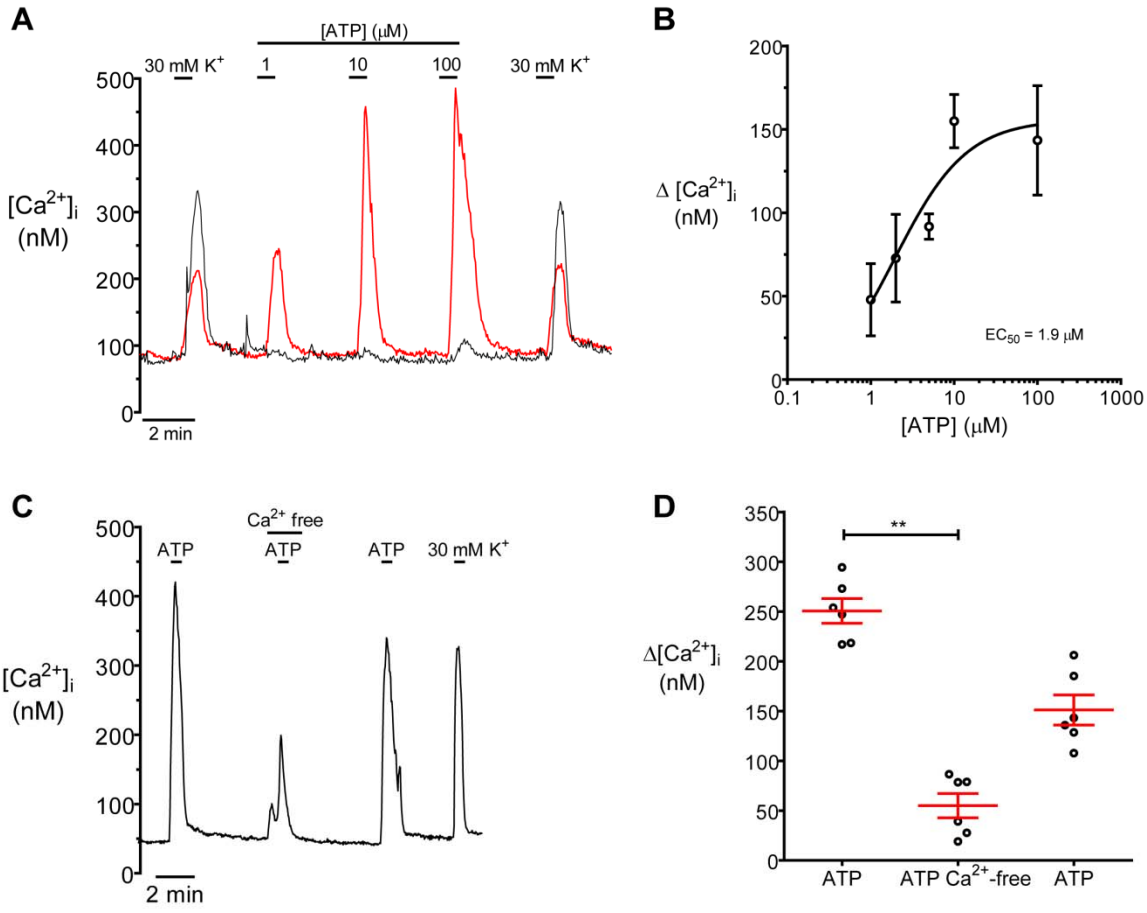
A
[ATP] (μM)
30 mM K+
1
10
100
30 mM K+
[Ca2+]i (nM)
500
400
300
200
100
0
2 min
B
Δ [Ca2+]i (nM)
200
150
100
50
0
EC50 = 1.9 μM
0.1
1
10
100
1000
[ATP] (μM)
C
Ca2+ free
ATP
ATP
ATP
30 mM K+
[Ca2+]i (nM)
500
400
300
200
100
0
2 min
D
**
Δ[Ca2+]i (nM)
350
300
250
200
150
100
50
0
ATP
ATP Ca2+-free
ATP

Figure 4. Characterization of ACh-evoked Ca^{2+} responses in aortic body (AB) neurons.

A, Intracellular Ca^{2+} responses evoked by 10 μM ACh (left) and 10 μM nicotine (Nic, right) in 3 neurons from different cultures. **B**, Effect of the nicotinic ACh receptor blocker, mecamylamine (mec, 10 μM), on the ACh-induced Ca^{2+} rise in AB neurons; note that mec reversibly blocks the entire Ca^{2+} response. **C**, Example Ca^{2+} traces illustrating that although all neurons are sensitive to nicotinic ACh receptor agonists, e.g. nicotine (Nic), only some are ATP sensitive (upper trace), whereas others are ATP-insensitive (lower trace).

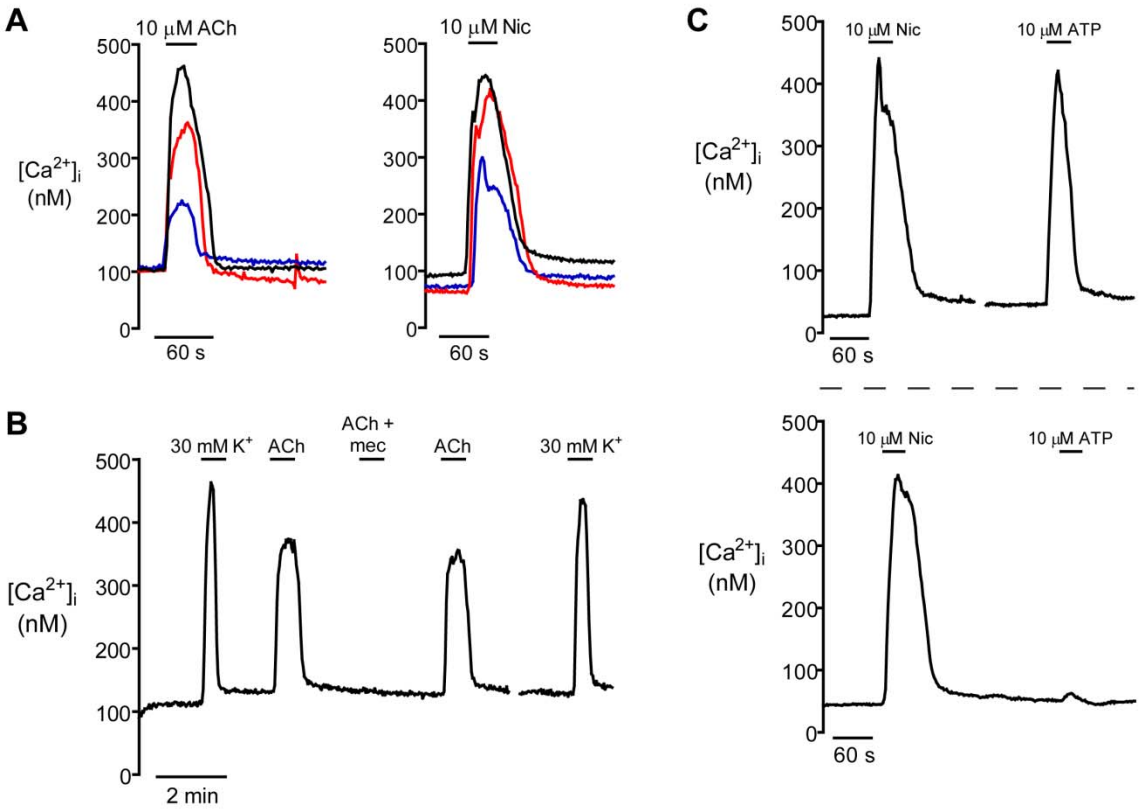
A
10 μM ACh
10 μM Nic
[Ca2+]i (nM)
500
400
300
200
100
0
60 s
B
30 mM K+
ACh
ACh + mec
ACh
30 mM K+
2 min
C
10 μM Nic
10 μM ATP
60 s

Figure 5. Electrical and dye coupling among nearby or juxtaposed aortic body (AB) neurons after 24 hr in culture.

A, **B**, **D**, Simultaneous current-clamp recordings from double-patched AB neurons, N1 and N2; spatial relationship of patched neurons is indicated in (**C**). Injection of 500 ms depolarizing current pulses into one neuron (indicated by the arrow) causes membrane depolarization in that neuron, as well as membrane depolarization of similar size and time course in the nearby neuron. **B**, Hyperpolarizing current pulses (500 ms) injected into either N1 or N2 causes membrane hyperpolarization in both neurons. **C**, Confocal image showing green fluorescence in N1, N2, and a third neuron, N3, caused by Lucifer Yellow (0.5%) injection into N2 only. **D**, Lack of effect of ATP (10 μM) on the membrane potential of neurons N1 and N2 indicated in **C**. **F**, ***left***, Phase contrast micrograph showing a group of 3 juxtaposed AB neurons from a different culture; ***right***, simultaneous current-clamp recordings from neurons N1 and N2 reveal almost identical ATP-evoked membrane depolarizations with similar latencies; the high incidence of electrical synapses means that only one of the 3 neurons need be directly ATP-sensitive, whereas the response of the others may be indirect, i.e. secondary to electrical coupling.

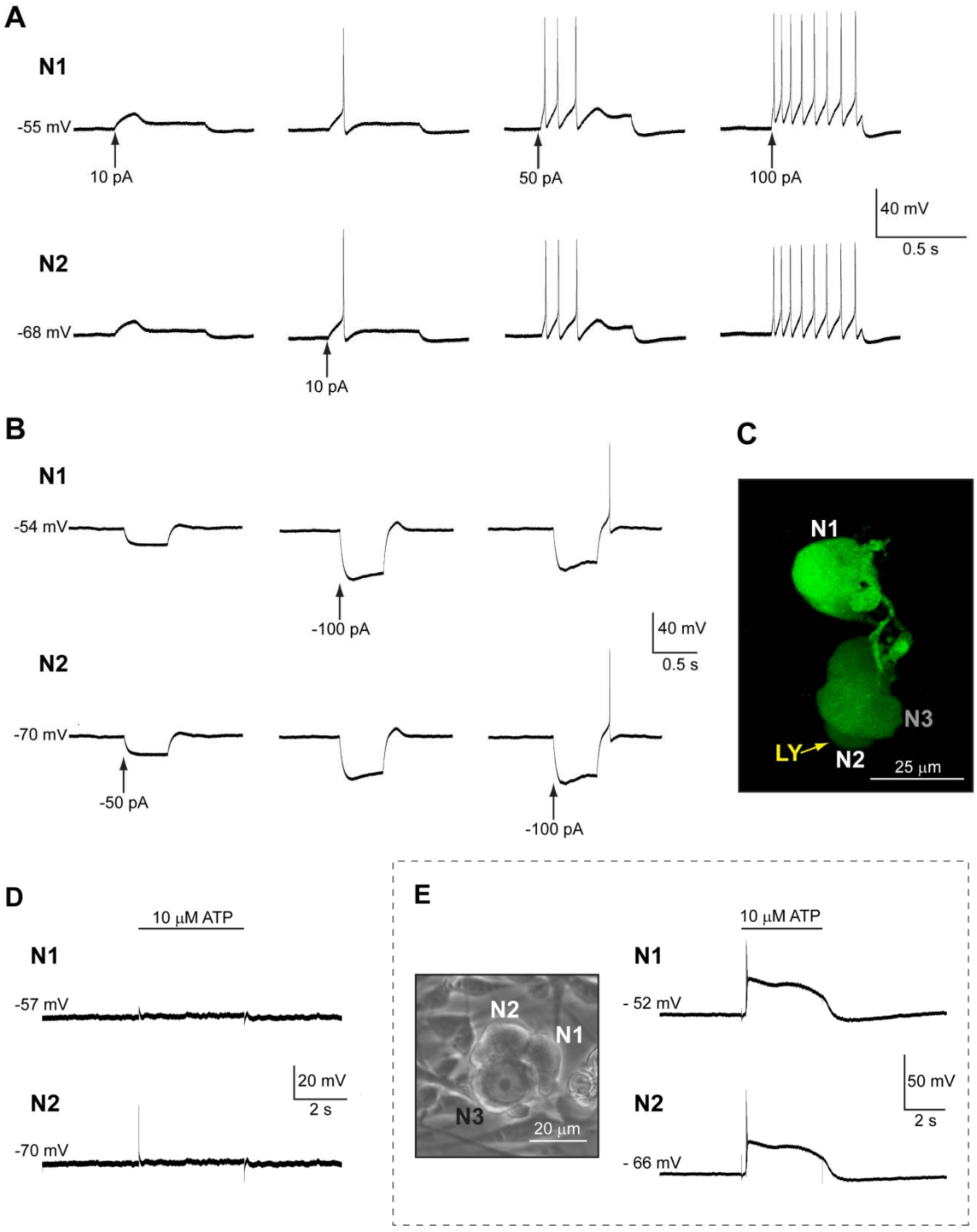
A
N1
-55 mV
10 pA
50 pA
100 pA
40 mV
0.5 s
N2
-68 mV
10 pA
B
N1
-54 mV
-100 pA
40 mV
0.5 s
N2
-70 mV
-50 pA
-100 pA
C
N1
N3
LY
N2
25 μm
D
10 μM ATP
N1
-57 mV
20 mV
2 s
N2
-70 mV
E
N2
N1
N3
20 μm
10 μM ATP
N1
- 52 mV
50 mV
2 s
N2
- 66 mV

Figure 6. Presence of viable red blood cells (RBCs) in 1 d old aortic body (AB) cultures.

A-**C**, Phase contrast micrographs of RBCs in 1 d old cultures; in **C**, an RBC (arrow) is located close to the soma of an AB neuron with a distinct nucleus and nucleolus. **D**, Histogram illustrating the size distribution of RBCs in AB cultures; RBC diameter is normally distributed with a mean of ~5.9 μm (n=300). **E**, High-magnification confocal image of an RBC immunopositive for carbonic anhydrase II (CAII), an enzyme involved in CO_2 transport by RBCs; note CAII distribution around the outer periphery of the RBC cytoplasm close to the plasma membrane, as expected for viable RBCs (Vince & Reithmeier, 1998). The random distribution of CAII-immunoreactive RBCs in an AB culture is shown in **G**. **F**, Double-labeling of RBCs and type I cells using CAII (green) and a typical type I cell marker, tyrosine hydroxylase (TH, red), shows the two markers are present in distinct cell populations.

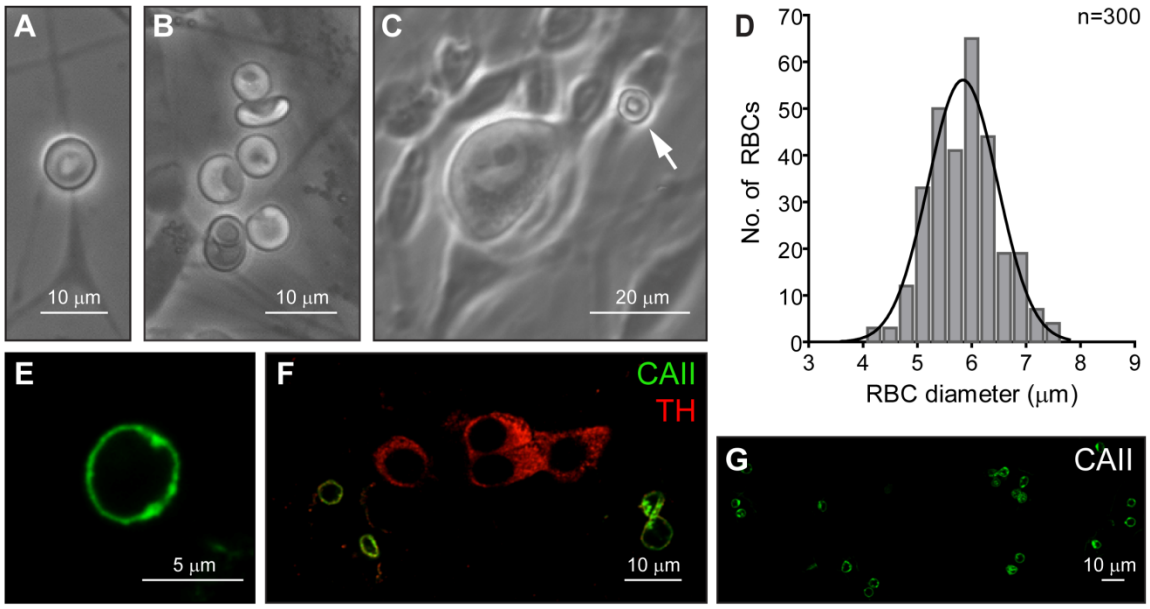
A
10 μm
B
10 μm
C
20 μm
D
n=300
No. of RBCs
RBC diameter (μm)
E
5 μm
F
CAII
TH
10 μm
G
CAII
10 μm

Figure 7. Evans Blue dye staining of aortic body (AB) paraganglia and endogenous neurons.

A, **D**, **G**, **K**, Brightfield (BF) images of left vagus and recurrent laryngeal nerves, labeled by intra-cardiac perfusion of Evans Blue dye. **A-C**, Presumptive AB paraganglion within the cervical vagus nerve labeled by Evans Blue. Texas Red epifluorescence (TR, 594 nm excitation) revealed the presence of extravascular dye in the interstitium surrounding putative type I cells; an overlay of the brightfield and epifluorescence images is shown in **C**. **D-F**, Attached to the recurrent laryngeal nerve near its bifurcation with the main vagal trunk, 3 blue-stained paraganglia, one of which is encircled (**D**), are not fluorescent themselves, but are adjacent to a group of fluorescent presumptive neuronal cell bodies (arrows) (**E**). **F**, Confocal image of the area in **D-E** after immunostaining with tyrosine hydroxylase (TH); note that the Evans Blue stained paraganglia are immunopositive for TH. Large-diameter TH-negative background cells are neuronal cell bodies. **G**, Pocket of blue-stained presumptive neurons embedded in the vagus nerve, just beyond its bifurcation with the recurrent laryngeal nerve. Neurons in **G** exhibit red fluorescence in **H**; the brightest fluorescence is in extravascular dye in the surrounding interstitium (e.g. arrows). A similar result is shown in **J**; note especially red fluorescent dye in the interstitium. **I**, A group of neuronal cell bodies within a thin branch of the vagus nerve shows red fluorescence. Note the presence of a putative blood vessel (bv, arrows) surrounding the neurons. **K**, Blue-stained paraganglion in a nerve fibre emerging from the recurrent laryngeal nerve. **L**, Z-projection of 3 consecutive confocal images of the paraganglion shown in **K**, after double-immunolabeling with TH and P2X2. **L *inset*** is a magnified view of part of the paraganglion in a different optical plane.

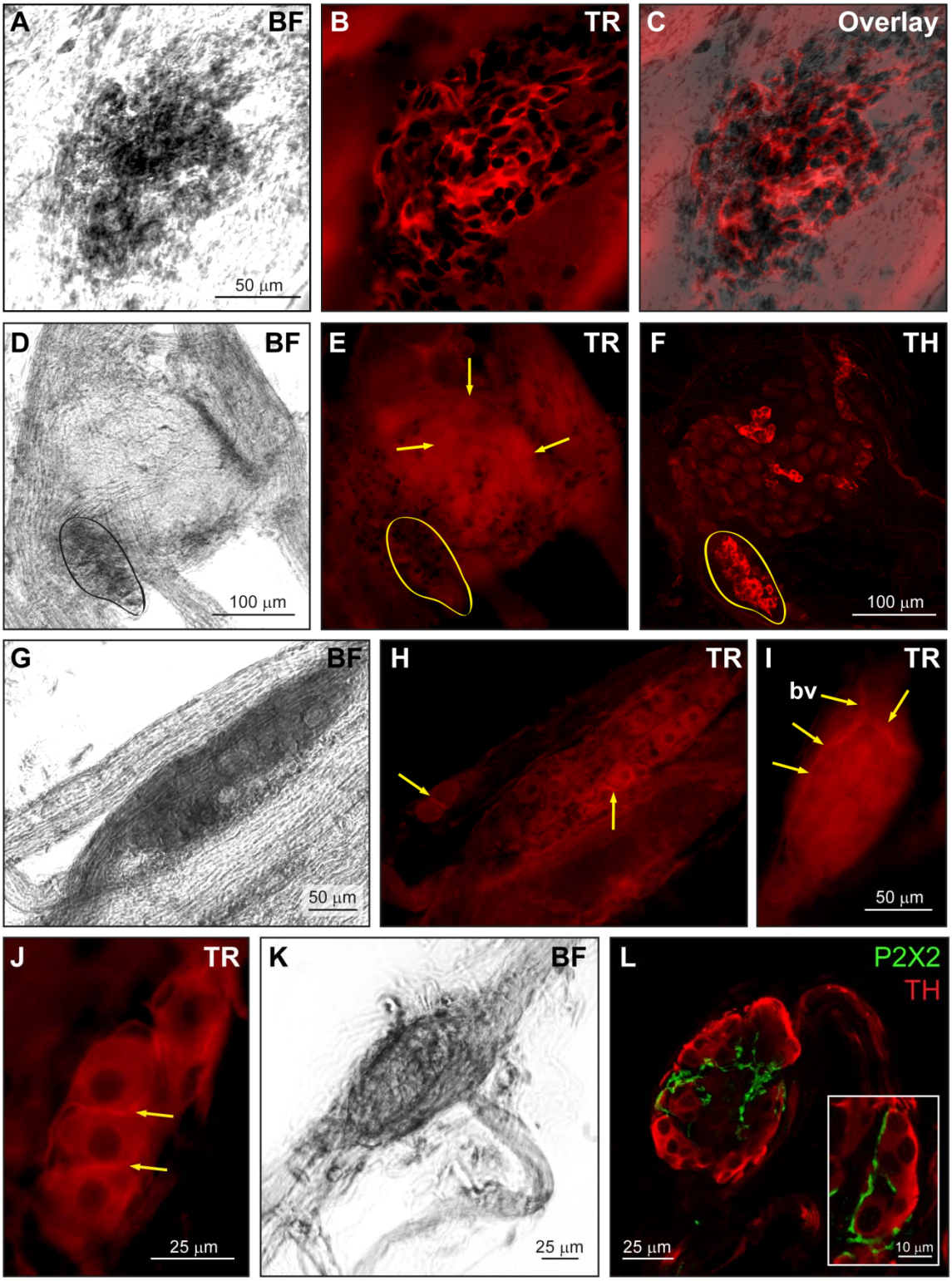
A
BF
50 µm
B
TR
C
Overlay
D
BF
100 µm
E
TR
F
TH
100 µm
G
BF
50 µm
H
TR
I
TR
bv
50 µm
J
TR
25 µm
K
BF
25 µm
L
P2X2
TH
25 µm
10 µm

Figure 8. Proposed mechanism by which the aortic body (AB) senses O_2 content. The aortic body (AB) at the bifurcation of the vagus and recurrent laryngeal nerves consists of a large type I cell cluster amid many neuronal cell bodies. Type I cells are presumed to release neurotransmitters including ACh and ATP, as suggested by the expression of immunoreactivity against the vesicular ACh transporter (VAChT) and by the presence of P2X2- and P2X3-immunoreactive (IR) nerve fibres and endings around type I clusters (Piskuric *et al.*, 2011). Some local neurons are excited by ATP via purinergic P2X2/3-containing receptors. All neurons are VAChT-IR and express functional nicotinic ACh receptors. This paraganglion is penetrated by fenestrated capillaries permeable to large molecules such as Evans Blue and ATP. We propose that in response to hypoxia, type I cells release ACh and ATP onto afferent nerve endings. At O_2 tensions <45 mmHg, below which significant unloading of O_2 from hemoglobin occurs, red blood cells (RBCs) release ATP into the microcirculation (Jagger *et al.*, 2001). ATP leaves the blood vessels through fenestrated capillaries, and floods the interstitium surrounding local neurons and their terminals. ATP binds to purinergic P2X2/3 receptors on a subset of local neurons causing excitation and action potential propagation. This signal is then transmitted to other local neurons, including ATP-insensitive ones, via electrical and possibly chemical (cholinergic) synapses, causing a coordinated electrical response to the hypoxic stimulus. Notably, ATP released from RBCs could also activate P2X2/3-expressing nodose ganglion neurons (Burnstock, 2009) whose axons terminate on AB paraganglia (Hansen, 1981; Kummer & Neuhuber, 1989; Dahlqvist *et al.*, 1994). We suggest this is the principle mechanism by which the AB senses O_2 content. Finally, endogenous neurons transmit chemosensory information to their targets in the central nervous system or local vasculature.

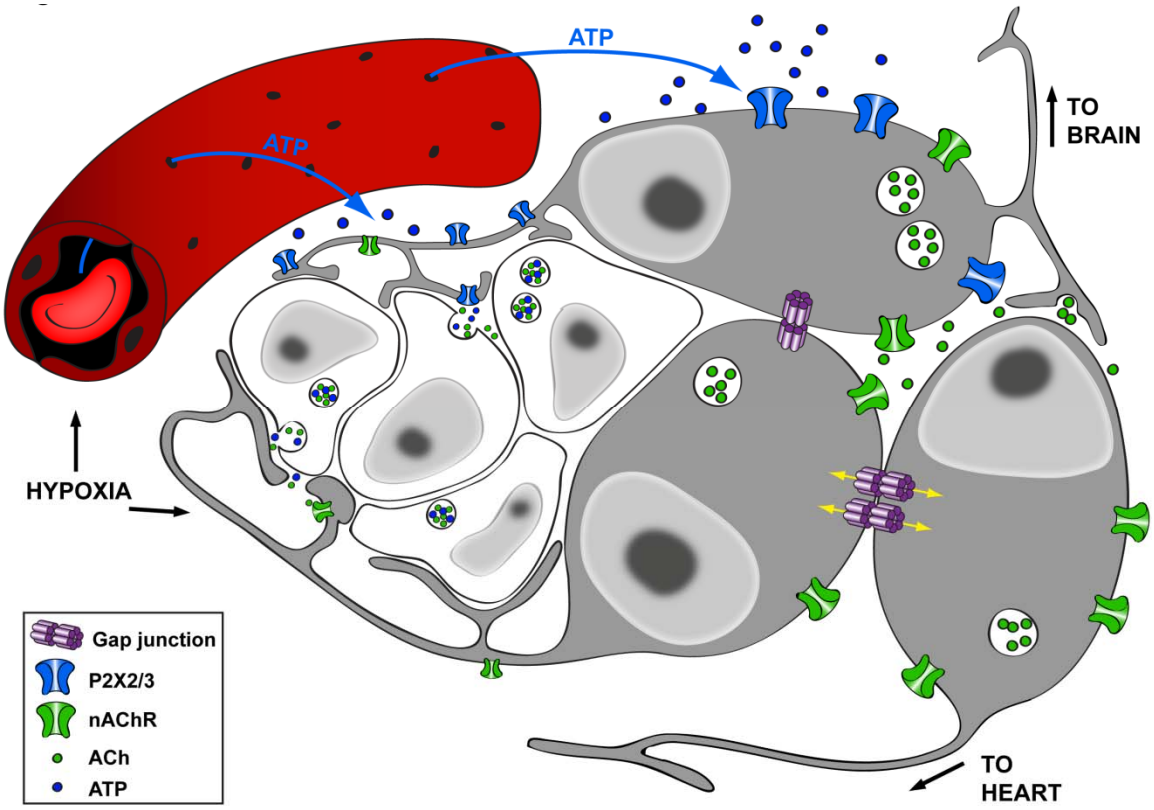
ATP
ATP
TO
BRAIN
HYPOXIA
Gap junction
P2X2/3
nAChR
ACh
ATP
TO
HEART

CHAPTER 5

General Discussion

Although the presence of chemoreceptors in the aortic arch region has been known for some 85 years, their functional significance is still a matter of debate. Anatomically, paraganglia that conspicuously resemble the carotid body (CB) chemoreceptors exist diffusely within the thoracic and cervical nerves as well as in the cardiac vasculature, though it is unknown which, if any, of these so-called aortic bodies (ABs) possess a chemoreceptor function. In the cat and rat, respiratory stimulants (e.g. hypoxia or cyanide) excite the aortic nerve (a branch of the vagus nerve) (Lahiri *et al.*, 1981a; Brophy *et al.*, 1999), which comprises the axons of sensory afferent neurons whose cell bodies lie in the nodose ganglion (Hansen, 1981; Kummer & Neuhuber, 1989). However, it is unclear whether this nerve activity translates into physiologically relevant systemic reflexes, especially in the rat, which is thought to be devoid of "functional" ABs (Kobayashi *et al.*, 1999). In the cat and dog, hypoxia-evoked AB activation initiates primarily cardiovascular reflexes (i.e. hypertension) (Comroe, 1939), an appropriate response given that AB chemoreceptors are hypothesized to be sensitive to O_2 *content*, and therefore function as circulatory O_2 monitors (Lahiri *et al.*, 1981b). Still, the physiological function of AB chemoreceptors remained speculative, partly because, prior to this thesis, the direct chemosensitivity of the putative receptor type I (glomus) cells was never demonstrated in mammals. Moreover, the general assumption that AB chemosensing mechanisms are analogous to those of the CBs could not explain how the

ABs sense O_2 content whereas the CBs sense PO_2. This thesis provides novel insights into both of these areas.

In order to generate a relevant *in vitro* model of mammalian ABs, I first investigated the anatomy of the juvenile rat AB via confocal microscopic examination of immunolabeled left vagus nerve and recurrent laryngeal nerve (RLN) whole mounts (Chapter 2). Consistent with previous reports, a relatively large AB was regularly found at the bifurcation of these nerves; notably, many (>30) neuronal cell bodies were located at the periphery of this paraganglion (Piskuric *et al.*, 2011). A novel role for ATP as a putative AB neurotransmitter emerged from the finding that P2X2- and P2X3-immunoreactive nerve fibres and terminals intimately surrounded type I cells; moreover, local, P2X2- and P2X3-immunopositive neurons appeared to be a source of at least part of this innervation. Upon dissociation of the vagus nerve and RLN, both AB type I cells as well as local neurons survived in short term culture, and this proved advantageous for my studies. Moreover, intracellular Ca^{2+} measurements revealed that both AB receptor type I cells and local neurons responded to multiple chemostimuli, including hypoxia, hypercapnia and acidity, and the type I cell responses were not obviously different from those of CB type I cells derived from the same animals (Piskuric & Nurse, 2012). Although not proven, the functional demonstration of heteromeric P2X2/3 purinoceptors on some, and nicotinic ACh receptors (nAChRs) on all, cultured neurons suggested that ATP and ACh could mediate chemotransmission from type I cells to local (sensory) neurons, as is the case in the CB. Finally, the unexpected observation of apparently viable red blood cells (RBCs) in AB cultures, along with the demonstration that AB paraganglia have access to blood-borne factors, suggested an alternate route for the activation of local purinergic neurons via hypoxia-induced ATP release from RBCs. Taken together, these data show for the first time that AB type I cells are chemosensitive at the cellular level, and suggest an important role for ATP in AB chemotransmission. The implication that RBCs contribute to the ATP signal provides an explanation for how the ABs might sense O_2 content and delivery, a function that is unique to the AB chemoreceptors.

Ca^{2+}_i responses of CB versus AB type I cells to chemostimuli

Chemoreceptor (type I) cells of the mammalian CB, which are developmentally and functionally related to AB type I cells, respond to chemostimuli via cellular mechanisms that converge on increases in cytosolic Ca^{2+} concentration, $[Ca^{2+}]_i$. Indeed, Ca^{2+}_i plays a fundamental role in stimulus-secretion coupling by triggering the exocytotic machinery to induce vesicle fusion (see Pang & Sudhof, 2010). A vital role for Ca^{2+}_i in CB neurosecretion was demonstrated in rabbit CB type I cells, in which cytosolic $[Ca^{2+}]$ and catecholamine secretion were simultaneously recorded. Hypoxia caused an increase in $[Ca^{2+}]_i$ that was coincident with catecholamine secretion, and both of these responses could be blocked with the non-selective voltage-gated Ca^{2+} channel antagonist, Ni^{2+} (Urena *et al.*, 1994). The release of other CB neurotransmitters, including ATP and adenosine, also depends upon extracellular Ca^{2+} entry through voltage-gated channels (Buttigieg & Nurse, 2004; Conde & Monteiro, 2006).

In neonatal rat CB type I cells, low PO_2 induces a rise in $[Ca^{2+}]_i$ that is graded to the degree of hypoxia, whereas acidic stimuli (high PCO_2 and/or low pH_e) produce effects on $[Ca^{2+}]_i$ that correlate inversely with their effects on pH_i (Buckler & Vaughan-Jones, 1993; Buckler *et al.*, 1993; Buckler & Vaughan-Jones, 1994a, b). Though the kinetics of the Ca^{2+}_i responses were not studied in detail, I found that moderate hypoxia (~25 mmHg, pH ~7.4), isohydric hypercapnia (10% CO_2, pH ~7.4), isocapnic acidosis (5% CO_2, pH ~6.8), and acidic hypercapnia (10% CO_2, pH ~7.1) were all effective at eliciting increases in $[Ca^{2+}]_i$ in subsets of AB type I cells from small (<5 cell) clusters (Chapter 3). Importantly, the $[Ca^{2+}]_i$ responses observed in AB type I cells were not obviously different from those in CB type I cells derived from the same animals. Though the percentage of responsive cells appeared low (i.e. range = 29-65% for AB and 45-67% for CB) many contributing factors must be considered. First, in terms of the hypoxia response, several *in vitro* studies have demonstrated that $[Ca^{2+}]_i$ in CB type I cells only begins to increase when the PO_2 is in the range of 20-40 mmHg, even though the CSN discharge rate increases at PO_2 levels between ~70-100 mmHg (see Dasso *et al.*,

2000). It is assumed that this discrepancy between $[Ca^{2+}]_i$ and CSN activity is attributable to PO_2 gradients within the CB; given that the CB capillary PO_2 is ~50-60 mmHg in normoxia, the PO_2 at the receptor cells must be even lower. Second, it is known that CB type I cells have variable thresholds of activation in response to chemostimuli; in one preparation for example, moderate hypoxia (i.e. ~20 mmHg) only activated ~ 60% of *single* CB type I cells (Dasso *et al.*, 2000). Third, the $[Ca^{2+}]_i$ responses of AB type I cells show a reduced chemosensitivity relative to the O_2-sensitive K^+ currents. This reflects the fact that inhibition of K^+ channels occurs upstream of extracellular Ca^{2+} entry, and that in order to observe a cytosolic Ca^{2+} response, the membrane potential must be depolarized enough to reach the threshold of voltage-gated Ca^{2+} channel activation. Finally, it is difficult to compare the proportion of responsive cells from one study to another, since different authors assign different criteria to classify a cell as "responsive". In fact, in most cases, the criteria for classifying a cell as responsive are not described at all.

That the $Ca^{2+}{}_i$ responses of isolated AB type I cells were similar to those of the CB supports the idea that the basic properties of AB and CB receptor cells are not different; rather, it is probably their microenvironment *in vivo* that renders them differentially sensitive to chemostimuli. Indeed, the $Ca^{2+}{}_i$ responses of these two chemoreceptors do not reflect the striking differences between AB and CB chemoafferent activity evoked by hypoxia or hypercapnia (Lahiri *et al.*, 1981a). A future worthwhile experiment would be to generate dose-response curves showing the $[Ca^{2+}]_i$ responses of isolated AB and CB type I cells to various levels of PO_2, and to compare their sensitivities at the cellular level to the sensitivity of their chemoafferent nerves *in vivo*. Interestingly, Lahiri and co-workers found that asphyxia evoked the same level of nerve discharge in both AB and CB chemoafferents, suggesting that the chemoreceptors are equally capable of responding to chemoexcitation (Lahiri *et al.*, 1981a). Perhaps complete asphyxia caused the same level of hypoxia (i.e. anoxia) at the tissue level in both the AB and CB, thereby activating the cells equally. In any case, the demonstration that AB type I cells respond to low PO_2 is consistent with the view that a change in PO_2 secondary to a decrease in arterial O_2 content is actually the adequate stimulus for AB

receptor cells. Nevertheless, this does not preclude the possibility that AB type I cells directly sense blood O_2 content, though this idea remains to be tested.

Neurotransmitter profile and chemosensitivity of local aortic body neurons

The existence and abundance of ganglion cells at the periphery of vagal and laryngeal paraganglia is a unique feature of the AB (McDonald & Blewett, 1981; Kummer & Neuhuber, 1989; Dahlqvist *et al.*, 1994; Dvorakova & Kummer, 2005; Piskuric *et al.*, 2011). In the CB, the ratio of autonomic neurons to type I cells is much lower than in the AB. The conspicuous and consistent presence of local neurons, as well as their ability to survive in cultures of the vagus nerve and RLN (Piskuric *et al.*, 2011; Piskuric & Nurse, 2012), implicates them as important players in AB chemosensing. These endogenous, AB-associated neurons have been variously described as autonomic efferent or sensory, though, prior to this thesis, no physiological evidence existed to support either role.

Neurotransmitter and electrical circuitry of local neurons

If ATP and acetylcholine (ACh) are major excitatory transmitters in the CB, sensory afferent petrosal neurons (PNs) must express the appropriate corresponding receptors. Indeed, molecular and physiological techniques have demonstrated that PNs express functional ionotropic ATP (i.e. P2X) and ACh (i.e. nicotinic) receptors, which are capable of mediating fast, excitatory neurotransmission. As is the case for many peripheral sensory nerves (Burnstock, 2009), PNs express the P2X2 and P2X3 subunits in their cell bodies and nerve endings in heteromeric and possibly homomeric forms (Zhang *et al.*, 2000; Prasad *et al.*, 2001; Rong *et al.*, 2003). Though it is clear that at least some PNs respond to ACh via nicotinic ACh receptor (nAChR) activation (for review, see Shirahata *et al.*, 2007), only the α7 subunit has so far been localized to the nerve terminals surrounding CB type I cells (Shirahata *et al.*, 1998), whereas α3, α4, α7, β2 and β4 are all expressed in the cat petrosal ganglion (Hirasawa *et al.*, 2003).

Using a battery of complementary techniques, I found that ~45% of local AB neurons derived from the left vagus nerve and RLN express functional heteromeric P2X2/3 purinoceptors in 1 d old cultures (Chapter 4). This observation confirmed my previous confocal immunofluorescence results, i.e. that subsets of local neurons adjacent to tyrosine hydroxylase (TH)-positive AB paraganglia were P2X2- and/or P2X3-immunoreactive (Chapter 2). Furthermore, all neurons tested *in vitro* were sensitive to the nAChR agonists, ACh and nicotine, and the ACh responses were completely and reversibly blocked by the nAChR antagonist, mecamylamine (Chapter 4). Therefore, at least in terms of their ATP- and ACh-sensitivity, this subset of local neurons resembles the CB sensory afferents. It is important to note, however, that this receptor profile also coincides with that of CB autonomic *efferent* neurons, which are located in discrete microganglia in the CSN and glossopharyngeal nerve (GPN), i.e. GPN neurons, and at the periphery of the CB. Autonomic efferent GPN neurons express a wide variety of P2X receptor subtypes, including P2X2, P2X3, P2X4, and P2X7, as well as several nAChRs, especially α3β4, and α4β2 (Campanucci *et al.*, 2006; Campanucci *et al.*, 2012). Further studies using natural chemostimuli will be required to decipher whether these ATP- and ACh-sensitive neurons are sensory afferents (see below), autonomic efferents, or even interneurons.

My investigations of the receptor profiles of local neurons provided valuable information regarding the potential neurotransmitter circuitry within the local AB 'microganglion'. That is, in addition to the potential for local neurons to sense ATP and ACh released from type I cells, local neurons may form chemical synapses with each other. Indeed, all local neurons are VAChT-immunoreactive, suggesting that they package ACh for stimulus-evoked release, and all are ACh-sensitive via nAChR (Chapters 2 and 4). I did not test for chemical synapses between neurons in this thesis [(in part because of the confounding presence of electrical coupling (see below)], however, dual patch clamp electrophysiology can be used to address this in future studies. If stimulating one neuron causes a post-synaptic potential in the unstimulated neuron, which is blocked by the nAChR antagonist mecamylamine, this would support the hypothesis of

chemical synapses between neurons. Interestingly, in a dual patch clamp study of similar design, we found that stimulating one neuron caused a potential of similar shape and magnitude in the unstimulated neuron; given the short synaptic delay and the fact that subthreshold depolarizations and hyperpolarizations were transferred to the unstimulated cell, these results suggested the presence of electrical synapses between adjoined or nearby neurons. As far as I am aware, such strong, bidirectional, non-rectifying electrical coupling has not been observed between petrosal ganglion or GPN neurons. It is tempting to speculate that this intercellular signaling between local neurons may be a way of amplifying or coordinating signals within this microganglion. Conceivably, this would be advantageous when transmitting responses from tiny organs, such as the ABs.

Chemosensitivity of aortic body neurons

If local neurons are chemoafferents that receive sensory input from AB type I cells, then in dissociated AB 'co-cultures', neurons that form functional synapses with type I cells should respond (indirectly) to chemoexcitation. Indeed, this is the case for sensory PNs, which when co-cultured with CB type I cells, are electrically excited by a variety of chemostimuli (Zhang *et al.*, 2000; Zhang & Nurse, 2004; Zhang *et al.*, 2007). Using intracellular [Ca^{2+}] measurements as an assay of responsiveness, a significant proportion of local neurons in 1 d old AB cultures were sensitive to hypoxia, isohydric hypercapnia, isocapnic acidosis and acidic hypercapnia; in fact, neuronal $[Ca^{2+}]_i$ responses were often rapid and robust (Chapter 3). Multiple factors may have contributed to the latency and magnitude of the $[Ca^{2+}]_i$ responses, including the strength and number of synaptic connections with activated receptor cells, the distance between the type I cells and the recorded neuron, and the density of voltage-gated Ca^{2+} channels in the neuronal cell body, where the $[Ca^{2+}]_i$ transients were monitored. Unfortunately, there are no comparable studies assaying $[Ca^{2+}]_i$ responses in CB afferent neurons (e.g. PNs) to chemostimuli to which these responses can be compared.

Though consistent with a sensory role, the high frequency of positive $[Ca^{2+}]_i$ responses exhibited by local neurons was surprising, given the low yield of type I cells in

AB cultures. This raised the question whether local neurons are *directly* chemosensitive. I attempted to address this using a combination of purinergic and cholinergic blockers to inhibit the CO_2/H^+-evoked $[Ca^{2+}]_i$ responses in a few neurons; however, the outcome was inconclusive because even though the responses to acidic hypercapnia were inhibited in some cases, they did not recover after washout of the drugs. Ideally, one could address the question of direct chemosensitivity in local neurons by assaying their sensitivity *in vitro* in the *absence* of type I cells. However, though this experiment can be done easily for CB afferent neurons by dissociating the petrosal ganglion alone, the close proximity of type I cells and local neurons within the vagus nerve and RLN makes it difficult to separate these cellular components *in vitro*. Therefore, given the limitations of the AB culture preparation, the most convenient way to determine whether neuronal responses are direct or indirect would be to use pharmacological tools to block the responses. In light of the data presented in Chapter 4, i.e. that red blood cells (RBCs) may contribute to the hypoxia- and acid-sensitivity of the AB, and that local neurons may be extensively coupled, deciphering the origin of the chemosensory responses remains a challenging task (see Future Directions).

The possibility that some local neurons are *directly* chemosensitive cannot, however, be overlooked. Indeed, it is well known that specific central and peripheral neurons possess an inherent sensitivity to O_2, CO_2 and H^+. In the central nervous system, hypoxia-activated neurons are present in the caudal hypothalamus and in the rostral ventrolateral medulla (VLM), specifically, in the nucleus tractus solitarius (NTS), the C_1 sympathoexcitatory region, and the pre-Bötzinger complex (i.e. the putative site of respiratory rhythm generation) (Neubauer & Sunderram, 2004). In response to hypoxia, O_2-sensitive central neurons increase sympathetic and respiratory activity independent of peripheral chemoreceptor activation. In the C_1 region, the mechanism of O_2-sensitivity involves the inhibition of outward K^+ currents and an increased Ca^{2+} conductance, analogous to the effect of hypoxia on CB type I cells (Sun & Reis, 1994; Wang *et al.*, 2001). Probably of greater physiological importance are the CO_2/H^+-sensitive central neurons, which stimulate breathing in response to respiratory (i.e. hypercapnic) acidosis.

CO_2-activated neurons have been localized to various brainstem regions including the NTS, the locus coeruleus (LC), medullary raphe, nucleus ambiguus, and VLM; though the study of their respective chemosensory mechanisms is in its infancy, it appears that inhibition of acid-sensitive K^+ channels (e.g. TASK) is a common feature. Interestingly, many putative central chemosensitive neurons, including those in the NTS, LC, and pre-Bötzinger complex, have been shown to be coupled by gap junctions (Putnam *et al.*, 2004). In the NTS, for example, there is both molecular evidence (i.e. presence of connexins) as well as physiological evidence (i.e. electrical coupling) for gap junctions in both neonatal and adult rats (see Putnam *et al.*, 2004). Though the significance of electrical coupling among central chemosensitive neurons is unknown, the reasons for it may also apply to local AB neurons.

Few studies have focused on chemosensing in peripheral neurons. In the rat dorsal root ganglion, hypoxia activates sensory neurons via inhibition of voltage-sensitive K^+ channels, leading to increased excitability and extracellular Ca^{2+} entry through L-type Ca^{2+} channels (Lukyanetz *et al.*, 2003; Gruss *et al.*, 2006). In the GPN and CSN, autonomic efferent neurons that innervate the CB also possess an inherent O_2-sensitivity (Campanucci *et al.*, 2003). Hypoxic stimulation of GPN neurons is presumed to contribute to the activation of neuronal nitric oxide (NO) synthase (nNOS), ultimately causing synthesis and release of the inhibitory gasotransmitter, NO, onto CB chemoreceptors. Interestingly, a small percentage (i.e. <10%) of local AB neurons were nNOS-immunopositive (Chapter 2); thus, it is possible that they are analogous to CB autonomic efferents, possessing an innate O_2 sensitivity and providing efferent inhibition to the AB.

Besides the function of local AB neurons, their central and peripheral targets remain unknown. One possibility is that these neurons have central projections to the vasomotor centre, contributing to cardiovascular chemoreflexes (e.g. changes in blood pressure). Another possibility is that they project to the cardiac vasculature directly, providing local circulatory regulation. Recently, it was shown that P2X2- and P2X3-immunoreactive nerve terminals of unknown origin are distributed widely in the aortic

arch, atrium, vena cava and ventricles (Song *et al.*, 2012). This innervation could derive from local AB neurons.

Red blood cells as O_2 sensors: Potential role in aortic body chemosensing

Ever since the ABs were theorized to sense O_2 content, the involvement of oxygenated hemoglobin, Hb (and thus, RBCs) has been implicated (Lahiri *et al.*, 1981b). The dependence of ABs on oxyhemoglobin is thought to arise from microvascular impediments within the AB. In contrast, dissolved O_2 is sufficient for the CBs because of their high blood flow. In this thesis, a more fundamental role for RBCs in AB chemosensing was implicated by the unexpected finding that many, apparently viable, RBCs were present in short term AB cultures, but *not* in CB cultures generated under the same conditions. Though unproven, it is possible that the AB provides a favourable microenvironment that attracts, or promotes the survival of, RBCs. Certainly, this would be advantageous for a poorly vascularized tissue, particularly in light of the current view that RBCs are mobile O_2-sensors that match microvascular O_2 supply with local tissue demand (Ellsworth *et al.*, 2009; Jensen, 2009). In fact, the trigger for RBC activation is a decrease in O_2 *content*, i.e. Hb desaturation (Ellsworth *et al.*, 2009), which coincidentally also stimulates AB chemoafferents (Lahiri *et al.*, 1981b). Therefore, RBCs may participate in AB activation evoked by decreases in O_2 content.

The mechanism of O_2-sensing by RBCs involves a hypoxia-evoked conformational change in Hb (i.e. desaturation), which triggers an intracellular signaling cascade that culminates in ATP release via pannexin-1 channels (Ellsworth *et al.*, 2009; Sridharan *et al.*, 2010). Traditionally, released ATP is thought to increase local blood flow by binding to metabotropic P2Y purinoceptors on the vascular endothelium, leading to the production and release of vasodilators (e.g. NO) (Ellsworth *et al.*, 2009). However, given that smooth-muscle ringed arterioles are absent in the AB (see Kummer & Neuhuber, 1989), this pathway would not be effective at increasing AB perfusion. Rather, I propose that RBC-released ATP extravasates through the highly permeable AB blood

vessels, and floods the interstitial fluid. Here, extravasated ATP could activate the P2X2/3-expressing nerve terminals that surround AB type I cells; these terminals are supplied by local AB neurons or afferent nodose ganglion neurons, which, when activated, initiate cardiovascular reflexes. Indeed, as illustrated by McDonald and Blewett (1981) and confirmed in Chapter 4 using Evans Blue, AB paraganglia in the vagus nerve and RLN do have access to blood-borne factors (e.g. RBC-derived ATP), and the highly permeable paraganglia are surrounded by purinergic nerve terminals. Therefore, interactions between RBCs and (local or sensory vagal) neurons/ nerve terminals may reflexly initiate circulatory adjustments that increase O_2 delivery to the body tissues! It is noteworthy that the role of the type I cell in this scenario is redundant (or perhaps involved in minor respiratory chemoreflex functions), if ATP release from RBCs is sufficient to activate AB afferents. Therefore, perhaps the primary function of AB type I cells is not to activate afferent neurons, but to bring together or help organize the local circuitry (i.e. RBC, local neurons/ terminals) for sensing O_2 content in a strategic area near the heart.

The aortic body 'tripartite synapse' – a working model

The data presented in this thesis provide a unique cellular view of AB function, and reveal potential signaling roles for previously-unexplored cell types in this chemosensory tissue. Specifically, at least 4 distinctive cell types were identified in 1 d old cultures based on their morphological, immunocytochemical and physiological characteristics, including (1) chemoreceptor type I (glomus) cells, (2) local neurons, (3) glia-like type II cells, and (4) RBCs (Figure 1). This *in vitro* model appears to satisfactorily approximate the main cell types of the *in vivo* AB, which consists of type I cell clusters enveloped by type II cells, interdigitated by blood vessels, and abutted by neuronal cell bodies (McDonald & Blewett, 1981; Kummer & Neuhuber, 1989).

Although the classical cellular elements involved in chemotransduction and chemotransmission include the receptor (type I) cell and afferent neuron, an increasingly

important role for glia in synaptic communication is emerging. Indeed, recent studies have shown that glia are capable of modulating neurotransmission by acting as bidirectional signaling partners for neurons (Perea *et al.*, 2009). That is, in addition to the usual 'supportive' roles attributed to glial cells, such as transmitter uptake and regulation of extracellular ion homeostasis, glia can respond to synaptic activity via G-protein coupled receptor activation and intracellular Ca^{2+} mobilization, and they can release neurotransmitters back into the synapse. Therefore, modern studies of synaptic communication consider the 'tripartite synapse', defined as the presynaptic nerve terminal, postsynaptic cell, and the glial process that ensheaths them (Eroglu & Barres, 2010).

In the CB, glia-like type II cells were recently hypothesized to serve as amplifiers of the excitatory neurotransmitter ATP at the chemosensory synapse (Zhang *et al.*, 2012). The proposed mechanism involves stimulus-evoked ATP release from type I cells acting at P2X receptors on afferent nerve endings and on P2Y2 receptors on type II cells (Xu *et al.*, 2003). P2Y2 receptor activation mobilizes Ca^{2+} from intracellular stores, which, via an unknown pathway, leads to the opening of ATP-permeable pannexin-1 channels in type II cells (Zhang *et al.*, 2012). The released ATP from type II cells activates P2X2/3 receptors on petrosal nerve terminals, thereby augmenting afferent nerve excitation. Interestingly, in dissociated AB cultures, Ca^{2+} imaging studies revealed the presence of ATP-sensitive, non-excitable cells; approximately half of these were also sensitive to the P2Y2 receptor agonist, UTP, suggesting that they were analogous to CB type II cells (Chapter 3). Presumably, these ATP-sensitive, non-excitable cells correspond to at least a subpopulation of the abundant glial fibrillary acidic protein (GFAP)-positive cells identified in short term AB cultures (Chapters 2 and 3).

The anatomical and functional data presented in this thesis have led to the following 'working model' of AB chemosensing, which includes the contributions of all 4 cellular components of the AB. This model embraces the view of the 'tripartite synapse' and includes the glia-like type II cell as an important contributor to chemosensory signaling. In fact, the proposed involvement of RBCs would extend this

view even further to encompass a fourth element; indeed, the idea of the "quadripartite synapse' which includes the 'extracellular space' has been suggested in the literature (Sykova, 2004). This model is summarized in Figure 2. (1) Various chemostimuli, including hypoxia (low PO_2), hypercapnia (high PCO_2) and acidity (low pH), initiate a depolarizing receptor potential in AB type I cells, leading to voltage-gated Ca^{2+} channel (VGCC) activation and extracellular Ca^{2+} entry. Although the channels responsible for the membrane depolarization remain unknown, they may include the high-conductance voltage- and Ca^{2+}-activated K^+ channel (BK) or the background TASK-like K^+ channel, as in the CB (Buckler, 2007; Peers & Wyatt, 2007). The involvement of VGCCs is suggested by the Ni^{2+}-sensitivity of the Ca^{2+} responses to acidic hypercapnia (Chapter 3). The resulting rise in $[Ca^{2+}]_i$ triggers neurosecretion of putative AB transmitters, including ATP, acetylcholine (ACh), dopamine (DA) and serotonin (5-HT). (2) ATP and ACh bind to P2X2/3 receptors and nicotinic ACh receptors (nAChRs), respectively, on the post-synaptic nerve terminals of either local AB neurons or nodose ganglion neurons (Chapter 3; Cooper, 2001; Burnstock, 2009). Activation of these ionotropic receptors leads to membrane depolarization and a rise in $[Ca^{2+}]_i$; additionally, ATP has minor actions on metabotropic P2Y receptors on some local neurons, which contribute to increases in cytosolic $[Ca^{2+}]$. Ultimately, post-synaptic (afferent) neurons are excited and transmit the chemosensory signal in the form of increased action potential firing to either the CNS or to local targets (e.g. cardiac vasculature). (3) ATP released from type I cells may also excite nearby type II cells via P2Y2 receptor activation, causing Ca^{2+} release from intracellular stores. The downstream effects of ATP-signaling in type II cells are not known in the AB, but may involve the opening of ATP-permeable pannexin-1 channels and further ATP release into the synapse as proposed for the CB (Zhang *et al.*, 2012). (4) Concomitant with receptor type I cell activation, hypoxia also causes ATP release from RBCs in response to Hb desaturation (i.e. decreased SO_2) (Ellsworth *et al.*, 2009). Given the high vascular permeability of AB paraganglia, blood-borne ATP could extravasate into the interstitial fluid surrounding type I cells and purinergic nerve terminals, further adding to the pool of ATP available at the chemosensory synapse (Chapter 4). It is

proposed that RBCs play a greater role in the AB than in the CB because the AB has a lower blood flow and tissue PO_2.

Physiological functions of central and peripheral chemoreceptors

A complex network of lower brainstem neurons – which together comprise the respiratory central pattern generator (CPG) – regulate breathing by controlling the rate and timing of respiratory muscle contraction (see Guyenet *et al.*, 2009). The output of the CPG depends on afferent sensory input received from the central and peripheral chemoreceptors. In this regard, the current consensus is that CO_2 chemoreception is largely, if not exclusively, attributable to CO_2-sensitive neurons located on the ventral surface of the medulla oblongata, whereas O_2 chemoreception is solely accomplished by the peripheral arterial chemoreceptors, mainly the CBs (Nattie, 2006). Thus, the ventilatory responses to CO_2 and hypoxia are mainly initiated by the medullary and CB chemoreceptors, respectively; however, the CBs provide the initial, rapid component of the CO_2-induced ventilatory response (as opposed to the steady-state response) (Nattie, 2006). [Note that although O_2- and CO_2-*sensitive* neurons have been identified in many brain regions (see above), the demonstration that they are true central *chemoreceptors* (i.e. that they supply chemosensory information to the CPG) remains unproven in most cases (Guyenet *et al.*, 2008; Powell *et al.*, 2009).]

The reason for the existence of multiple peripheral O_2 chemoreceptors, i.e. CBs and ABs, is a matter of debate. Upon examination of the literature, two plausible explanations are evident, and these are not mutually exclusive. First, it is possible that the ABs and CBs have different stimulus specificities (i.e. PO_2 vs. O_2 content), and act to produce different reflexes to regulate O_2 uptake (i.e. respiration) and delivery to tissues (i.e. circulation). Indeed, Comroe's classical experiments on dogs and cats showed that CBs are primarily responsible for eliciting hypoxia-evoked hyperventilation whereas ABs elicit mainly hypertension (Comroe, 1939). Furthermore, Lahiri's group determined that CB afferents are more sensitive to low arterial PO_2, whereas AB afferents are sensitive to

low O_2 content, and these differences were attributed to microvascular impediments in the AB not present in the CB (Lahiri *et al.*, 1980a; Lahiri *et al.*, 1981b). Interestingly, Milsom and Burleson (2007) suggested that the ability to distinguish between arterial PO_2 and O_2 content is highly adaptive; indeed, many vertebrates appear capable of distinguishing between these stimuli. Furthermore, in many vertebrate species, the hypoxic ventilatory response is more strongly correlated with O_2 content than with PO_2; for example, fish hyperventilate in response to a decrease in O_2 content independent of PO_2, indicative of arterial chemoreceptors that respond to O_2 delivery (see Milsom & Burleson, 2007). In mammals, the ABs are the only purportedly O_2-content sensitive chemoreceptors, though unlike their counterparts in fish, they stimulate mainly circulatory reflexes. Consistent with the proposals from Lahiri's group, Milsom and Burleson suggest that the presence of distinct populations of chemoreceptors may be attributable to the local tissue PO_2 in the vicinity of the receptor cells, which depends on the metabolic rate and blood flow in that tissue. In fact, they speculate that although the O_2-sensing mechanisms of all peripheral chemoreceptors may be the same, their locations may have evolved so as to make one population of receptors more sensitive to changes in O_2 delivery than the others (Milsom & Burleson, 2007).

A second explanation for the presence of two peripheral arterial chemoreceptors is that the ABs may provide a 'back-up' system in case of CB dysfunction in disease conditions. Evidence from multiple species suggests that the ABs are responsible for the recovery of the hypoxic ventilatory response after chronic CB denervation (Prabhakar & Peng, 2004). For example, in newborn (5 d old) piglets, AB denervation had no effect on eupneic (in room air) breathing whereas significant hypoventilation was observed in CB denervated animals (Serra *et al.*, 2002). After a 2 week recovery period, however, the CB denervated animals were breathing normally, indicating a compensatory upregulation of non-CB chemoafferents. The site of chemosensitivity was localized to the ABs, based on injections of sodium cyanide into the ascending aorta, whereas cyanide injection into the carotid arteries had no effect on ventilation (indicating that the CBs had not simply been re-innervated). Therefore, the redundancy and plasticity within the ventilatory control

system may be advantageous to the maintenance of O_2 homeostasis in certain diseased states where CB function is impaired.

Future Directions

The work presented in this thesis has raised several questions that require further investigation.

1. *Are the responses of local AB neurons to chemostimuli direct or indirect?*

   Assuming that the Ca^{2+} responses of local AB neurons to chemostimuli are indirect, as is the case for CB chemosensory neurons, their responses may be mediated via one or more of the following pathways, (i) binding of type I cell-released neurotransmitter(s) onto their respective receptors on local neurons, (ii) binding of RBC-released ATP onto neuronal P2X2/3 receptors, or (iii) chemical or electrical coupling with adjacent neurons. The existence of at least three separate possibilities makes it difficult to isolate one contribution from the other; indeed, my attempts to block the CO_2/H^+-evoked Ca^{2+}_i responses in neurons by combined purinergic-cholinergic block were unsuccessful in a few cases (see Chapter 3). Nevertheless, a role for ATP in AB chemotransmission (regardless of the source) could be tested using P2X2 and P2X3 knockout mice; this model was elegantly used to demonstrate that the P2X2 subunit is pivotal in CB hypoxic chemotransmission (see Rong *et al.*, 2003). For example, the effects of hypoxia on P2X2-deficient mice versus wild-type mice could be compared at the cellular level (i.e. measure Ca^{2+}_i responses of cultured neurons), or at the systemic level (i.e. measure blood pressure), to test whether P2X2-deficient mice exhibit attenuated responses.

   The potential contribution of RBCs to neuronal excitability could be tested in a number of ways. First, the effect of RBC-mediated ATP release on the neuronal Ca^{2+}_i responses could be investigated using the pannexin channel antagonist, carbenoxolone. At low concentrations, carbenoxolone should selectively block ATP

release from RBCs without affecting neurotransmitter release from type I cells, or electrical coupling between neurons. Second, testing the chemosensitivity of neurons in long-term (i.e. >2 day) cultures, in which RBCs have mostly died off, could identify a potential contribution from RBCs. Finally, pannexin-1 knockout mice would provide insight as to whether ATP release via these channels contributes to the neuronal Ca^{2+}_i responses *in vitro*, or to nerve activity *in situ*. Unfortunately, because RBCs are anucleated when mature, their potential for genetic manipulation is limited.

2. *What are the cellular targets of local AB neurons?*

Immunocytochemical studies suggest that local AB neurons provide peptidergic (Kummer & Neuhuber, 1989; Dahlqvist *et al.*, 1994) and/or purinergic (Chapter 2) innervation to type I cells. Furthermore, local neurons appear to make intimate contacts with type I cells *in vitro* (Chapter 2). Still, the functional innervation of AB type I cells by local neurons has not been confirmed. Neurotransmission between type I cells and local neurons can be investigated *in vitro* using dual patch clamp recording (as in Chapter 4), to investigate whether stimulation of a type I cell can cause an electrical potential in a juxtaposed neuron. Selective receptor blockers can then identify which neurotransmitters and receptor subtypes mediate chemical transmission, if it exists. Notably, this study is limited by the low yield of type I cells and neurons in dissociated AB cultures, and the relative rarity of their association. Moreover, the identification of chemical synapses *in vitro* does not assure their existence *in vivo*.

More importantly, the central or peripheral targets of local neurons are of interest, since they may provide clues as to how ABs exert their systemic effects. Tracer injection into the 'microganglion' at the bifurcation of the left vagus nerve and RLN would be very difficult, given its small size (<200 μm). In an attempt to investigate whether neurons in the vagus nerve and/or RLN project to the cardiac ganglia, I injected the lipophilic tracer, DiI, into the atria of newborn (~2 d old) rats in an excised heart-vagus nerve preparation. Though I did not observe any retrograde

labeling of vagal or laryngeal neurons, it is unclear whether this was because the site of dye injection was inaccurate, the axons connecting local neurons to cardiac ganglia were severed during dissection, or simply because the local neurons do not innervate cardiac ganglia.

3. *Do AB type I cells release ACh and ATP in response to chemostimulation?*

Activity-dependent release of ACh and ATP from AB type I cells must be demonstrated in order to validate that they act as neurotransmitters at the AB chemosensory synapse. Given that type I cells, type II cells, and RBCs are all proposed to release ATP, traditional methods of ATP measurement including HPLC and luciferin-luciferase bioluminescence may not be ideal for this preparation (though a low dose of carbenoxolone might block pannexin channels, thereby blocking ATP release from type II cells and RBCs). Ideally, ATP- or ACh-biosensors (e.g. CHO cells heterologously expressing P2X or nicotinic receptors) would provide reliable measurements of ATP or ACh released from single or small groups of type I cells.

4. *What steps precede Ca^{2+} entry in the AB type I cell O_2-, CO_2- and acid-sensing pathways?*

In this thesis, I demonstrated that hypoxia, hypercapnia, and acidosis led to increases in cytosolic [Ca^{2+}] in AB type I cells; however, the mechanisms upstream of Ca^{2+} entry were not explored. In CB type I cells, Ca^{2+} entry is preceded by (1) activation of an O_2- or CO_2/H^+-sensor, (2) modulation of various K^+ or non-selective cation channels, and (3) membrane depolarization. Future studies will be required to address these steps in AB type I cells, in particular, to identify whether the chemosensing mechanisms are conserved within these two separate (and potentially functionally distinct) peripheral chemoreceptors. Given the current controversy surrounding the molecular identity of the O_2 sensor in CB type I cells, it would be appropriate to investigate whether blockers of mitochondrial metabolism or H_2S production have any effect on the hypoxia-evoked $[Ca^{2+}]_i$ responses in AB type I

cells. Electrophysiological experiments would provide valuable information concerning the types of ion channels that are modulated by chemostimuli; in the CB, these include the O_2-sensitive BK and TASK channels, as well as the CO_2/H^+-sensitive TASK and acid-sensing ion channels (ASICs). Electrophysiological recording of the CO_2-induced membrane depolarization in AB type I cells in the absence and presence of a membrane permeable carbonic anhydrase inhibitor, e.g. azetazolamide, would provide clues as to whether this enzyme plays a role in the CO_2 response, as it does in the CB. Finally, the molecular and immunocytochemical detection of specific ion channel subunits thought to be involved in chemosensing (e.g. TASK1) in AB type I cells would nicely supplement physiological studies.

5. *What are the autocrine/paracrine effects of ACh, ATP, Ado, 5-HT and DA on type I cells?*

In the past decade, CB research has been dominated by investigations of the autocrine/paracrine effects of CB neurotransmitters on the chemoreceptor cells (Nurse, 2010). Importantly, CB plasticity in response to chronic or intermittent hypoxia may be related to changes in neurotransmitter production, release, and/or sensitivity. Considering that the AB tissue PO_2 is slightly hypoxic relative to the CB (Lahiri *et al.*, 1981b), it would be interesting to compare the effects of ACh, ATP, Ado, 5-HT and DA on AB versus CB type I cells. Using Ca^{2+} imaging, I briefly investigated the effects of ATP and ACh on AB type I cells. The results were inconclusive because it was difficult to distinguish type I cell responses from type II cell responses, particularly in large clusters. It would be worthwhile to re-examine the effects of these neurotransmitters and neuromodulators on single or small groups of type I cells.

Figure 1. Aortic body (AB) cultures contain several viable cell types after 1 d *in vitro*.

Dissociation of the left vagus nerve and recurrent laryngeal nerve yields heterogeneous AB cultures that contain chemoreceptor type I cells (**A**, **B**), endogenous neurons (**C**, **D**), red blood cells (RBCs; **E**, **F**) and glia-like cells (**B**, **G**; arrowheads). Panel **C** is a montage of 2 images of the same neuron captured in different focal planes; the result clearly illustrates the cell body and an emerging, pseudounipolar process (arrow). In **G**, type I cells and glia-like cells are immunolabeled using antibodies against tyrosine hydroxylase (TH, green) and glial fibrillary acidic protein (GFAP, red), respectively. Note that the arrowheads in **G** indicate 2 glial cell bodies that ensheath type I cell clusters; in **B**, the arrowheads indicate 2 putative glia-like cells. Scale bars: 20 μm.

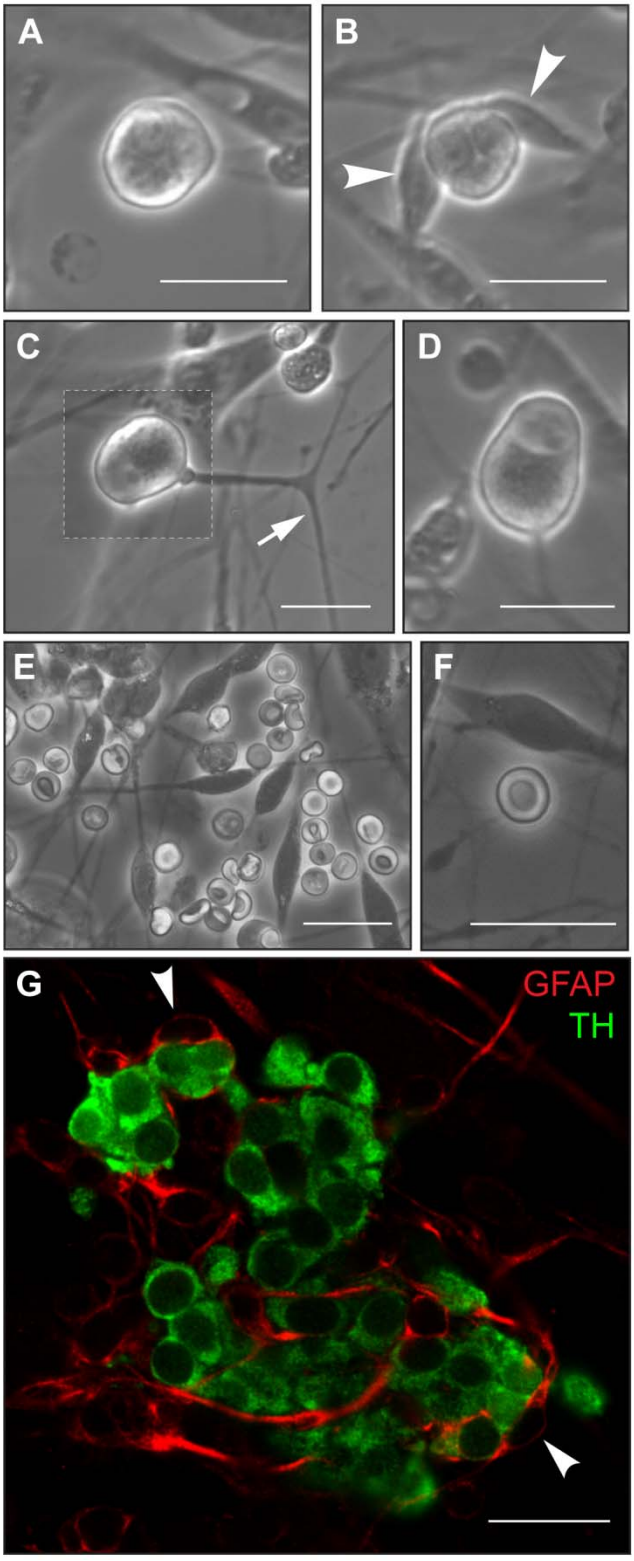
A
B
C
D
E
F
G
GFAP
TH

Figure 2. Working model of aortic body (AB) chemoreception.

(**1**) In response to hypoxia (low PO_2), hypercapnia (high PCO_2) and acidity (low pH), type I cells are depolarized (ΔV_m) leading to Ca^{2+} entry via voltage-gated Ca^{2+} channels (VGCCs). The increase in cytosolic [Ca^{2+}] triggers neuroscretion of putative AB transmitters, including ATP, acetylcholine (ACh), dopamine (DA) and serotonin (5-HT). (**2**) ATP and ACh bind to heteromeric P2X2/3 receptors and nicotinic ACh receptors (nAChRs), respectively, on the post-synaptic nerve terminals of local AB neurons and/or nodose ganglion neurons. This leads to membrane depolarization and Ca^{2+} entry, and presumably action potential propagation to central and peripheral targets. (**3**) ATP released from type I cells may also activate P2Y2 receptors on glia-like type II cells, mobilizing Ca^{2+} from intracellular stores and possibly leading to ATP release via pannexin-1 channels. (**4**) Hypoxia also activates red blood cells (RBCs), causing hemoglobin desaturation (decreased SO_2) and a signaling cascade that ends in ATP release via pannexin-1 channels. Therefore, extravasated ATP released from RBCs may also contribute to the synaptic ATP pool, augmenting chemoafferent activity, and accounting largely for the ability of ABs to sense O_2 content.

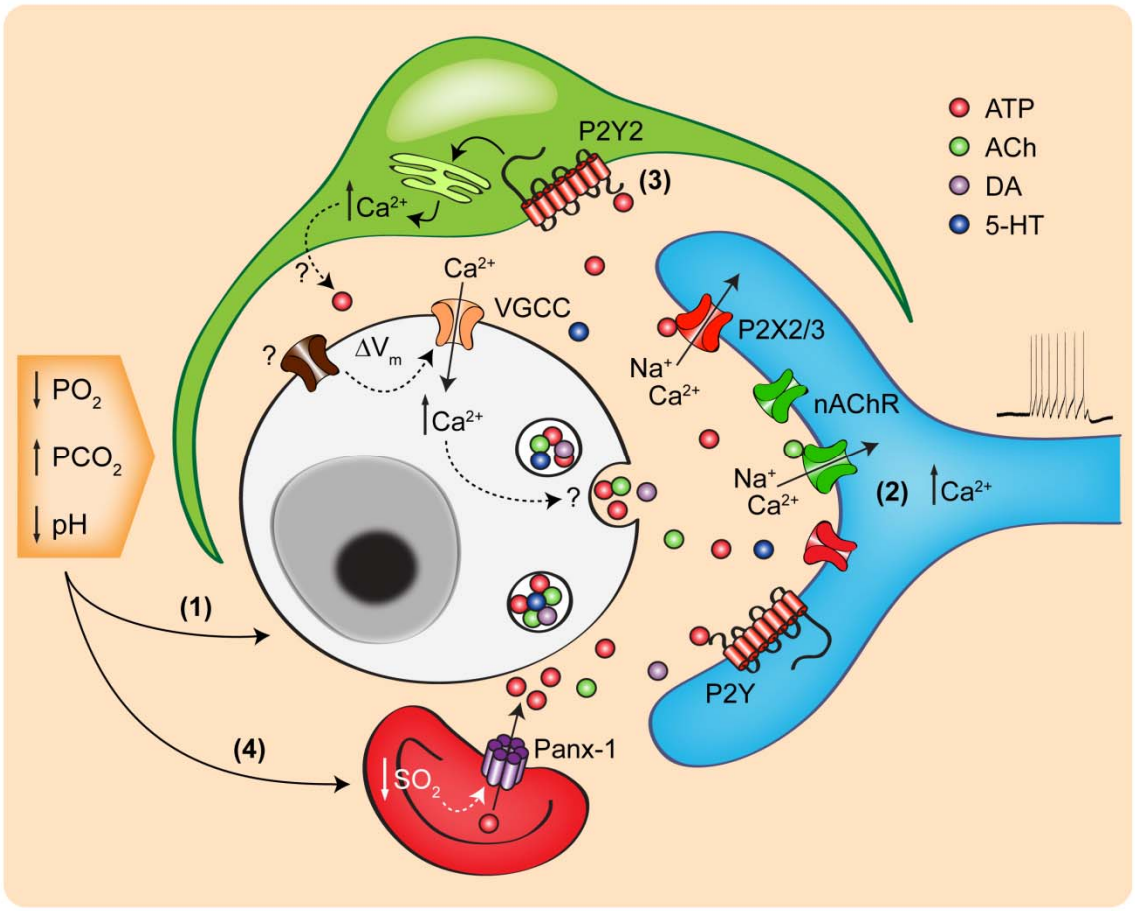
ATP
ACh
DA
5-HT
P2Y2
(3)
↑Ca2+
?
Ca2+
VGCC
?
ΔVm
↑Ca2+
?
↓PO2
↑PCO2
↓pH
(1)
(4)
↓SO2
Panx-1
P2X2/3
Na+
Ca2+
nAChR
Na+
Ca2+
(2) ↑Ca2+
P2Y

REFERENCES

Abudara V, Garces G & Saez JC (1999). Cells of the carotid body express connexin43 which is up-regulated by cAMP. *Brain Res* **849,** 25-33.

Afework M & Burnstock G (2000). Age-related changes in the localization of P2X (nucleotide) receptors in the rat adrenal gland. *Int J Dev Neurosci* **18,** 515-520.

Alcayaga J, Cerpa V, Retamal M, Arroyo J, Iturriaga R & Zapata P (2000). Adenosine triphosphate-induced peripheral nerve discharges generated from the cat petrosal ganglion in vitro. *Neurosci Lett* **282,** 185-188.

Alcayaga J, Soto CR, Vargas RV, Ortiz FC, Arroyo J & Iturriaga R (2006). Carotid body transmitters actions on rabbit petrosal ganglion *in vitro*. *Adv Exp Med Biol* **580,** 331-337; discussion 351-339.

Arvidsson U, Riedl M, Elde R & Meister B (1997). Vesicular acetylcholine transporter (VAChT) protein: a novel and unique marker for cholinergic neurons in the central and peripheral nervous systems. *J Comp Neurol* **378,** 454-467.

Bairam A, Joseph V, Lajeunesse Y & Kinkead R (2007). Developmental profile of cholinergic and purinergic traits and receptors in peripheral chemoreflex pathway in cats. *Neuroscience* **146,** 1841-1853.

Bennett MV (1966). Physiology of electrotonic junctions. *Ann N Y Acad Sci* **137,** 509-539.

Brophy S, Ford TW, Carey M & Jones JF (1999). Activity of aortic chemoreceptors in the anaesthetized rat. *J Physiol* **514 (Pt 3),** 821-828.

Buckler KJ (1997). A novel oxygen-sensitive potassium current in rat carotid body type I cells. *J Physiol* **498 (Pt 3),** 649-662.

Buckler KJ (2007). TASK-like potassium channels and oxygen sensing in the carotid body. *Respir Physiol Neurobiol* **157,** 55-64.

Buckler KJ (2012). Effects of exogenous hydrogen sulphide on calcium signalling, background (TASK) K channel activity and mitochondrial function in chemoreceptor cells. *Pflugers Arch* **463,** 743-754.

Buckler KJ & Vaughan-Jones RD (1993). Effects of acidic stimuli on intracellular calcium in isolated type I cells of the neonatal rat carotid body. *Pflugers Arch* **425,** 22-27.

Buckler KJ & Vaughan-Jones RD (1994a). Effects of hypercapnia on membrane potential and intracellular calcium in rat carotid body type I cells. *J Physiol* **478 (Pt 1),** 157-171.

Buckler KJ & Vaughan-Jones RD (1994b). Effects of hypoxia on membrane potential and intracellular calcium in rat neonatal carotid body type I cells. *J Physiol* **476,** 423-428.

Buckler KJ, Vaughan-Jones RD, Peers C, Lagadic-Gossmann D & Nye PC (1991a). Effects of extracellular pH, PCO_2 and HCO_3^- on intracellular pH in isolated type-I cells of the neonatal rat carotid body. *J Physiol* **444,** 703-721.

Buckler KJ, Vaughan-Jones RD, Peers C, Lagadic-Gossmann D & Nye PC (1993). The modulation of intracellular pH in carotid body glomus cells by extracellular pH and pCO_2. *Adv Exp Med Biol* **337,** 103-109.

Buckler KJ, Vaughan-Jones RD, Peers C & Nye PC (1991b). Intracellular pH and its regulation in isolated type I carotid body cells of the neonatal rat. *J Physiol* **436,** 107-129.

Buckler KJ, Williams BA & Honore E (2000). An oxygen-, acid- and anaesthetic-sensitive TASK-like background potassium channel in rat arterial chemoreceptor cells. *J Physiol* **525 Pt 1,** 135-142.

Burnstock G (2009). Purines and sensory nerves. *Handb Exp Pharmacol***,** 333-392.

Buttigieg J & Nurse CA (2004). Detection of hypoxia-evoked ATP release from chemoreceptor cells of the rat carotid body. *Biochem Biophys Res Commun* **322,** 82-87.

Campanucci VA, Dookhoo L, Vollmer C & Nurse CA (2012). Modulation of the carotid body sensory discharge by NO: An up-dated hypothesis. *Respir Physiol Neurobiol*.

Campanucci VA, Fearon IM & Nurse CA (2003). O_2-sensing mechanisms in efferent neurons to the rat carotid body. *Adv Exp Med Biol* **536,** 179-185.

Campanucci VA & Nurse CA (2007). Autonomic innervation of the carotid body: role in efferent inhibition. *Respir Physiol Neurobiol* **157,** 83-92.

Campanucci VA, Zhang M, Vollmer C & Nurse CA (2006). Expression of multiple P2X receptors by glossopharyngeal neurons projecting to rat carotid body O_2-chemoreceptors: role in nitric oxide-mediated efferent inhibition. *J Neurosci* **26,** 9482-9493.

Cardenas H & Zapata P (1983). Ventilatory reflexes originated from carotid and extracarotid chemoreceptors in rats. *Am J Physiol* **244,** R119-125.

Cheng Z, Powley TL, Schwaber JS & Doyle FJ, 3rd (1997a). A laser confocal microscopic study of vagal afferent innervation of rat aortic arch: chemoreceptors as well as baroreceptors. *J Auton Nerv Syst* **67,** 1-14.

Cheng Z, Powley TL, Schwaber JS & Doyle FJ, 3rd (1997b). Vagal afferent innervation of the atria of the rat heart reconstructed with confocal microscopy. *J Comp Neurol* **381,** 1-17.

Comroe JH, Jr. (1939). The location and function of the chemoreceptors of the aorta. *Am J Physiol* **127,** 176-191.

Comroe JH, Jr. & Mortimer L (1964). The Respiratory and Cardiovascular Responses of Temporally Separated Aortic and Carotid Bodies to Cyanide, Nicotine, Phenyldiguanide and Serotonin. *J Pharmacol Exp Ther* **146,** 33-41.

Conde SV, Gonzalez C, Batuca JR, Monteiro EC & Obeso A (2008). An antagonistic interaction between A2B adenosine and D2 dopamine receptors modulates the function of rat carotid body chemoreceptor cells. *J Neurochem* **107,** 1369-1381.

Conde SV & Monteiro EC (2006). Profiles for ATP and adenosine release at the carotid body in response to O_2 concentrations. *Adv Exp Med Biol* **580,** 179-184; discussion 351-179.

Cooper E (2001). Nicotinic acetylcholine receptors on vagal afferent neurons. *Ann N Y Acad Sci* **940,** 110-118.

Dahlqvist A, Carlsoo B, Domeij S & Hellstrom S (1984). Morphometric analysis of glomus cells within the recurrent laryngeal nerve of the rat. *J Neurocytol* **13,** 407-416.

Dahlqvist A, Neuhuber WL & Forsgren S (1994). Innervation of laryngeal nerve paraganglia: an anterograde tracing and immunohistochemical study in the rat. *J Comp Neurol* **345,** 440-446.

Daly MDB, Lambertsen CJ & Schweitzer A (1954). Observations on the volume of blood flow and oxygen utilization of the carotid body in the cat. *Journal of Physiology* **125,** 67-89.

Dasso LL, Buckler KJ & Vaughan-Jones RD (2000). Interactions between hypoxia and hypercapnic acidosis on calcium signaling in carotid body type I cells. *Am J Physiol Lung Cell Mol Physiol* **279,** L36-42.

Debus E, Weber K & Osborn M (1983). Monoclonal antibodies specific for glial fibrillary acidic (GFA) protein and for each of the neurofilament triplet polypeptides. *Differentiation* **25,** 193-203.

del Valle J, Camins A, Pallas M, Vilaplana J & Pelegri C (2008). A new method for determining blood-brain barrier integrity based on intracardiac perfusion of an Evans Blue-Hoechst cocktail. *J Neurosci Methods* **174,** 42-49.

Dvorakova MC & Kummer W (2005). Immunohistochemical evidence for species-specific coexistence of catecholamines, serotonin, acetylcholine and nitric oxide in glomus cells of rat and guinea pig aortic bodies. *Ann Anat* **187,** 323-331.

Easton J & Howe A (1983). The distribution of thoracic glomus tissue (aortic bodies) in the rat. *Cell Tissue Res* **232,** 349-356.

Ellsworth ML, Ellis CG, Goldman D, Stephenson AH, Dietrich HH & Sprague RS (2009). Erythrocytes: oxygen sensors and modulators of vascular tone. *Physiology (Bethesda)* **24,** 107-116.

Eroglu C & Barres BA (2010). Regulation of synaptic connectivity by glia. *Nature* **468,** 223-231.

Evans AM, Mustard KJ, Wyatt CN, Peers C, Dipp M, Kumar P, Kinnear NP & Hardie DG (2005). Does AMP-activated protein kinase couple inhibition of mitochondrial oxidative phosphorylation by hypoxia to calcium signaling in O_2-sensing cells? *J Biol Chem* **280,** 41504-41511.

Eyzaguirre C (2007). Electric synapses in the carotid body-nerve complex. *Respir Physiol Neurobiol* **157,** 116-122.

Fearon IM, Zhang M, Vollmer C & Nurse CA (2003). GABA mediates autoreceptor feedback inhibition in the rat carotid body via presynaptic $GABA_B$ receptors and TASK-1. *J Physiol* **553,** 83-94.

Fitzgerald RS (2000). Oxygen and carotid body chemotransduction: the cholinergic hypothesis - a brief history and new evaluation. *Respir Physiol* **120,** 89-104.

Fitzgerald RS, Shirahata M & Wang HY (1999). Acetylcholine release from cat carotid bodies. *Brain Res* **841,** 53-61.

Gauda EB, Cooper R, Johnson SM, McLemore GL & Marshall C (2004). Autonomic microganglion cells: a source of acetylcholine in the rat carotid body. *J Appl Physiol* **96,** 384-391.

Gonzalez C, Almaraz L, Obeso A & Rigual R (1994). Carotid body chemoreceptors: from natural stimuli to sensory discharges. *Physiol Rev* **74,** 829-898.

Gorham JD, Baker H, Kegler D & Ziff EB (1990). The expression of the neuronal intermediate filament protein peripherin in the rat embryo. *Brain Res Dev Brain Res* **57,** 235-248.

Gruss M, Ettorre G, Stehr AJ, Henrich M, Hempelmann G & Scholz A (2006). Moderate hypoxia influences excitability and blocks dendrotoxin sensitive K^+ currents in rat primary sensory neurones. *Mol Pain* **2,** 12.

Grynkiewicz G, Poenie M & Tsien RY (1985). A new generation of Ca^{2+} indicators with greatly improved fluorescence properties. *J Biol Chem* **260,** 3440-3450.

Guyenet PG, Bayliss DA, Stornetta RL, Fortuna MG, Abbott SB & DePuy SD (2009). Retrotrapezoid nucleus, respiratory chemosensitivity and breathing automaticity. *Respir Physiol Neurobiol* **168,** 59-68.

Guyenet PG, Stornetta RL & Bayliss DA (2008). Retrotrapezoid nucleus and central chemoreception. *J Physiol* **586,** 2043-2048.

Hansen JT (1981). Innervation of the rat aortic (subclavian) body: an ultrastructural study following axonal degeneration. *J Ultrastruct Res* **74,** 83-94.

Hatcher JD, Chiu LK & Jennings DB (1978). Anemia as a stimulus to aortic and carotid chemoreceptors in the cat. *J Appl Physiol* **44,** 696-702.

He L, Chen J, Dinger B, Stensaas L & Fidone S (2006). Effect of chronic hypoxia on purinergic synaptic transmission in rat carotid body. *J Appl Physiol* **100,** 157-162.

He L, Dinger B & Fidone S (2005). Effect of chronic hypoxia on cholinergic chemotransmission in rat carotid body. *J Appl Physiol* **98,** 614-619.

Hirasawa S, Mendoza JA, Jacoby DB, Kobayashi C, Fitzgerald RS, Schofield B, Chandrasegaran S & Shirahata M (2003). Diverse cholinergic receptors in the cat carotid chemosensory unit. *Adv Exp Med Biol* **536,** 313-319.

Hohler B, Mayer B & Kummer W (1994). Nitric oxide synthase in the rat carotid body and carotid sinus. *Cell Tissue Res* **276,** 559-564.

Ito S, Ohta T & Nakazato Y (1997). Release of 5-hydroxytryptamine by hypoxia from epithelioid cells of chicken thoracic aorta. *Br J Pharmacol* **122,** 799-801.

Ito S, Ohta T & Nakazato Y (1999). Characteristics of 5-HT-containing chemoreceptor cells of the chicken aortic body. *J Physiol* **515 (Pt 1),** 49-59.

Iturriaga R & Alcayaga J (2004). Neurotransmission in the carotid body: transmitters and modulators between glomus cells and petrosal ganglion nerve terminals. *Brain Res Brain Res Rev* **47,** 46-53.

Iturriaga R, Lahiri S & Mokashi A (1991). Carbonic anhydrase and chemoreception in the cat carotid body. *Am J Physiol* **261,** C565-573.

Jackson A & Nurse C (1997). Dopaminergic properties of cultured rat carotid body chemoreceptors grown in normoxic and hypoxic environments. *J Neurochem* **69,** 645-654.

Jagger JE, Bateman RM, Ellsworth ML & Ellis CG (2001). Role of erythrocyte in regulating local O_2 delivery mediated by hemoglobin oxygenation. *Am J Physiol Heart Circ Physiol* **280,** H2833-2839.

Jarvis MF & Khakh BS (2009). ATP-gated P2X cation-channels. *Neuropharmacology* **56,** 208-215.

Jensen FB (2009). The dual roles of red blood cells in tissue oxygen delivery: oxygen carriers and regulators of local blood flow. *J Exp Biol* **212,** 3387-3393.

Jiang RG & Eyzaguirre C (2003). Dye and electric coupling between carotid nerve terminals and glomus cells. *Adv Exp Med Biol* **536,** 247-253.

Jones JF (2000). Aortic body chemoreflex of the anaesthetized rat. Electrophysiological, morphological, and reflex studies. *Adv Exp Med Biol* **475,** 789-792.

Katz DM & Black IB (1986). Expression and regulation of catecholaminergic traits in primary sensory neurons: relationship to target innervation *in vivo*. *J Neurosci* **6,** 983-989.

Kemp PJ (2006). Detecting acute changes in oxygen: will the real sensor please stand up? *Exp Physiol* **91,** 829-834.

Kim D, Cavanaugh EJ, Kim I & Carroll JL (2009). Heteromeric TASK-1/TASK-3 is the major oxygen-sensitive background K^+ channel in rat carotid body glomus cells. *J Physiol* **587,** 2963-2975.

Kim DK, Prabhakar NR & Kumar GK (2004). Acetylcholine release from the carotid body by hypoxia: evidence for the involvement of autoinhibitory receptors. *J Appl Physiol* **96,** 376-383.

Kim YS, Paik SK, Cho YS, Shin HS, Bae JY, Moritani M, Yoshida A, Ahn DK, Valtschanoff J, Hwang SJ, Moon C & Bae YC (2008). Expression of P2X3 receptor in the trigeminal sensory nuclei of the rat. *J Comp Neurol* **506,** 627-639.

Kobayashi M, Cheng ZB, Tanaka K & Nosaka S (1999). Is the aortic depressor nerve involved in arterial chemoreflexes in rats? *J Auton Nerv Syst* **78,** 38-48.

Kumar P & Bin-Jaliah I (2007). Adequate stimuli of the carotid body: more than an oxygen sensor? *Respir Physiol Neurobiol* **157,** 12-21.

Kummer W & Neuhuber WL (1989). Vagal paraganglia of the rat. *J Electron Microsc Tech* **12,** 343-355.

Lahiri S, Mokashi A, Mulligan E & Nishino T (1981a). Comparison of aortic and carotid chemoreceptor responses to hypercapnia and hypoxia. *J Appl Physiol* **51,** 55-61.

Lahiri S, Mulligan E, Nishino T & Mokashi A (1979). Aortic body chemoreceptor responses to changes in PCO_2 and PO_2 in the cat. *J Appl Physiol* **47,** 858-866.

Lahiri S, Mulligan E, Nishino T, Mokashi A & Davies RO (1981b). Relative responses of aortic body and carotid body chemoreceptors to carboxyhemoglobinemia. *J Appl Physiol* **50,** 580-586.

Lahiri S, Nishino T, Mokashi A & Mulligan E (1980a). Relative responses of aortic body and carotid body chemoreceptors to hypotension. *J Appl Physiol* **48,** 781-788.

Lahiri S, Nishino T, Mulligan E & Mokashi A (1980b). Relative latency of responses of chemoreceptor afferents from aortic and carotid bodies. *J Appl Physiol* **48,** 362-369.

Lewis C, Neidhart S, Holy C, North RA, Buell G & Surprenant A (1995). Coexpression of P2X2 and P2X3 receptor subunits can account for ATP-gated currents in sensory neurons. *Nature* **377,** 432-435.

Li Q, Sun B, Wang X, Jin Z, Zhou Y, Dong L, Jiang LH & Rong W (2010). A crucial role for hydrogen sulfide in oxygen sensing via modulating large conductance calcium-activated potassium channels. *Antioxid Redox Signal* **12,** 1179-1189.

Lopez-Barneo J (2003). Oxygen and glucose sensing by carotid body glomus cells. *Curr Opin Neurobiol* **13,** 493-499.

Lopez-Barneo J, Lopez-Lopez JR, Urena J & Gonzalez C (1988). Chemotransduction in the carotid body: K^+ current modulated by PO_2 in type I chemoreceptor cells. *Science* **241,** 580-582.

Lukyanetz EA, Stanika RI, Koval LM & Kostyuk PG (2003). Intracellular mechanisms of hypoxia-induced calcium increase in rat sensory neurons. *Arch Biochem Biophys* **410,** 212-221.

Mayer C, Quasthoff S & Grafe P (1998). Differences in the sensitivity to purinergic stimulation of myelinating and non-myelinating Schwann cells in peripheral human and rat nerve. *Glia* **23,** 374-382.

McDonald DM (1981). Peripheral chemoreceptors: structure–function relationships of the carotid body. In *Regulation of Breathing. Lung Biol. Health Dis.*, vol. 17. ed. Hornbein Tf, pp. 105-320. Marcel Dekker, New York.

McDonald DM & Blewett RW (1981). Location and size of carotid body-like organs (paraganglia) revealed in rats by the permeability of blood vessels to Evans blue dye. *J Neurocytol* **10,** 607-643.

McDonald DM & Larue DT (1983). The ultrastructure and connections of blood vessels supplying the rat carotid body and carotid sinus. *J Neurocytol* **12,** 117-153.

McDonald DM & Mitchell RA (1975). The innervation of glomus cells, ganglion cells and blood vessels inthe rat carotid body: a quantitative ultrastructural analysis. *Journal of Neurocytology* **4,** 177-230.

Milsom WK & Burleson ML (2007). Peripheral arterial chemoreceptors and the evolution of the carotid body. *Respir Physiol Neurobiol* **157,** 4-11.

Nattie E (2006). Why do we have both peripheral and central chemoreceptors? *J Appl Physiol* **100,** 9-10.

Neubauer JA (2004). Comroe's study of aortic chemoreceptors: a path well chosen. *J Appl Physiol* **97,** 1595-1596.

Neubauer JA & Sunderram J (2004). Oxygen-sensing neurons in the central nervous system. *J Appl Physiol* **96,** 367-374.

Niane L, Joseph V & Bairam A (2009). Role of cholinergic-nicotinic receptors on hypoxic chemoreflex during postnatal development in rats. *Respir Physiol Neurobiol* **169,** 323-332.

Niane LM, Donnelly DF, Joseph V & Bairam A (2011). Ventilatory and carotid body chemoreceptor responses to purinergic P2X receptor antagonists in newborn rats. *J Appl Physiol* **110,** 83-94.

North RA (2002). Molecular physiology of P2X receptors. *Physiol Rev* **82,** 1013-1067.

Nurse CA (1990). Carbonic anhydrase and neuronal enzymes in cultured glomus cells of the carotid body of the rat. *Cell Tissue Res* **261,** 65-71.

Nurse CA (2005). Neurotransmission and neuromodulation in the chemosensory carotid body. *Auton Neurosci* **120,** 1-9.

Nurse CA (2010). Neurotransmitter and neuromodulatory mechanisms at peripheral arterial chemoreceptors. *Exp Physiol* **95,** 657-667.

Nurse CA & Fearon IM (2002). Carotid body chemoreceptors in dissociated cell culture. *Microsc Res Tech* **59,** 249-255.

Nurse CA & Zhang M (1999). Acetylcholine contributes to hypoxic chemotransmission in co-cultures of rat type 1 cells and petrosal neurons. *Respir Physiol* **115,** 189-199.

O'Leary DM, Murphy A, Pickering M & Jones JF (2004). Arterial chemoreceptors in the superior laryngeal nerve of the rat. *Respir Physiol Neurobiol* **141,** 137-144.

Olson KR (2011). Hydrogen sulfide is an oxygen sensor in the carotid body. *Respir Physiol Neurobiol* **179,** 103-110.

Paintal AS & Riley RL (1966). Responses of aortic chemoreceptors. *J Appl Physiol* **21,** 543-548.

Pang ZP & Sudhof TC (2010). Cell biology of Ca^{2+}-triggered exocytosis. In *Curr Opin Cell Biol*, vol. 22, pp. 496-505.

Peers C (1990). Hypoxic suppression of K^+ currents in type I carotid body cells: selective effect on the Ca^{2+}-activated K^+ current. *Neurosci Lett* **119,** 253-256.

Peers C & Wyatt CN (2007). The role of maxiK channels in carotid body chemotransduction. *Respir Physiol Neurobiol* **157,** 75-82.

Peng YJ, Nanduri J, Raghuraman G, Souvannakitti D, Gadalla MM, Kumar GK, Snyder SH & Prabhakar NR (2010). H_2S mediates O_2 sensing in the carotid body. *Proc Natl Acad Sci U S A* **107,** 10719-10724.

Perea G, Navarrete M & Araque A (2009). Tripartite synapses: astrocytes process and control synaptic information. *Trends Neurosci* **32,** 421-431.

Piskuric NA & Nurse CA (2012). Effects of chemostimuli on $[Ca^{2+}]_i$ responses of rat aortic body type I cells and endogenous local neurons: Comparison with carotid body cells. *J Physiol*.

Piskuric NA, Vollmer C & Nurse CA (2011). Confocal immunofluorescence study of rat aortic body chemoreceptors and associated neurons *in situ* and *in vitro*. *J Comp Neurol* **519,** 856-873.

Pokorski M & Lahiri S (1983). Aortic and carotid chemoreceptor responses to metabolic acidosis in the cat. *Am J Physiol* **244,** R652-658.

Powell FL, Kim BC, Johnson SR & Fu Z (2009). Oxygen sensing in the brain--invited article. *Adv Exp Med Biol* **648,** 369-376.

Prabhakar NR (2012). Carbon monoxide (CO) and hydrogen sulfide (H_2S) in hypoxic sensing by the carotid body. *Respir Physiol Neurobiol*.

Prabhakar NR & Peng YJ (2004). Peripheral chemoreceptors in health and disease. *J Appl Physiol* **96,** 359-366.

Prasad M, Fearon IM, Zhang M, Laing M, Vollmer C & Nurse CA (2001). Expression of P2X2 and P2X3 receptor subunits in rat carotid body afferent neurones: role in chemosensory signalling. *J Physiol* **537,** 667-677.

Putnam RW, Filosa JA & Ritucci NA (2004). Cellular mechanisms involved in CO_2 and acid signaling in chemosensitive neurons. *Am J Physiol Cell Physiol* **287,** C1493-1526.

Radford KM, Virginio C, Surprenant A, North RA & Kawashima E (1997). Baculovirus expression provides direct evidence for heteromeric assembly of P2X2 and P2X3 receptors. *J Neurosci* **17,** 6529-6533.

Reyes EP, Fernandez R, Larrain C & Zapata P (2007a). Carotid body chemosensory activity and ventilatory chemoreflexes in cats persist after combined cholinergic-purinergic block. *Respir Physiol Neurobiol* **156,** 23-32.

Reyes EP, Fernandez R, Larrain C & Zapata P (2007b). Effects of combined cholinergic-purinergic block upon cat carotid body chemoreceptors in vitro. *Respir Physiol Neurobiol* **156,** 17-22.

Rocher A, Geijo-Barrientos E, Caceres AI, Rigual R, Gonzalez C & Almaraz L (2005). Role of voltage-dependent calcium channels in stimulus-secretion coupling in rabbit carotid body chemoreceptor cells. *J Physiol* **562,** 407-420.

Rong W, Gourine AV, Cockayne DA, Xiang Z, Ford AP, Spyer KM & Burnstock G (2003). Pivotal role of nucleotide P2X2 receptor subunit of the ATP-gated ion channel mediating ventilatory responses to hypoxia. *J Neurosci* **23,** 11315-11321.

Sapru HN, Gonzalez E & Krieger AJ (1981). Aortic nerve stimulation in the rat: cardiovascular and respiratory responses. *Brain Res Bull* **6,** 393-398.

Sapru HN & Krieger AJ (1977). Carotid and aortic chemoreceptor function in the rat. *J Appl Physiol* **42,** 344-348.

Serra A, Brozoski D, Hodges M, Roethle S, Franciosi R & Forster HV (2002). Effects of carotid and aortic chemoreceptor denervation in newborn piglets. *J Appl Physiol* **92,** 893-900.

Shirahata M, Balbir A, Otsubo T & Fitzgerald RS (2007). Role of acetylcholine in neurotransmission of the carotid body. *Respir Physiol Neurobiol* **157,** 93-105.

Shirahata M, Ishizawa Y, Rudisill M, Schofield B & Fitzgerald RS (1998). Presence of nicotinic acetylcholine receptors in cat carotid body afferent system. *Brain Res* **814,** 213-217.

Shirahata M, Ishizawa Y, Rudisill M, Sham JS, Schofield B & Fitzgerald RS (2000). Acetylcholine sensitivity of cat petrosal ganglion neurons. *Adv Exp Med Biol* **475,** 377-387.

Song X, Gao X, Guo D, Yu Q, Guo W, He C, Burnstock G & Xiang Z (2012). Expression of P2X2 and P2X3 receptors in the rat carotid sinus, aortic arch, vena cava, and heart, as well as petrosal and nodose ganglia. *Purinergic Signalling* **8,** 15–22.

Spyer KM & Gourine AV (2009). Chemosensory pathways in the brainstem controlling cardiorespiratory activity. *Philos Trans R Soc Lond B Biol Sci* **364,** 2603-2610.

Sridharan M, Adderley SP, Bowles EA, Egan TM, Stephenson AH, Ellsworth ML & Sprague RS (2010). Pannexin 1 is the conduit for low oxygen tension-induced ATP release from human erythrocytes. *Am J Physiol Heart Circ Physiol* **299,** H1146-1152.

Sun MK & Reis DJ (1994). Hypoxia-activated Ca^{2+} currents in pacemaker neurones of rat rostral ventrolateral medulla *in vitro*. *J Physiol* **476,** 101-116.

Sykova E (2004). Extrasynaptic volume transmission and diffusion parameters of the extracellular space. *Neuroscience* **129,** 861-876.

Tan ZY, Lu Y, Whiteis CA, Benson CJ, Chapleau MW & Abboud FM (2007). Acid-sensing ion channels contribute to transduction of extracellular acidosis in rat carotid body glomus cells. *Circ Res* **101,** 1009-1019.

Teppema LJ & Dahan A (2010). The ventilatory response to hypoxia in mammals: mechanisms, measurement, and analysis. *Physiol Rev* **90,** 675-754.

Thompson RJ, Jackson A & Nurse CA (1997). Developmental loss of hypoxic chemosensitivity in rat adrenomedullary chromaffin cells. *J Physiol* **498 (Pt 2),** 503-510.

Urena J, Fernandez-Chacon R, Benot AR, Alvarez de Toledo GA & Lopez-Barneo J (1994). Hypoxia induces voltage-dependent Ca^{2+} entry and quantal dopamine secretion in carotid body glomus cells. *Proc Natl Acad Sci U S A* **91,** 10208-10211.

Varas R, Alcayaga J & Iturriaga R (2003). ACh and ATP mediate excitatory transmission in cat carotid identified chemoreceptor units *in vitro*. *Brain Res* **988,** 154-163.

Varas R, Alcayaga J & Zapata P (2000). Acetylcholine sensitivity in sensory neurons dissociated from the cat petrosal ganglion. *Brain Res* **882,** 201-205.

Vince JW & Reithmeier RA (1998). Carbonic anhydrase II binds to the carboxyl terminus of human band 3, the erythrocyte Cl^-/HCO_3^- exchanger. *J Biol Chem* **273,** 28430-28437.

von Kugelgen I (2006). Pharmacological profiles of cloned mammalian P2Y-receptor subtypes. *Pharmacol Ther* **110,** 415-432.

Vulchanova L, Riedl MS, Shuster SJ, Buell G, Surprenant A, North RA & Elde R (1997). Immunohistochemical study of the P2X2 and P2X3 receptor subunits in rat and monkey sensory neurons and their central terminals. *Neuropharmacology* **36,** 1229-1242.

Wang G, Zhou P, Repucci MA, Golanov EV & Reis DJ (2001). Specific actions of cyanide on membrane potential and voltage-gated ion currents in rostral ventrolateral medulla neurons in rat brainstem slices. *Neurosci Lett* **309,** 125-129.

Wang ZZ, Bredt DS, Fidone SJ & Stensaas LJ (1993). Neurons synthesizing nitric oxide innervate the mammalian carotid body. *J Comp Neurol* **336,** 419-432.

Wang ZZ, Stensaas LJ, Dinger B & Fidone SJ (1989). Immunocytochemical localization of choline acetyltransferase in the carotid body of the cat and rabbit. *Brain Res* **498,** 131-134.

Weiss ML & Cobbett P (1992). Intravenous injection of Evans Blue labels magnocellular neuroendocrine cells of the rat supraoptic nucleus *in situ* and after dissociation. *Neuroscience* **48,** 383-395.

Wyatt CN & Evans AM (2007). AMP-activated protein kinase and chemotransduction in the carotid body. *Respir Physiol Neurobiol* **157,** 22-29.

Wyatt CN, Wright C, Bee D & Peers C (1995). O_2-sensitive K^+ currents in carotid body chemoreceptor cells from normoxic and chronically hypoxic rats and their roles in hypoxic chemotransduction. *Proc Natl Acad Sci U S A* **92,** 295-299.

Xiang Z, Bo X & Burnstock G (1998). Localization of ATP-gated P2X receptor immunoreactivity in rat sensory and sympathetic ganglia. *Neurosci Lett* **256,** 105-108.

Xu J, Tse FW & Tse A (2003). ATP triggers intracellular Ca^{2+} release in type II cells of the rat carotid body. *J Physiol* **549,** 739-747.

Yamamoto M, Kondo H & Nagatu I (1989). Immunohistochemical demonstration of tyrosine hydroxylase, serotonin and neuropeptide tyrosine in the epithelioid cells within arterial walls and carotid bodies of chicks. *J Anat* **167,** 137-146.

Yamamoto Y & Taniguchi K (2003). Heterogeneous expression of TASK-3 and TRAAK in rat paraganglionic cells. *Histochem Cell Biol* **120,** 335-339.

Zhang M, Buttigieg J & Nurse CA (2007). Neurotransmitter mechanisms mediating low-glucose signalling in cocultures and fresh tissue slices of rat carotid body. *J Physiol* **578,** 735-750.

Zhang M, Clarke K, Zhong H, Vollmer C & Nurse CA (2009). Postsynaptic action of GABA in modulating sensory transmission in co-cultures of rat carotid body via $GABA_A$ receptors. *J Physiol* **587,** 329-344.

Zhang M, Fearon IM, Zhong H & Nurse CA (2003). Presynaptic modulation of rat arterial chemoreceptor function by 5-HT: role of K^+ channel inhibition via protein kinase C. *J Physiol* **551,** 825-842.

Zhang M & Nurse CA (2000). Does endogenous 5-HT mediate spontaneous rhythmic activity in chemoreceptor clusters of rat carotid body? *Brain Res* **872,** 199-203.

Zhang M & Nurse CA (2004). CO_2/pH chemosensory signaling in co-cultures of rat carotid body receptors and petrosal neurons: role of ATP and ACh. *J Neurophysiol* **92,** 3433-3445.

Zhang M, Piskuric NA, Vollmer C & Nurse CA (2012). P2Y2 receptor activation opens pannexin-1 channels in rat carotid body type II cells: Potential role in amplifying the neurotransmitter ATP. *J Physiol*. **In press.**

Zhang M, Zhong H, Vollmer C & Nurse CA (2000). Co-release of ATP and ACh mediates hypoxic signalling at rat carotid body chemoreceptors. *J Physiol* **525 Pt 1,** 143-158.

Zhong H & Nurse CA (1997). Nicotinic acetylcholine sensitivity of rat petrosal sensory neurons in dissociated cell culture. *Brain Res* **766,** 153-161.

Zhong H, Zhang M & Nurse CA (1997). Synapse formation and hypoxic signalling in co-cultures of rat petrosal neurones and carotid body type 1 cells. *J Physiol* **503 (Pt 3),** 599-612.